BIMETALLIC CATALYSTS FOR ENANTIOSELECTIVE EPOXIDE POLYMERIZATION: ESTABLISHING AND USING MECHANISTIC HYPOTHESES TO DEVELOP ENHANCED CATALYST SYSTEMS

A Dissertation

Presented to the Faculty of the Graduate School

of Cornell University

In Partial Fulfillment of the Requirements for the Degree of

Doctor of Philosophy

by

Syud Momtaz Ahmed

August, 2012

BIMETALLIC CATALYSTS FOR ENANTIOSELECTIVE EPOXIDE POLYMERIZATION: ESTABLISHING AND USING MECHANISTIC HYPOTHESES TO DEVELOP ENHANCED CATALYST SYSTEMS

Syud Momtaz Ahmed, Ph. D.

Cornell University 2012

In 2008, the Coates group reported a bimetallic cobalt catalyst that enantioselectively polymerized terminal epoxides to form highly isotactic polyethers and enantiopure epoxides. The complex catalyst system, which consisted of the catalyst and a cocatalyst, was extremely difficult to study due to the paramagnetism of the catalyst, short reaction times, exothermic nature of the reaction, induction periods, and precipitation of polyether during polymerization. Despite these challenges, a viable mechanistic hypothesis for the enchainment of epoxides was established using experimental observations and theoretical calculations focused on the structural features of the catalyst, the oxidation state of the metal center, the role of the cocatalyst, and free-energy changes during propagation of epoxide. The mechanistic insight gained was used to develop enhanced catalysts through systematic ligand variations, enabling higher activity and selectivity for isotactic polyether synthesis under milder and more controlled reaction conditions.

BIOGRAPHICAL SKETCH

Syud Momtaz Ahmed was born in Hong Kong on December 5, 1984 to Syud Iqbal Ahmed and Pervin Ahmed. Momtaz was the youngest of three sons, and was named after his maternal grandfather, Dr. Momtazuddin Ahmed, a respected and very accomplished educator. It was at a very young age (around 3) that Momtaz conducted his first science experiment – he threw certain of his toys out the window of their apartment on the 21st floor to see if they would shatter (also known as quality testing). After a one sided "discussion" with his mother, he realized the repercussions of being an experimental scientist were far too severe, and that he would be a doctor instead. At the age of 5, his parents moved back to their home country, Bangladesh, and lived in the capital city, Dhaka.

Momtaz's parents were strong believers in providing their children with the best education available, and admitted him to a private school, Sunbeams, where English was the medium of instruction. During his 12 years at Sunbeams, he made amazing friends, played cricket, and prepared for the GCE O' level examinations (administered by the University of London). Momtaz was awarded a "Nation Builder's Award" (1 of 300, among thousands of examinees) for his exemplary results on the exams. Soon after, he reluctantly applied to colleges in the United States and attained an international scholarship to attend Wabash College in Crawfordsville, IN (notably, both his brothers also attended the same college).

On arriving at Wabash in 2003, Momtaz's name was mispronounced repeatedly – it made everyone's lives easier once he started introducing himself as 'Taz,' a nickname he was given by his cricket teammates because of his similarities with the Tazmanian devil (yes, the looney toons character). Momtaz wanted to pursue a career in medicine and very randomly picked chemistry as a suitable major and mathematics as a minor. He began doing research his freshman year in

the lab of Dr. Lon Porter, making gold nanoparticles for drug delivery systems and functionalizing silicon wafers for use in medical devices. During his time at Wabash, Momtaz received multiple awards for academic excellence, was inducted in academic honors societies, and in 2006, was awarded a grant that allowed him to work in Prof. Robert Hamers' lab at the University of Wisconsin, Madison. It was while working there that he realized how much he enjoyed research, and decided to go to graduate school for physical chemistry instead of applying to medical school. After graduating *Magna Cum Laude* from Wabash College, Momtaz moved to Ithaca, NY to attend Cornell University in 2007.

At Cornell, Momtaz joined the lab of Prof. Geoffrey Coates (not doing physical chemistry), where he worked towards developing catalysts for polyether synthesis. During his time there, he synthesized good and bad catalysts, prepared biodegradable and biocompatible materials, made amazing friends, hired people of specific height to help with his work to prove a point, attended and enlivened his labmates' weddings, and was a strong instigator of group activities at the Chapter House, Pixel and Level-B. On completion of his degree, Momtaz will be moving to Minnesota where he accepted a position as a senior scientist at 3M.

Aside from academics and doing research, Momtaz played the tabla, a South-Asian percussion instrument, from a very young age and accompanied many renowned artists throughout Bangladesh. He was best known as the percussionist of a band named AJOB, a fusion band that released a commercial album under the label of Ektaar Records (now available on i-Tunes). Momtaz has performed over a 100 shows throughout Bangladesh and the United States, and has been a guest performer on multiple commercial albums. In 2008, he had the honor of receiving instruction from the maestro, Zakir Hussain, the best tabla player in the world.

Dedicated to my dearest friend, Nabilah Shabnam Khan.

Remembered forever for her toothy smile and lively spirit.

ACKNOWLEDGMENTS

I'm quite sure that my list of people to thank at this point in life is endless, so if I haven't mentioned you and you're reading this – thank you for being a part of my adventure called life.

First and foremost, I'd like to thank my parents for their endless love, encouragement and prayers – they've been pivotal to my success throughout the years and I don't know what I'd do without them. I thank my brothers, Faisal and Amer, for their support, encouragement, and friendship that has brought me a long way. Bhabi, Lesley, Naasiah, Inayah, and Armaan also get high fives for being awesome.

The person most instrumental to my success (or claim to it), is Geoff Coates. I sincerely thank him for everything – accepting me into his group, being a great advisor and mentor, his endless patience, trust, constant support and guidance, freedom in the lab, providing motivation when most needed, helping me develop into the best scientist I can be, introducing me to Mollydooker and buying me Giordano's pizza. The list goes on and on. Working with Geoff has been a pleasure and an extraordinary learning experience I cherish and appreciate.

I thank Pete Wolczanski and Bruce Ganem for not only serving on my committee, but for being great professors and role models as scientists. I could always rely on Bruce to provide me with a solution to my synthetic challenges in lab, while also providing me with profound career advice. My conversations with him ranged from discussing science to talking about establishing businesses, and I can't remember any conversations I didn't enjoy (except the one about my first 665 exam). Pete has been no less than awesome during my time at Cornell – he taught me all about metals and how to make them do my bidding, provided me answers that explained mystery results, and taught me to think of organometallics as an art. I'm definitely grateful to the both of them. Thank you Frank Disalvo for serving on my committee while Pete's away.

Big thanks to Renee Thomas, Pete Widger, Ryan Jeske, Ian Childers and Anne LaPointe – people I worked closest with. Renee taught me the ways of epoxide polymerization; Pete and I worked side by side for 4 years trying to overcome the everyday challenges of synthesizing isotactic polyethers and it was during that time I learned the most about research; Jeske showed me how to master Schlenk technique; Anne was pivotal in my development as a scientist, preparation of papers, understanding of high throughput experimentation, and I'd probably not be graduating on time without her help; finally, Ian has been a great help in wrapping up things, and a great person to work with. He has definitely contributed towards my development as a scientist and I wish him all the best in the years to come.

I'm grateful for having been able to learn from and be friends with amazing people in the Coates group, past and present: Rachna, C, Julie, Mulzer, Chad, B-Long, Hisashi, Joe-Bot, J-Ro, Greggy D., Amelia, Hisashi, Nick, Kristina, Nate-dawg, Tam-slam, Yuki, Giang, Sarker, Dan Joh and the list goes on. I will say my life would not have been the same without Kelly Case – provider of candy and chemicals, sharer of muffins, and a person who I depend upon quite a bit (thanks Kerry!). A special thank you to Angie, for always being there, keeping up in good spirits, being inspirational and listening to me complain. I thank Erin too, for all the awesome times, and being a great classmate – I look forward to continue working with her at 3M.

What truly made Cornell an exceptional experience were some very special people who I'm so happy I met and became close friends with. Bryan Whiting, Pasquale Iacono, Kevin Noonan, and Henry Kostalik – all amazing scientists who I learned a lot from, shared laughs with, celebrated with, and spent the most time with. Henry was coined my work spouse because of the endless hours we worked together in 565. He has been one of my closest friends and his dedication to his work, friends and family is unparalleled – I learned so much from him. The standards held for story telling was never the same after meeting Bryan – he's ridiculously

intelligent and I learned so much chemistry from him. He had the ability to make a story about pulling out of the parking lot seem interesting. I'm convinced Kevin is a different breed of man (maybe because he's Canadian) – super intelligent, mentoring, fun, and the fastest beer chugger I know. Pasquale continues to surprise me all the time – he's talented, comes up with amazing ideas out of the blue and delivers hilarious one-liners I wish I could claim. MEN!

Last but not least, I'd like to thank Tim Clark. Tim's mentoring nature, friendship, and help when I first joined the group helped me become the scientist I am today. He really had a huge role to play in my development as a researcher, and his continued friendship is greatly cherished.

Thanks to Alti, Adnan, Auyon, Atef, Fahmi, Mahshid, Yasinul, Mariana, KQ, Farhan, Shez, Nas, Nab, Armeen, Labik, Shov, Chin-face, Ryan, hot-Marie, Srikant-Paleo-Iyer, Ry, Inish, Ali, Nabil, Rishad, Rashad, Aritro, Emuna, Omar, AOL friends, Shanon and Doug Hudson, Ivan Keresztes, Emil Lobkovsky, Dr. Lon Porter, Dr. Feller, Dr. Dallinger, Prof. Bob Hamers and people in the chemistry department for all their help, support, and encouragement over the years. Thanks also to my family members (cousins, uncles, aunts) for their support over the years. A special thanks to Heera, for her continued encouragement, inspiration, friendship and good wishes.

TABLE OF CONTENTS

Chapter 2: Mechanistic Insight into the Enantioselective Polymerization of Epoxides using a Bimetallic Cobalt Catalyst

Chapter 3: Systematic Ligand Variations to Enhance a Highly Active Bimetallic Catalyst for Enantioselective Epoxide Polymerization

LIST OF FIGURES

LIST OF SCHEMES

LIST OF TABLES

Chapter 1

Stereoselective Catalysts for the Ring-Opening Polymerization of Epoxides

Reproduced in part with permission from:

H. Ajiro, P. C. B. Widger, S. M. Ahmed, S. D. Allen, G. W. Coates

Comprehensive Polymer Science II

1.1. Introduction

1.1.1. Background

In the 1950s Baggett and Pruitt reported that iron (III) chloride polymerized racemic propylene oxide (PO) to give a polymeric material that could be separated into amorphous and crystalline materials using solvent fractionation.[1-4] Shortly thereafter, Natta[5] and Price[6,7] provided evidence that the crystalline material was isotactic poly(propylene oxide) (PPO), in which the main-chain stereogenic centers of each macromolecule were of the same relative configuration. This finding marked the first discovery of a stereoselective catalyst for epoxide polymerization. This chapter highlights the significant advances made in the field of stereoselective epoxide polymerization, including copolymerizations since the initial findings of Baggett, Pruitt, Natta and Price.

1.1.2 Scope of Chapter

Many of the important contributors to the field of stereoselective epoxide polymerization have written accounts of their research,[8-20] but there are few collective contemporary reviews of the work done in this area.[21] This chapter focuses on discrete catalysts for the stereoselective polymerization of racemic epoxides. Due to space limitations, only catalysts bearing at least one ancillary ligand that is not likely to react with epoxides are discussed; catalysts only bearing ligands that are well-known to react with epoxides are not covered. A discussion of strategies for controlling the relative configuration of main-chain stereogenic centers of epoxide polymers is

included. The polymerization of enantiopure epoxides[6] is not covered as the emphasis of this chapter is on stereochemical control of polymerization by the catalyst or initiator.

1.2. Basic Concepts in Stereselective Epoxide Polymerization

1.2.1. Regiochemistry

Both the ancillary ligands (L_n) surrounding the active metal center (M) and the growing polymer chain (OR) influence the regiochemistry and stereochemistry of epoxide polymerization.[22] When the epoxide is unsymmetrically substituted (i.e. PO), enchainment commonly occurs in two ways: (1) S_N2 attack by the polymer's alkoxide chain-end at the less substituted methylene with retention of the stereochemistry of the substituted carbon to give a secondary metal alkoxide; or (2) S_N2 attack at the substituted methine with inversion of stereochemistry to give a primary metal alkoxide. The polymer is regioregular when only one process dominates; the polymer is regioirregular when both processes occur. The regiochemistry of a polyether, such as PPO, can be readily determined by ^{13}C NMR spectroscopy.[23-25]

1.2.2. Analysis of Polymer Stereochemistry

NMR spectroscopy is the most useful method for determining polymer tacticity.[26,27] In many cases, the chemical shifts for the various polymer nuclei are sensitive to adjacent stereogenic centers, resulting in fine structure that can provide quantitative information about the polymer microstructure once the shift identities are assigned. For example, the methyl, methylene, and methine regions of a high-resolution ^{13}C NMR spectrum of regioregular atactic PPO display several resonances, each of which represents a different set of consecutive

stereocenters. As each resonance in the spectrum has been assigned (Scheme 1.1),[23,24,28] a routine ^{13}C NMR experiment can reveal both the tacticity and the degree of stereoregularity of a sample of PPO.

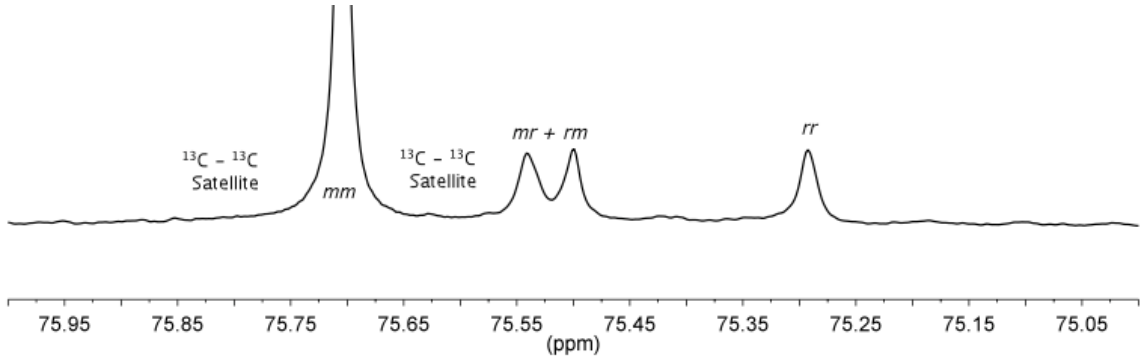

Scheme 1.1. Methine Region of the ^{13}C NMR Spectrum of Partially Isotactic Poly(propylene oxide) Showing Triad Stereoerrors.

1.2.3. Chain-End Control and Enantiomorphic-Site Control of Stereochemistry

In a chain-growth polymerization reaction, one end of the polymer chain remains at the active metal center during monomer enchainment. Thus, the stereogenic center in the polymer chain from the last enchained monomer unit will have an influence on the stereochemistry of monomer enchainment. If this influence is significant, the mode of stereochemical regulation is referred to as "polymer chain-end control" (Scheme 1.2a). If the active site is chiral and overrides the influence of the polymer chain end, the mechanism of stereochemical direction is termed "enantiomorphic-site control" (Scheme 1.2b).[9-11] The Bovey formalism is a convenient way to describe polymer tacticity, where an "*m*" for *meso* (same stereo-configuration), or an "*r*" for *racemic* (opposite stereo-configuration) describes relationships between adjacent stereogenic centers (dyads). These dyads are seen as unique signals in ^{13}C NMR. The monomer enchainment

mechanism can be easily identified by observing the stereochemical errors propagated in a polymer chain. The ratio of the signals in a ^{13}C NMR spectrum can be used to determine the mechanism of stereocontrol. In the case of an isotactic polymer, a "chain-end control" mechanism produces polymers in which stereoerrors are propagated (i.e. would display primarily *mm*, *mr*, and *rm* triads, Scheme 1.2a). In the "enantiomorphic-site control" mechanism, correction of stereoerrors occurs because the ligands direct the stereochemical events, leading to an isolated error (i.e. produces a polymer which would display primarily *mm*, *mr*, *rm*, and *rr* triads, Scheme 1.2b).

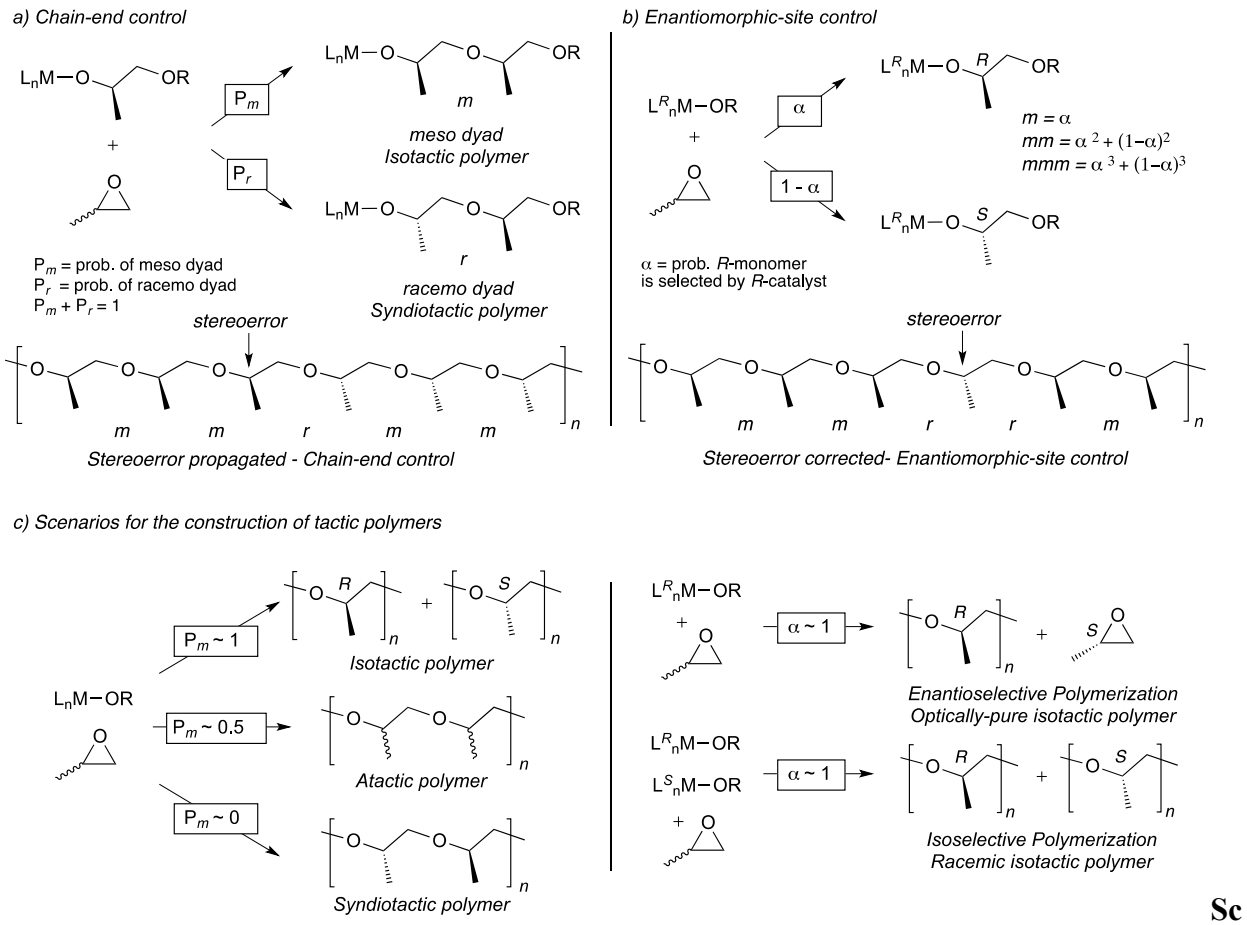

Scheme 1.2. a) Chain-End b) Enantiomorphic-Site Mechanisms of Stereocontrol in Epoxide Polymerization c) Scenarios for the Construction of Tactic Polymers (L^R_nM-OR is an

enantiomerically pure catalyst that prefers *R*-Monomer).

Optically active catalysts can kinetically resolve racemic monomers (Scheme 1.2c) via enantioselective polymerization producing optically active polymers as well as enantiomerically enriched monomers. The nonpreferred enantiomer remains enriched in the reaction mixture after the preferred enantiomer of monomer has been enchained as a polymer. The quantitative measure of stereocontrol in such a system is given by the selectivity factor (s = s-factor), which is the ratio of the rate constants for the polymerization of the fast enantiomer converted to polymer with respect to the slow enantiomer enchained [$s = k_{fast}/k_{slow} = \alpha/(1 - \alpha)$].[29] A racemic enantioselective catalyst can polymerize both enantiomers of racemic monomer via isoselective polymerization to give racemic isotactic polymer.

1.3. Stereoselective Epoxide Polymerization

The majority of papers reporting stereoselective epoxide polymerization focus on the polymerization of PO using different metal-based catalysts. Thus, this chapter is organized based on the metal of the active center of the catalyst. Aluminum, zinc, cobalt, tin and chromium are the most commonly used metals for discrete stereoselective epoxide polymerization catalysts and their use in this field of research forms the foundation of this chapter.

1.3.1 Aluminum-Based Catalysts

Although aluminum alkoxide- and aluminoxane-based catalysts have shown promise for the isoselective polymerization of epoxides, the poorly defined nature of these species has significantly hampered their use in such polymerizations due to the formation of large amounts of atactic polyether.[30] Some examples of discrete aluminum complexes have been reported herein.

Aluminum–acetylacetonate complexes

The prevailing theory for the mechanism of epoxide polymerization has been that epoxide coordination to the metal center precedes insertion. To support this mechanism, Vandenberg proposed that the addition of chelating agents such as acetylacetone (acac) to an R_3Al/H_2O (R = alkyl) polymerization system would block potential coordination sites on the metal center, thus hindering the reaction. Instead, these additives enhanced the polymerization rate and ushered in a new class of versatile and highly active catalysts.[12,31-33] The presumed structure of the active aluminum-acac catalyst is shown in Scheme 1.3. Although the precise structure of the active catalyst is unknown, a few structural features have been determined: (1) an oxygen atom bridges two aluminum centers (although the presence of multiple linkages, such as those in oligomeric aluminoxanes, cannot be ruled out); (2) alkyl groups are present on the aluminum atoms; and (3) the acac ligand is chelated to the aluminum center.[20]

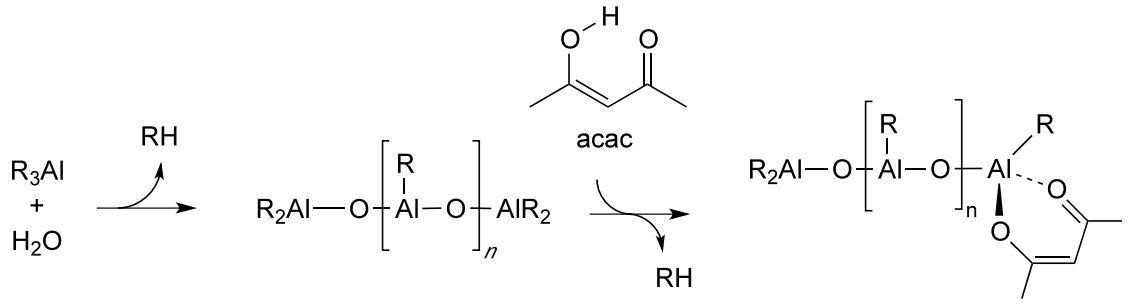

Scheme 1.3. Synthesis of AlR_3/H_2O/acac Epoxide Polymerization Catalysts (R = alkyl).

Tuning the AlR_3/H_2O/acac catalyst (R = alkyl) composition by varying the R groups and the ratio of components creates systems that conduct epoxide polymerizations to give high conversions, in many instances achieving >90% conversion to give high-molecular-weight, acetone-insoluble polyethers. The fraction of acetone-insoluble, isotactic polymer produced varies according to the exact composition of the catalyst system used, and is approximately 30% of the total mass of the ether-insoluble material, while the remaining 70% is acetone-soluble atactic polymer.[32,33]

In work investigating the mechanism of this system, Vandenberg used AlR_3/H_2O catalysts to polymerize *cis*- and *trans*-2,3-epoxybutane. Mechanistic information for the polymerization was obtained from the properties of the resultant polymers and the examination of the diol decomposition products. These results are summarized in Scheme 1.4.[12,20,34-36]

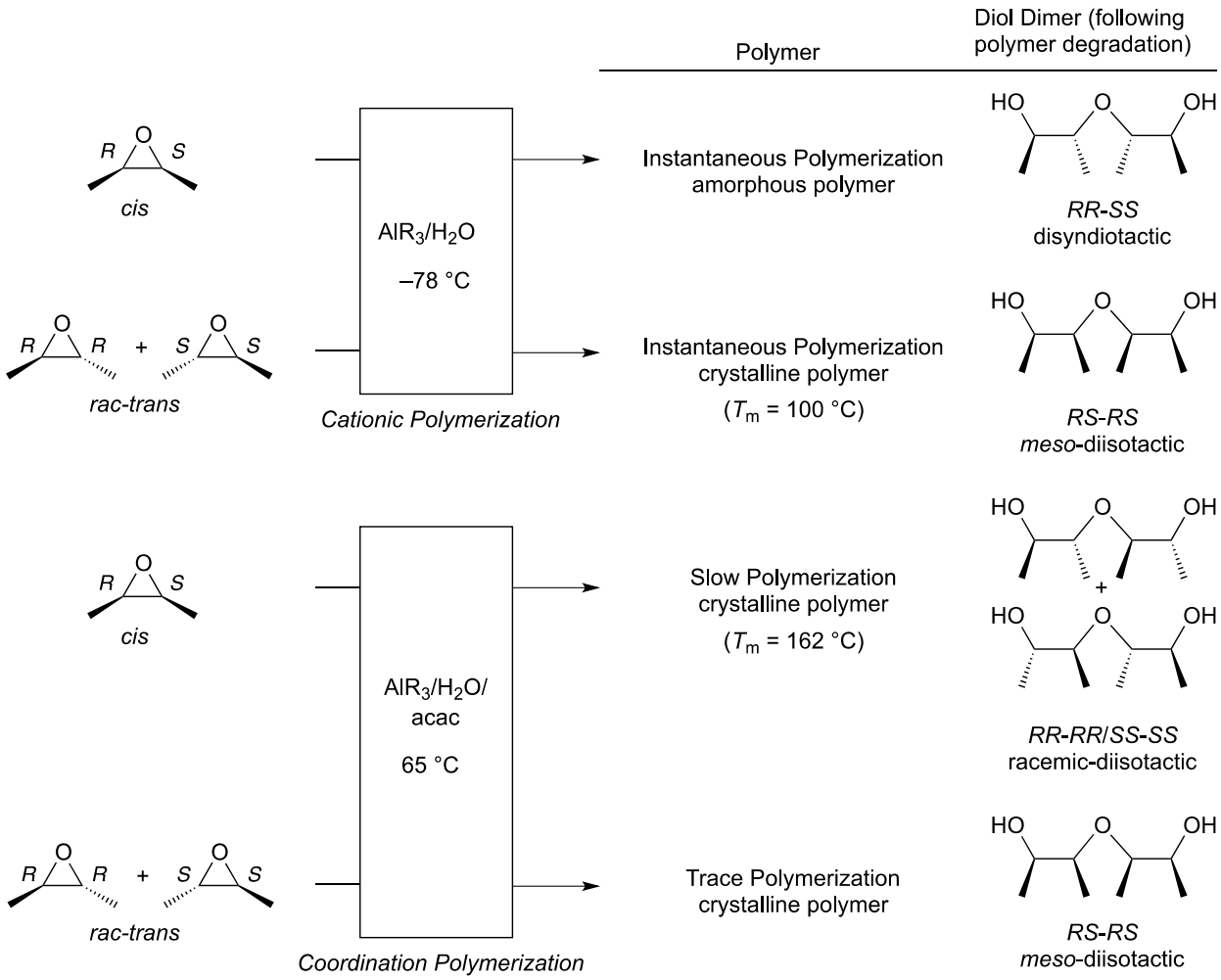

Scheme 1.4. Stereoselectivity of Polymerization of *cis*- and *trans*-2,3-Epoxybutane Using AlR_3/H_2O catalysts (R = alkyl).

The AlR_3/H_2O catalysts polymerize both *cis*- and *trans*-2,3-epoxy butane instantaneously at –78 °C, consistent with a cationic process for monomer enchainment. The polymer isolated from the *cis* isomer is an amorphous rubber, whereas the polymer isolated from the *trans* isomer is crystalline with a T_m of 100 °C. This finding is in contrast to the AlR_3/H_2O/acac system, which only slowly polymerizes the same monomers at 65 °C, presumably through a much slower coordination–insertion mechanism. The coordination polymerization of the *cis* isomer yields a crystalline polymer with a T_m of 162 °C, whereas the *trans* isomer polymerizes extremely

slowly, producing only trace amounts of a crystalline polymer with a T_m similar to that obtained with the cationic polymerization. Vandenberg attributes the extremely slow polymerization of the *trans* isomer to its increased steric bulk compared to the *cis* isomer at the metal coordination site. The steric bulk hinders the required pre-coordination to the metal center for monomer insertion.

Through the controlled degradation of the polyethers to diol dimers using *n*-butyl lithium, the stereochemistry of the monomer units in the polymer chain was determined.[34] The decomposition of all four polymers showed that inversion of stereochemistry at the site of attack on the epoxide ring occurred in both cationic and coordination-insertion polymerization mechanisms. The *cis* epoxides (*RS* stereocenters) produce monomeric units in the polymer chain with *RR* and *SS* stereocenters, and the *trans* epoxides (either *RR* or *SS*) produce monomeric units in the polymer chain with only *RS* units. This observation shows that both polymerizations are stereospecific, with inversion of configuration occurring at the site of attack, regardless of the polymerization mechanism.

To obtain the geometry required for a S_N2 attack in a coordination-insertion mechanism, Vandenberg proposed the transition structure shown in **Scheme 1.5**. In this scheme, an epoxide is activated by coordination to an aluminum center, while the adjacent aluminum center delivers the growing polymer chain. During this process, coordination bonds are exchanged to keep the charges balanced. Despite the evidence for bimetallic epoxide ring-opening events in other systems,[37-39] there is little evidence beyond the epoxide inversion, to show that it occurs in these heterogeneous aluminum-based systems.

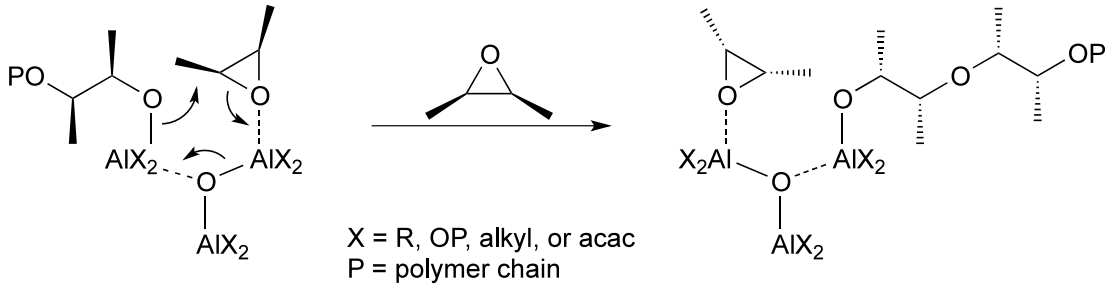

Scheme 1.5. Proposed Bimetallic Enchainment of Epoxides Using (acac)Al Complexes (acac = acetylacetonate, P = polymeryl).

Aluminum systems featuring chiral alkoxides

Haubenstock and coworkers synthesized chiral aluminum alkoxides for the stereoselective polymerization of PO.[40] Addition of 1.5 equiv. of (*R*)-(–)-3,3-dimethyl-1,2-butanediol ((*R*-dmbd)H_2) to AlH_3 generated the active complex $[(R\text{-dmbd})_{1.5}/Al]_n$. Alone, $[(R\text{-dmbd})_{1.5}/Al]_n$ displayed very low activity for the polymerization of PO, achieving 85% conversion in 3 weeks with negligible optical activity in the unreacted monomer. The addition of $ZnCl_2$ (Al:Zn = 1:1) to the $[(R\text{-dmbd})_{1.5}/Al]_n$ initiator generated a much more active catalyst, as shown in Scheme 1.6. Furthermore, the optical activity of the unreacted PO was observed to increase with increasing conversion to polymer, and based on the optical rotation of the unreacted monomer, Haubenstock and coworkers determined that the catalyst system preferentially reacted with (*R*)-PO because the reaction solution became enriched in the (*S*) enantiomer, although with modest selectivity (s = 1.05).[40] On fractionation, 10% of the total mass of the isolated polymer was acetone-insoluble and highly isotactic (>99% *m*-dyads), whereas the remainder of the polymer was acetone-soluble and atactic. Although a slight enantiomeric enrichment of monomer was achieved, this system did not significantly improve

the yield of isotactic PPO compared to similar systems,[41-43] and it is unclear whether the selective enchainment of the *R*-enantiomer was contributing to the formation of the 10% of crystalline polymer as opposed to it arising from a different mechanism.

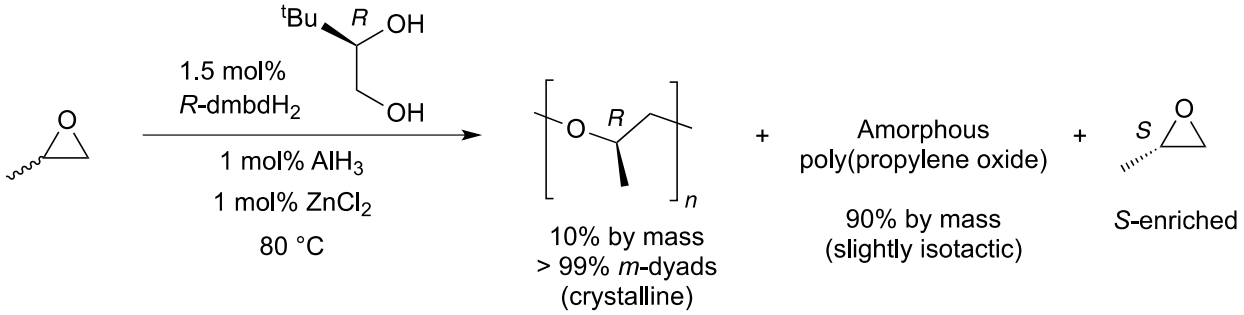

Scheme 1.6. Polymerization of Propylene Oxide with $[(R\text{-dmbd})_{1.5}Al]_n/ZnCl_2$ Catalysts (dmbd = 3,3-dimethyl-1,2-butanediolate).

Aluminum–porphyrin complexes

Inoue first reported that 5, 10, 15, 20-tetraphenylporphyrin (tpp) aluminum chloride (Figure 1.1, **1.1**) was active for the living polymerization of PO.[44-46] Although the polymer microstructure was not studied in great detail, ^{13}C NMR spectra showed the polymers to be highly regioregular and slightly isotactic.[44,45] The activity of (tpp)AlCl was relatively low, requiring 6 days to completely polymerize 200 equiv. of PO. The addition of Cl or OMe substituents on the porphyrin ligand, as in (*p*-Cl-tpp)AlCl (**1.2**) and (*p*-OMe-tpp)AlCl (**1.3**), increased the activity by a factor of two, but the tacticity of the resulting polymers was not discussed.[45] More detailed ^{13}C NMR analyses by Le Borgne and coworkers showed that the PPO derived from **1.1** was slightly isotactic, with an *m*-dyad content of 69% and an *mm*-triad content of 45%, confirming the initial results reported by Inoue.[24]

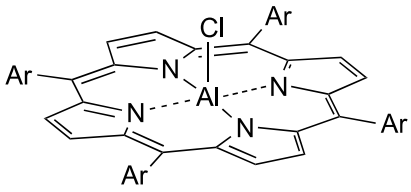

Ar = C_6H_5 (tpp); **1.1**
Ar = *p*-C_6H_4Cl (*p*-Cl-tpp); **1.2**
Ar = *p*-C_6H_4OMe (*p*-OMe-tpp); **1.3**

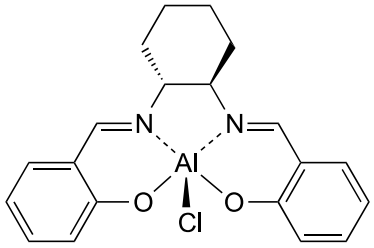

(*R,R*-salcy)AlCl; **1.4**

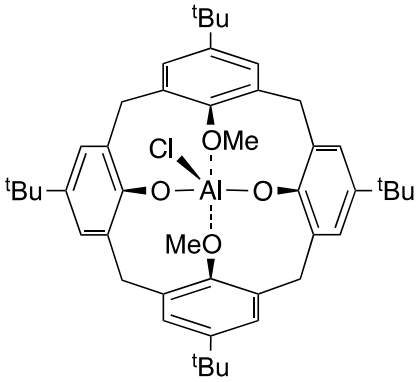

(dmca)AlCl; **1.5**

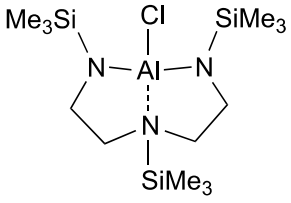

1.6

Figure 1.1. Well-defined complexes for the polymerization of epoxides (tpp = 5, 10, 15, 20-tetraphenylporphyrin; salcy = *N,N*′-bis-(2-hydroxybenzylidene)-(1*R*,2*R*)-1,2-cyclohexanediamine); dmca = dimethylcalixarene.

Aluminum–schiff-base complexes

Well-defined [*N,N*'-bis-(2-hydroxybenzylidene)-(1*R*,2*R*)-1,2-cyclohexane-diamine] (*R,R*-salcy) aluminum complexes (Figure 1.1, **1.4**) have been used as enantioselective epoxide polymerization catalysts.[47-49] Polymerization of racemic PO in the presence of 5 mol% **1.4** yields approximately 70% conversion to PPO after 62 hours. The remaining unreacted monomer exhibits an optical rotation of +1.85°, which corresponds to an *ee* of 15% (Scheme 1.7). The

modest *s*-factor of 1.3 obtained in this system is slightly higher than that observed for the previously discussed heterogeneous aluminum systems.[50] Examination of the isolated polymer reveals both chloro and hydroxyl end-groups, suggesting that each metal center produces a single polymer chain since each chain bears a Cl atom from initiation and a hydroxyl group from termination.[48]

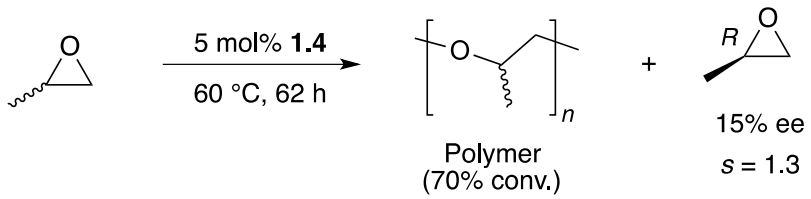

Scheme 1.7. Attempted Enantioselective Polymerization of Racemic Propylene Oxide Using **1.4**.

Aluminum–calixarene complexes

Kuran and coworkers synthesized a dimethylcalixarene-based system (Figure 1.1, **1.5**) that exhibited low activity for PO polymerization TOF = 0.06 h^{-1}.[51] The polymerization of PO produced predominantly isotactic PPO with an *m*-dyad content of approximately 74%.

Other well-defined aluminum systems

N,*N*′,*N*″-Tris(trimethylsilyl)diethylenetriamine complexes of aluminum have been shown to be active oligomerization catalysts for PO.[52] Over the course of 2 days, catalyst **1.6** (Figure 1.1) produces low-molecular-weight PPO (M_n < 500 g mol^{-1}) with predominantly head-to-tail linkages and an *m*-dyad content of 60%.

1.3.2. Zinc-Based Catalysts

During research on aluminum catalysts for the stereoselective polymerization of epoxides, it was discovered that the addition of zinc cocatalysts to these systems greatly enhanced catalyst activity.[41] These enhancements prompted a number of studies focusing on the design of zinc-based catalyst systems.

Zinc alkoxide catalysts

Furukawa and coworkers explored catalysts derived from the addition of methanol or ethanol to diethylzinc as epoxide polymerization systems,[53] and found that both the yield and crystallinity of the resulting polymers were inferior to those for polymers synthesized with the $ZnEt_2/H_2O$ system. The use of achiral alcohols as co-catalysts was revisited in 1994 when Kuran and coworkers reported the polymerization of PO and cyclohexene oxide (a *meso* substrate) with $ZnEt_2$/polyhydric phenol (such as 4-*tert*-butyl-catechol), phenol, or 1-phenoxy-2-propanol.[54] The PPO formed from these systems contained mostly isotactic dyads (72% *m*), while the poly(cyclohexene oxide) contained mostly syndiotactic dyads (80% *r*) (Scheme 1.8).

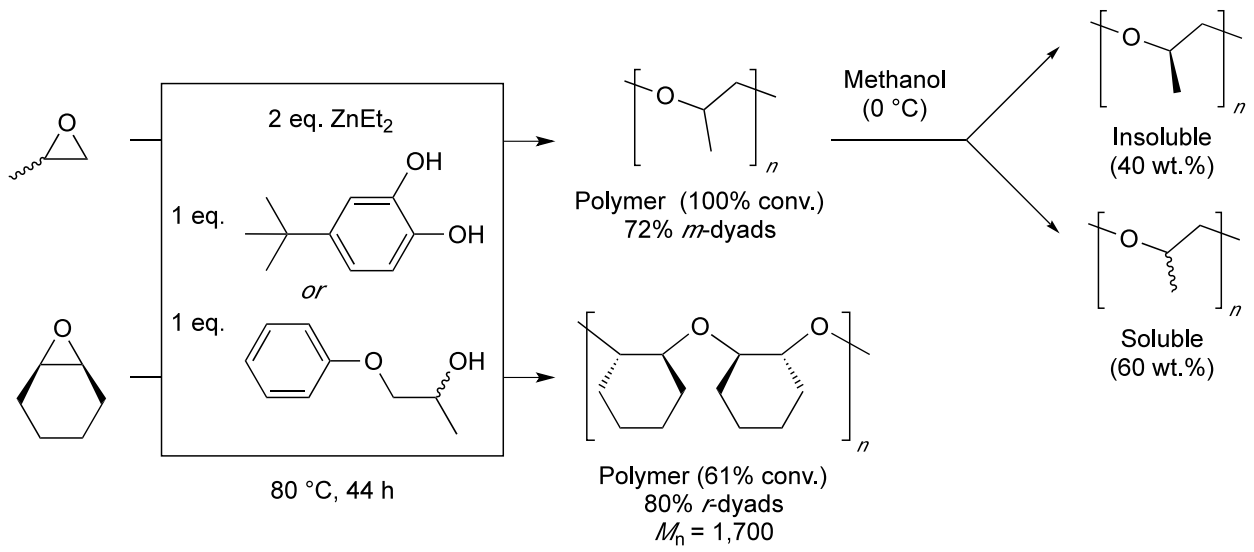

Scheme 1.8. Polymerization of Epoxides with $ZnEt_2$/1-Phenoxy-2-propanol or 4-*tert*-Butylcatechol.

Chiral zinc alkoxide catalysts

Sigwalt and coworkers noted higher stereoselectivity during the polymerization of propylene sulfide using a (*R*)-3,3-dimethyl-1,2-butanediol/$ZnEt_2$ system when compared to a similar chiral alcohol/$ZnEt_2$ system. Based on these results, they applied this system to PO polymerization, but noticed that stereoselectivity was actually lower than that for the polymerization of propylene sulfide.[16,55,56] This lower stereoselectivity was attributed to the weaker coordination of the "harder" epoxide oxygen atom to zinc, as compared to the "softer" coordination of the episulfide sulfur atom.

Sepulchre and coworkers investigated the polymerization of cyclohexene oxide using $ZnEt_2$ activated with water, alcohols, and chiral alcohols. In their study, a mixture of $ZnEt_2$ and 1-methoxy-2-propanol or (1*S*, 2*R*)-ephedrine simultaneously afforded a mixture of isotactic and syndiotactic poly(cyclohexene oxide) that was characterized using ^{1}H and ^{13}C NMR

spectroscopy (Scheme 1.9).[57,58] They proposed a "flip-flop" mechanism (similar to that proposed by Vandenberg as shown in **Scheme 1.5**) involving neighboring zinc centers to explain this observation.[20]

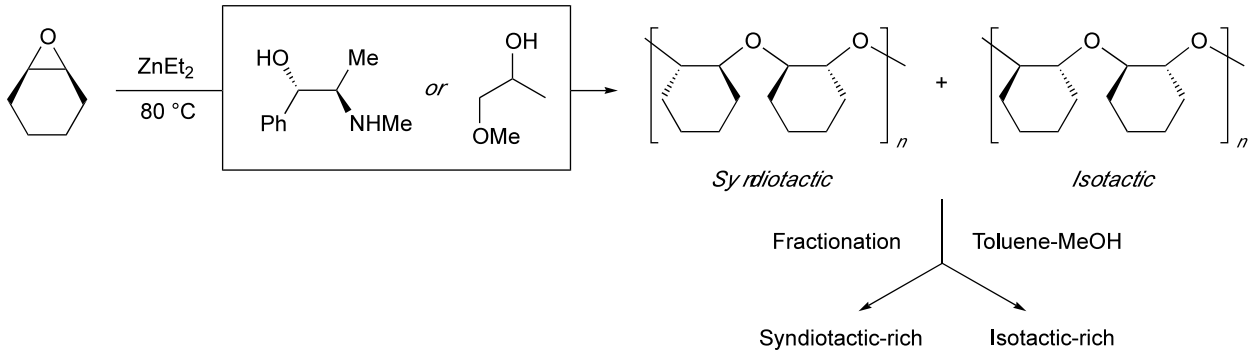

Scheme 1.9. Preparation of a Mixture of Isotactic and Syndiotactic Poly(cyclohexene oxide) Using Chiral Zinc Alkoxide Catalysts.

Zinc alkoxide clusters

Tsuruta and coworkers synthesized and investigated the epoxide polymerization activity of several well-defined zinc clusters (Figure 1.2).[59-68] Complexes $[Zn(OMe)_2{\bullet}(EtZnOMe)_6]$ (**7**), $[Zn(OCH_2CH_2OMe)_2{\bullet}(EtZnOCH_2CH_2OMe)_6]$ (**1.8**), and $[\{CH_3OCH_2CH(Me)OZnOCH(Me)CH_2OCH_3\}_2{\bullet}\{EtZnOCH(Me)CH_2OCH_3\}_2]$ ($[Zn\text{-}MP]_{2,2}$) (**1.9**), were synthesized by the dropwise addition of 1.1 equiv. of the corresponding alkoxyalcohols to $ZnEt_2$ in heptanes at 5 °C. Each complex was crystalline, and its molecular structure was determined using X-ray crystallography (Figure 1.2).[59,62,68]

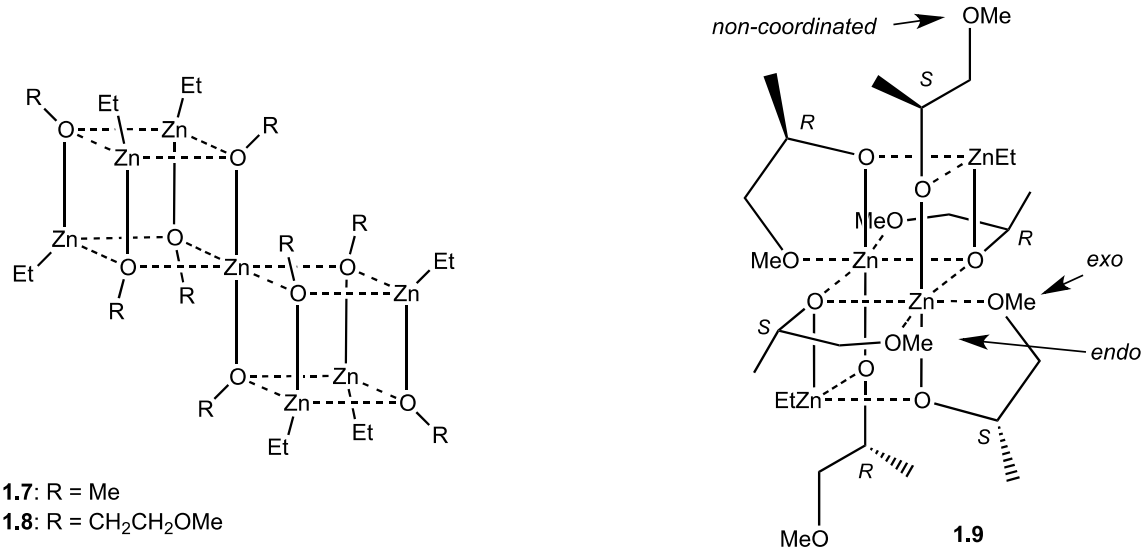

Figure 1.2. Structures of zinc cluster catalysts **1.7**, **1.8**, and **1.9**.

The PO polymerization activity for each complex is shown in Scheme 1.10. Surprisingly, isostructural complexes **1.7** and **1.8** had significantly different polymerization activities; **1.7** achieved 91% conversion in 216 hours, while **1.8** only attained 22% conversion in 240 hours. Catalyst **1.9**, however, was twice as active as complex **1.7**. This catalyst has a different molecular structure, as shown in Figure 1.2. Complex **1.9** bears six methoxy isopropyl groups in a chair-like structure in three different coordination environments; the methoxy groups are either *endo*- and *exo*-coordinated to the central zinc atoms through dative bonds, or non-coordinated.

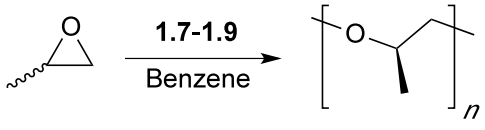

Catalyst	Temp. (°C)	Time (h)	Yield (%)	*m*-Dyads (%)
1.7	80	216	91	63
1.8	80	240	22	59
1.9	80	100	93	79
1.9	35	240	9	81

Scheme 1.10. Polymerization of Racemic Propylene Oxide with Zinc Alkoxide Cluster Catalysts **1.7**-**1.9**.

Studies using a deuterated analogue of **1.9** revealed that the non-coordinating methoxyisopropoxide groups initiated the polymerization by attack on the PO monomer, whereas the coordinated methoxyisopropoxide groups provided the chiral structure which remained unchanged during the polymerization.[63] When these complexes were screened for cyclohexene oxide polymerization, only **1.9** was found to be active.[69,70] Through ^{1}H NMR spectroscopic analysis of polymer decomposition products (using Vandenberg's method[34]), Tsuruta and coworkers determined that the poly(cyclohexene oxide) obtained was predominantly syndiotactic (Scheme 1.11).

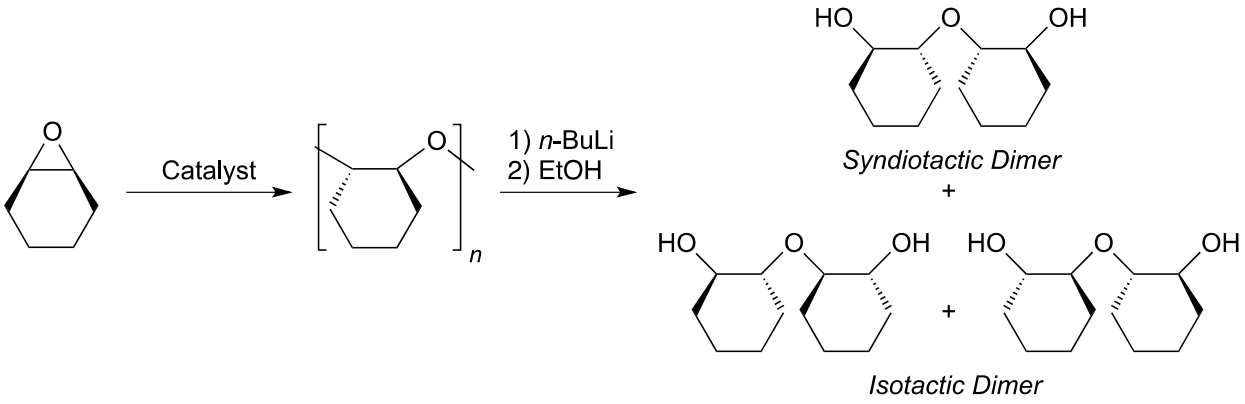

Catalyst	Syndiotactic Dimer (%)	Isotactic Dimer (%)
$ZnEt_2$	66	34
$(EtZnOMe)_4$	66	34
1.9	81	19

Scheme 1.11. Syndioselective Polymerization of Cyclohexene Oxide with **1.9** and Subsequent Degradation.

Zinc porphyrin–based catalysts

Inoue and coworkers reported that the polymerization of PO at 20 °C with the zinc porphyrin catalyst (Et_2Zn/*N*-methyl-5, 10, 15, 20-tetraphenylporphyrin, **1.10**) produced syndiotactic PPO (M_w = 31,000, 60% *r*) (**Scheme 1.12**). This result was in contrast to those seen for all other zinc-based systems, which afford isotactic PPO. The authors attributed the unexpected syndiotactic microstructure of the polymer to the planar ligand and the isolated nature of the zinc center, which is different than that present in most other zinc aggregate systems.[44]

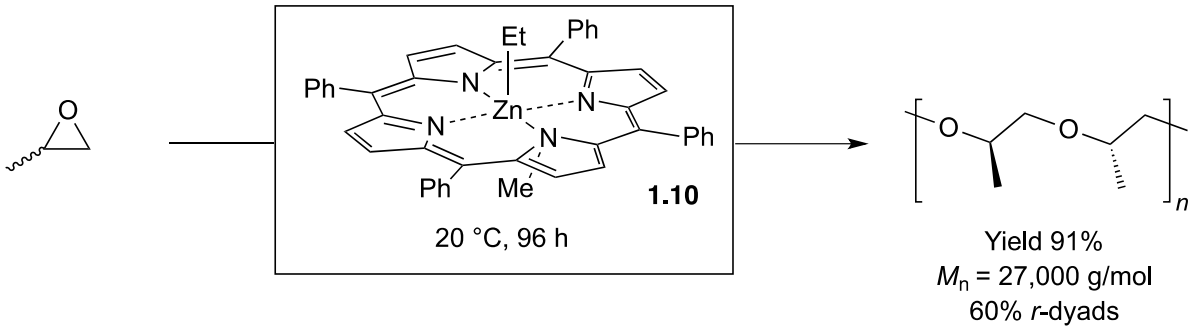

Scheme 1.12. Syndioselective Polymerization of Propylene Oxide with **1.10**.

Zinc catalysts for asymmetric cyclohexene oxide/CO_2 copolymerization

There is significant interest in controlling the absolute stereochemistry of ring-opening in epoxide/CO_2 copolymerization. Cyclohexene oxide, a *meso* molecule, is an ideal substrate for desymmetrization using chiral catalysts. In 1999, Nozaki reported that a 1:1 mixture of $ZnEt_2$ and (*S*)-α,α-diphenylpyrrolidine-2-yl-methanol (**1.11**) (Scheme 1.13) was active for stereoselective cyclohexene oxide/CO_2 copolymerization at 40 °C and 30 atm CO_2.[71] The resultant polycarbonate contained 100% carbonate linkages, had an M_n of 8,400 g mol^{-1}, and had a M_w/M_n of 2.2. Hydrolysis of this poly(cyclohexene carbonate) with base produced the corresponding *trans*-cyclohexane-1,2-diol with 73% *ee*. ^{13}C NMR spectroscopy studies of model polycarbonate oligomers afforded spectral assignments for the isotactic (153.7 ppm) and syndiotactic dyads (153.3–153.1 ppm) of poly(cyclohene oxide),[72] which agreed with those proposed by Coates *et. al.*[73] Finally, the ring-opening polymerization proceeded stereospecifically via complete inversion of configuration (S_N2 mechanism) of one carbon of each repeat unit; hence, no *cis*-cyclohexane-1,2-diol was observed after base-catalyzed degradation of the polycarbonate.

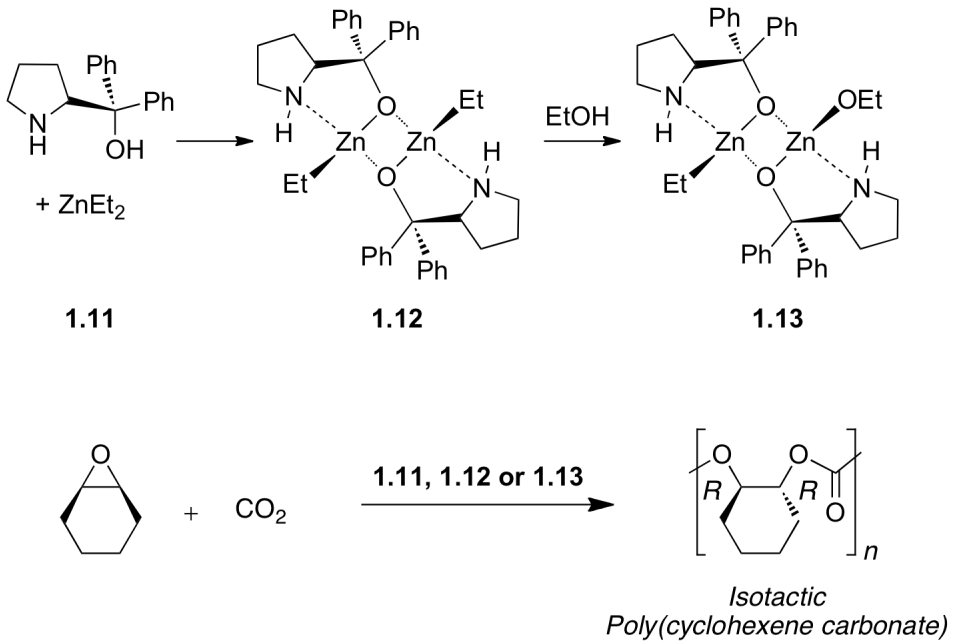

Scheme 1.13. Chiral Zinc Catalysts for the Stereoselective, Alternating Copolymerization of Cyclohexene Oxide and CO_2.

In a 2003 report, Nozaki and coworkers isolated presumed intermediates in the asymmetric alternating copolymerization of cyclohexene oxide with CO_2.[74] Reaction of a 1:1 mixture of $ZnEt_2$ and (*S*)-α,α-diphenylpyrrolidine-2-yl-methanol (**1.11**, Scheme 1.13) yielded dimeric **1.12**, which was structurally characterized by X-ray diffraction studies. At 40 °C and 30 atm CO_2, **1.12** catalyzed the formation of isotactic poly(cyclohexene carbonate) (M_n = 11,800 g mol^{-1}, M_w/M_n = 15.7) with a turnover frequency of 0.6 h^{-1}. Hydrolysis of the resulting poly(cyclohexene carbonate) yielded the *trans*-cyclohexane-1,2-diol of 49% *ee*, which was lower than that seen with catalyst **1.11**. When copolymerization was attempted using a catalyst system consisting of **1.12** and 0.2–1.0 equiv. EtOH (**1.12**/EtOH), the *ee* of the hydrolyzed cyclohexane diol increased up to 80%. The catalyst and EtOH combination resulted in better control of polymer molecular weights and molecular weight distributions in comparison to polymerization

using only **1.12**. Compound **1.13** (Scheme 1.13) was proposed to be the active initiating species in this polymerization. End-group analysis of the poly(cyclohexene carbonate)s prepared with **1.12** and **1.12**/0.2 EtOH by matrix-assisted laser desorption/ionization time-of-flight (MALDI-TOF) mass spectrometry revealed that in the absence of ethanol or in the presence of 0.2 eq. ethanol, end group signals assignable to an aminoalcohol-initiated polymerization were identified. However, as EtOH addition was increased from 0.2 to 1.0 equiv., signals corresponding to the aminoalcohol-initiated polycarbonate disappeared as signals corresponding to end-group structures for EtOH-initiated poly(cyclohexene carbonate) emerged. This result was further confirmed by end-group analysis using ^{1}H NMR spectroscopy. Finally, mechanistic studies suggested that the dimeric form of the catalyst, **1.13**, was in fact the active species.

In 2000, Coates and coworkers developed C_1-symmetric imine-oxazoline ligated zinc bis(trimethylsilyl)amido compounds (Figure 1.3, **1.14**) for the isoselective, alternating copolymerization of cyclohexene oxide and CO_2.[73] Through multiple electronic and steric manipulations of the imine-oxazoline ligand framework, compound **1.14** was found to exhibit the highest enantioselectivity for polymerization (*RR*:*SS* ratio in polymer = 86:14; 72% *ee*). Poly(cyclohexene carbonate) prepared with this catalyst possessed 100% carbonate linkages, an M_n of 14,700 g mol^{-1}, and an M_w/M_n of 1.35. This poly(cyclohexene carbonate) was crystalline with a glass transition temperature (T_g) of 120 °C, and a melting temperature (T_m) of 220 °C. Furthermore, stereocontrol was also achieved in the alternating copolymerization of cyclopentene oxide and CO_2, producing poly(cyclopentene carbonate) with an *RR*:*SS* ratio of 88:12 (76% *ee*). As revealed by ^{13}C NMR spectroscopy, the experimental carbonyl tetrad

concentrations of this material matched the predicted tetrad concentrations for an enantiomorphic-site control mechanism.[73]

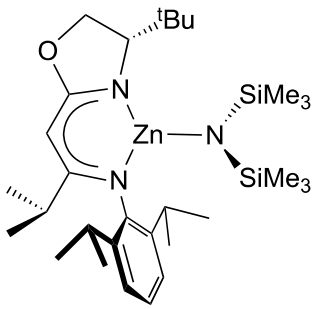

1.14

Figure 1.3. Chiral zinc catalyst **1.14** for the enantioselective, alternating copolymerization of cycloalkene oxides and CO_2.

1.3.3. Cobalt-Based Catalysts

Tsuruta found that the optically pure complex [(*R,R*-salcy)Co] (**1.15**) was active for epoxide polymerization (Scheme 1.14) when activated with $AlEt_3$. Although the system exhibited no enantioselectivity for the polymerization of PO, it was moderately selective ($s \sim 1.5$) for the enantioselective polymerization of *tert*-butyl ethylene oxide and epichlorohydrin (Scheme 1.14).[75]

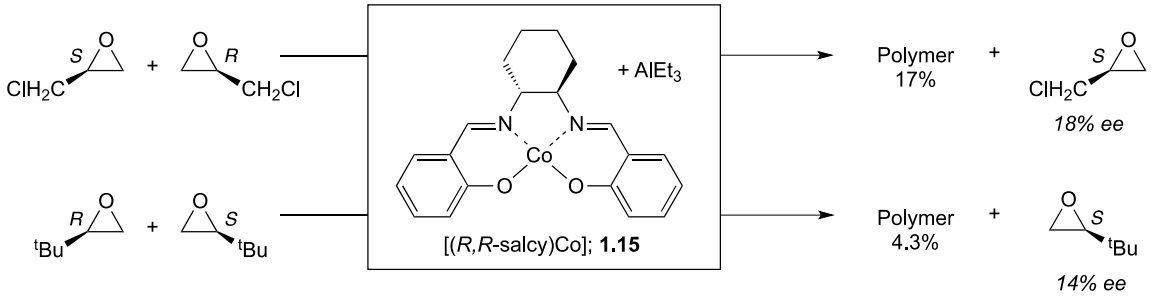

Scheme 1.14. Enantioselective Polymerization of Racemic *tert*-Butyl Ethylene Oxide and Epichlorohydrin Using **1.15**/$AlEt_3$.

Epoxide-carbon dioxide copolymerization systems

Coates and coworkers reported that [(*R,R*-salcy-^{t}Bu)CoOAc] (**1.16**) copolymerizes PO and CO_2 (Scheme 1.15).[76] Novel features of the catalyst are high regioregularity and alternation, coupled with high selectivity for polycarbonate formation (cyclic propylene carbonate is not formed). (*S*)-PO is consumed faster than (*R*)-PO with a modest *s*-factor of 2.8. Given the same absolute monomer configuration and similar *s*-factor observed by Jacobsen for the cobalt-catalyzed ring-opening of aliphatic epoxides with benzoic acid,[39] a related mechanism was

proposed to occur for polymerization with [(*R,R*-salcy-^{t}Bu)CoOAc], giving a cobalt-alkoxide catalyst resting state to produce the regioregular structure shown in Scheme 1.15.

Lu and coworkers found that the addition of quaternary ammonium salts increased the *s*-factor to 3.5.[77] The use of cobalt salen complexes, [SalenCo^{III}X] in conjunction with an ionic organic ammonium salt or a sterically hindered strong organic base allowed for the stereoselective alternating copolymerization of CO_2 and racemic aliphatic epoxides. By using a 7-methyl-1,5,7-triazabicyclo[4.4.0]dec-5-ene (MTBD) cocatalyst with the cobalt catalyst, it was possible to produce poly(propylene carbonates) with a *s*-factor of 5.6, >95% head-to-tail connectivity and >99% carbonate linkages. The same catalytic system was also used for the copolymerization of cyclohexene oxide and CO_2 to produce polycarbonates with an *ee* of 36.6% and greater than 99% carbonate linkages.[78] More recently, Coates and Cohen have reported that a combination of complex **1.17** and bis(triphenylphosphine)iminium chloride (PPNCl) exhibits an *s*-factor of 9.7 for the copolymerization of PO and CO_2 at –20 °C (Scheme 1.15).[79]

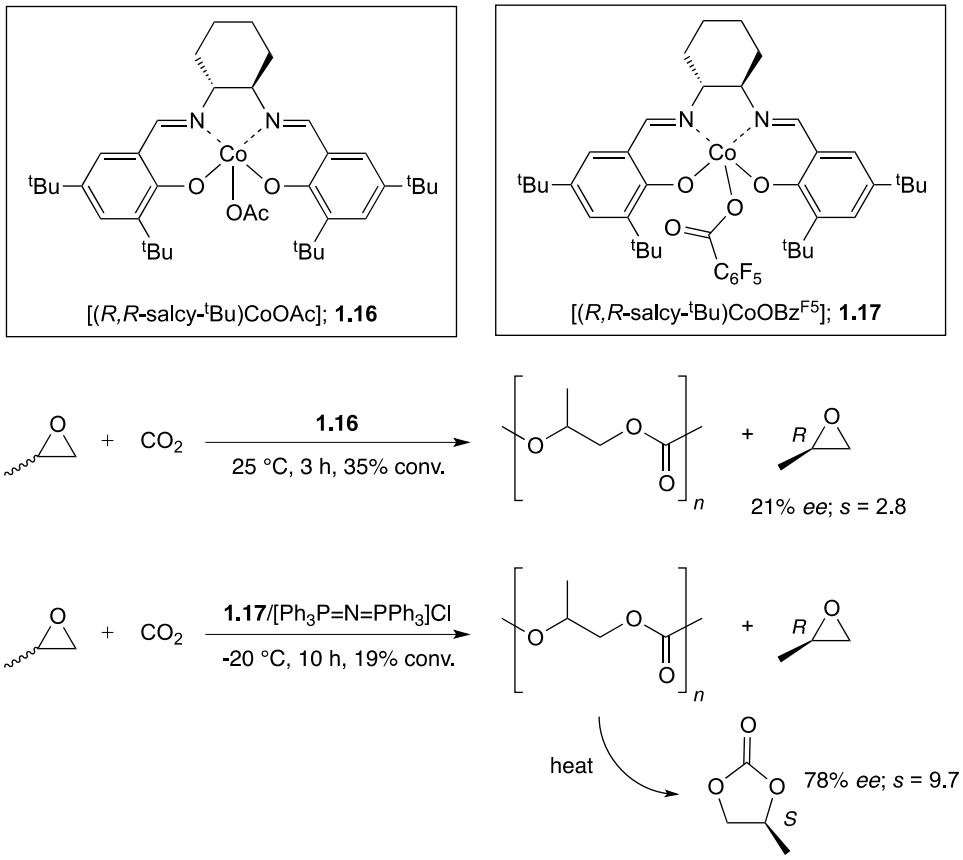

Scheme 1.15. Enantioselective Polymerization of Racemic Propylene Oxide Using **1.16** and **1.17**/[Ph_3PNPPh_3]Cl.

Coates and coworkers also reported the first syndioselective copolymerization of cyclohexene oxide and CO_2 (Scheme 1.16).[80] Using complex [*rac*-(salpr-^{t}Bu)CoBr] (**1.18**), poly(cyclohexene carbonate) was formed with 80% *r*-dyads, as determined by ^{13}C NMR spectroscopy. The carbonyl and methylene regions were best simulated using Bernoullian statistical methods, supporting a chain-end stereochemical control mechanism.

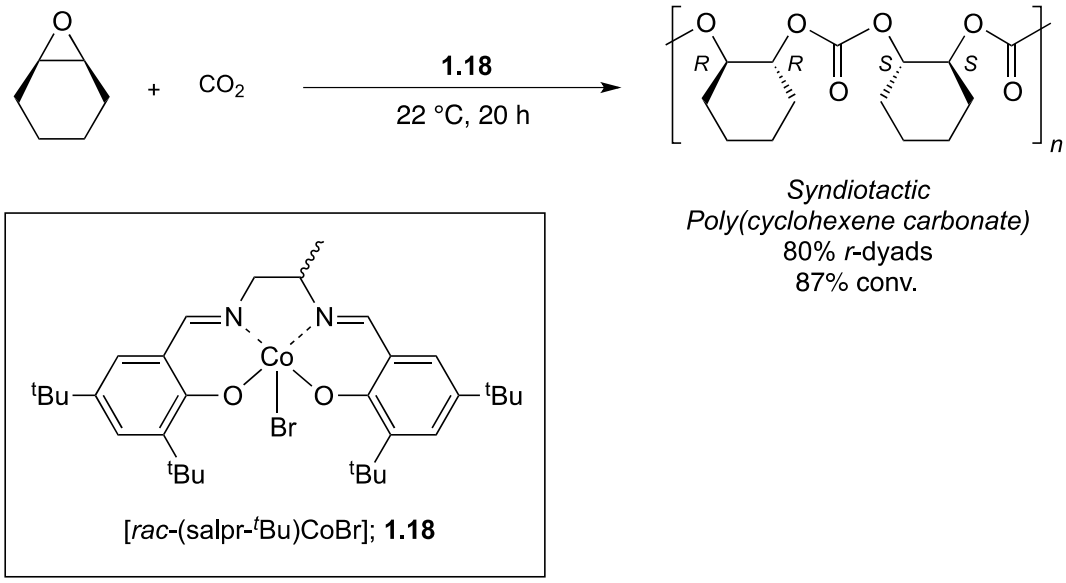

Scheme 1.16. Syndioselective Copolymerization of Cyclohexene Oxide and CO_2 with **1.18**.

The Nozaki group reported cobalt salcy complexes with pendant ammoniums for the synthesis of stereogradient iso-enriched poly(propylene carbonate) from racemic PO and CO_2 (Scheme 1.17).[81] The *s*-factors measured were between 1.1 and 3.5 but complete conversion of monomer was possible with minimal formation of cyclic propylene carbonate by-product. The stereo gradient poly(propylene carbonate) was found to have a higher decomposition temperature (T_d = 281 °C) than its isotactic analogue (T_d = 233 °C) which was attributed to intramolecular stereocomplex formation.

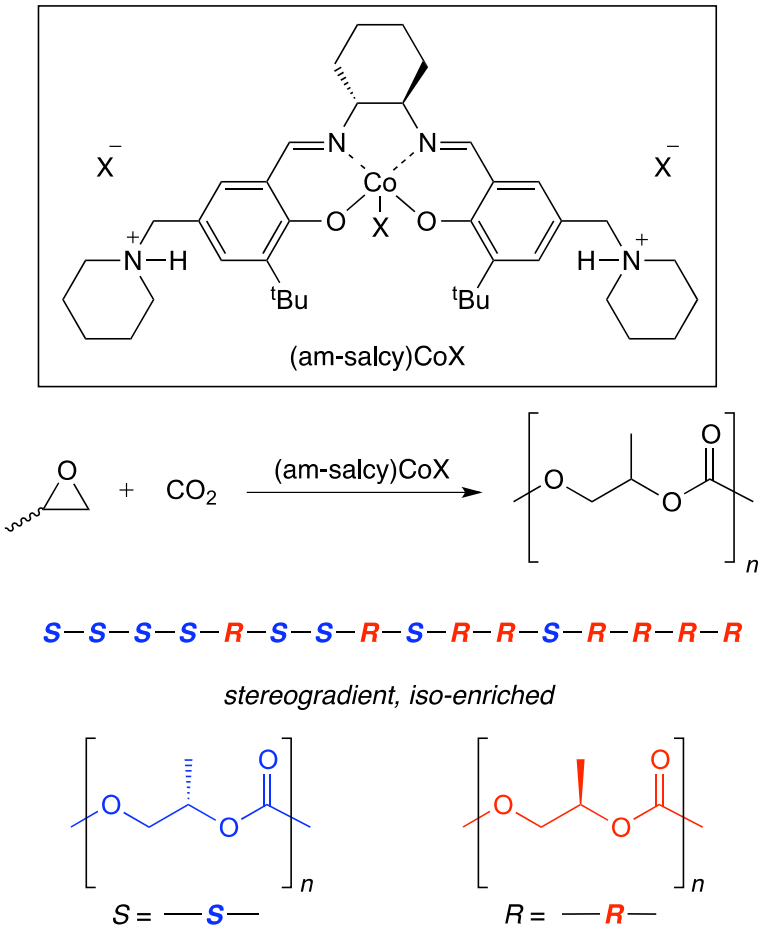

Scheme 1.17. Synthesis of Stereogradient Iso-enriched Poly(propylene carbonate).

Recent stereoselective epoxide homopolymerization systems

In 2005, Coates and coworkers reported a highly active and isoselective (TOF = 220 h^{-1}, *mm* > 99%) cobalt complex, [(salph-^{t}Bu)CoOAc] (**1.19**, Scheme 1.18a) for the polymerization of racemic PO.[82] This is the first example of highly isotactic PPO generation from racemic PO without concomitant atactic byproduct. 1-Butene oxide and 1-hexene oxide, though structurally similar to PO, displayed only trace activity with **1.19**, while all other substituted epoxides screened showed no activity. Though suitable crystals of **1.19** were not obtained, the crystal structure of the methoxide analogue **1.20**, revealed the formation of chiral clefts that are

proposed to facilitate its isoselective nature. Adjacent cobalts were separated by 7.13 Å with the salen planes oriented 52° to each other, as shown in Scheme 1.18b.[83] Studies found that samples of crystalline **1.20** that had been ground mechanically displayed significantly higher activity than unground **1.20**. This large increase in polymerization activity of **1.20** with increased surface area supports that polymerization occurs on the surface of crystalline **1.19** and **1.20**. The supramolecular structure of **1.19** and **1.20** limits any attempts at catalyst optimization through substituent modification due to the inability to accurately predict structural packing, leading to desire for a soluble modular system to synthesize isotactic polyethers.

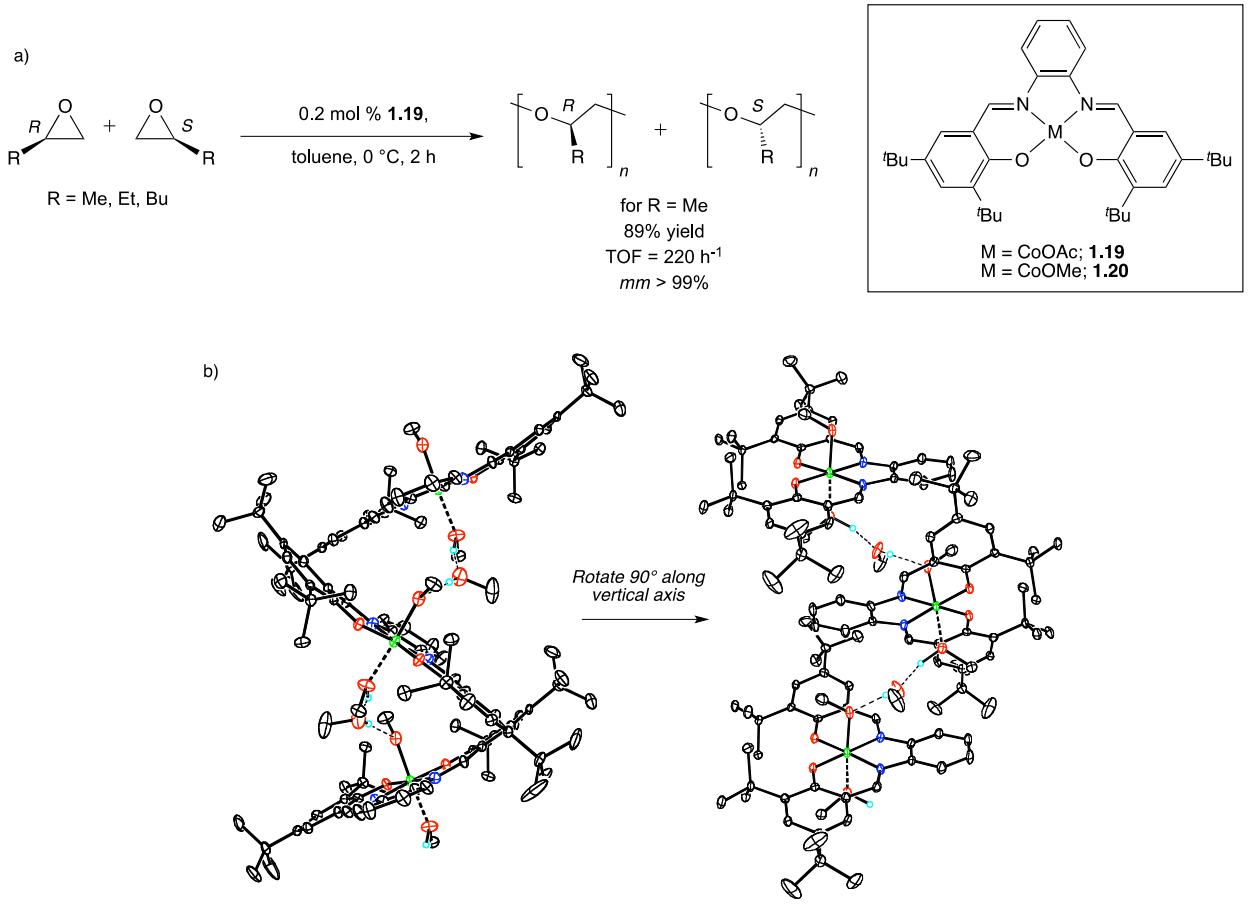

Scheme 1.18. a) Isoselective Polymerization of Propylene Oxide Using **1.19**; b) Molecular Structure of Methoxide Analogue **1.20**.

Mechanistic studies of **1.19** and **1.20** led to the design of the complex **1.21**, which was reported by Coates and coworkers in 2008.[84,85] An axially chiral binaphthol linker covalently oriented the cobalt centers in the appropriate geometry and maintained the ideal distance between metal centers for epoxide polymerization (**Scheme 1.19**). The catalytic system consisting of **1.21** and co-catalyst, [PPN] acetate (OAc), can enantioselectively polymerize PO with *s*-factor greater than 300 and TOF of 5400 h^{-1}. The system displayed enantiomorphic site control as determined by ^{13}C NMR spectroscopy. A variety of monosubstituted racemic monomers including alkyl, glycidyl, vinyl, styrenic, and fluorinated epoxides were shown to be enantioselectively polymerized to form highly isotactic enantiopure polyethers. This left valuable enantiopure epoxides in the starting material with *s*-factors ranging from 20-300. Racemic catalyst was shown to isoselectively polymerize epoxides in quantitative yield at low (0.1 mol%) catalyst loading. Many of the isotactic polyethers synthesized were crystalline unlike their atactic analogs and nearly all had high M_n values.

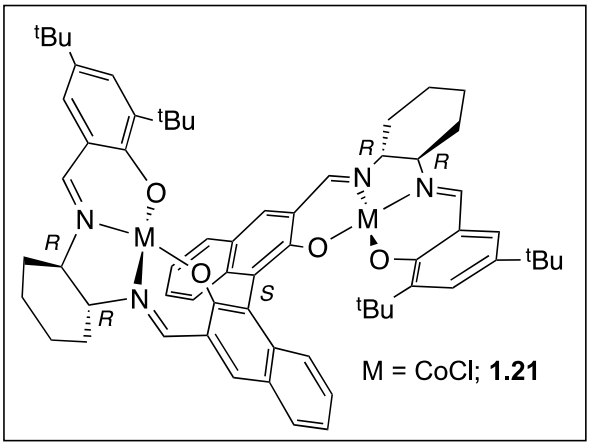

[PPN]OAc = $\left[Ph_3P{=}N{=}PPh_3 \right]^{+}\ ^{-}OAc$

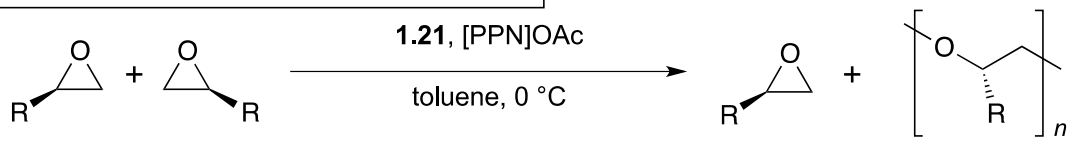

epoxide	TOF (min^{-1})	M_n (kg mol^{-1})	*s*-factor	epoxide	TOF (min^{-1})	M_n (kg mol^{-1})	*s*-factor
	91	26	>300	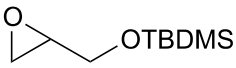	760	140	>70
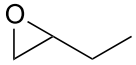	16	61	>300	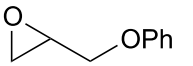	960	130	>70
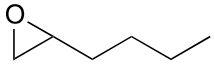	6	77	>100	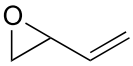	14	79	>20
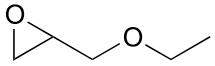	10	8	>50	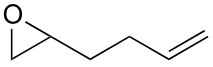	21	46	>300
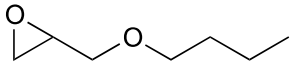	14	33	>50	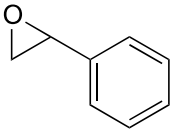	11	50	>70
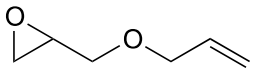	130	110	>100				
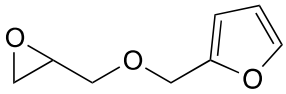	230	69	>80	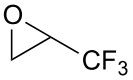	190	20	>300

Scheme 1.19. Enantioselective Polymerization of Epoxides with **1.21**.

Subsequent work developed a simplified isoselective variant of the catalyst (**1.22**) by substituting the cyclohexanediamine bridge for ethylenediamine and using a racemic binaphthol linker (Scheme 1.20).[86] This complex displayed low activity and selectivity for PO polymerization when combined with [PPN]OAc. The identity of the cocatalyst was found to dramatically affect reactivity, the bulkier [PPN] pivalate (OPiv) cocatalyst gave the highest rates and isoselectivities for a broad range of epoxides. This system displays the highest rate reported for highly isoselective PO polymerization (TOF = 1000 h^{-1}) and high tacticity, (*mm* = 97%).

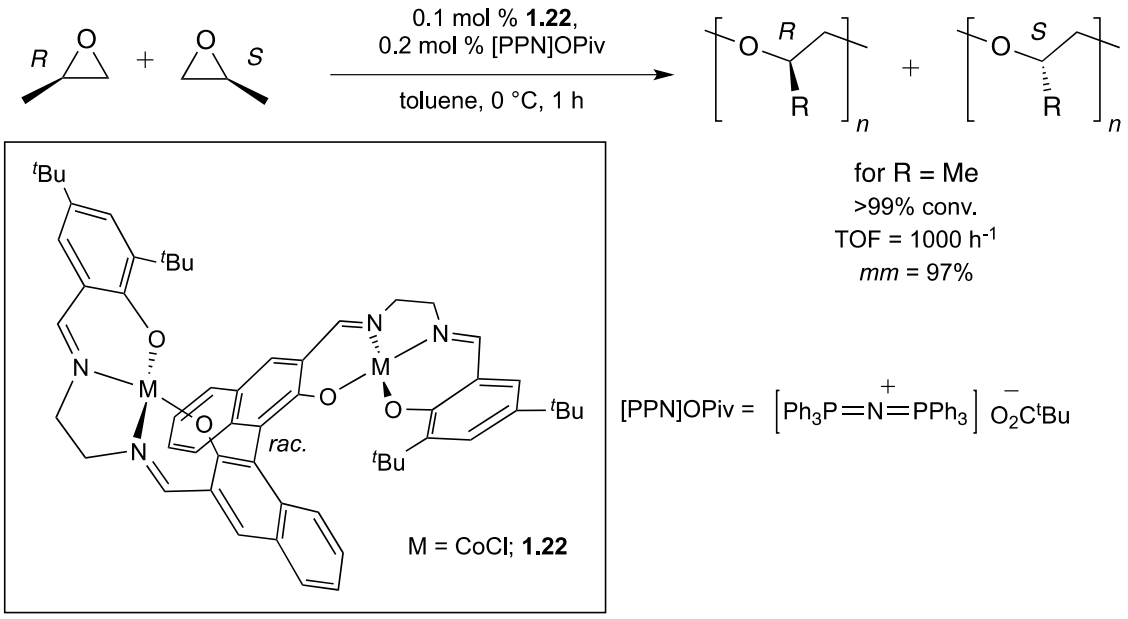

Scheme 1.20. Isoselective Polymerization of Epoxides with **1.22**.

Studies of these bimetallic systems have shown that the axial chirality of the binaphthol linker determines the enantiopreference for epoxide enchainment,[86] rather than the stereochemistry of the diamine, unlike related cobalt salen systems.[39,87] Complexes **1.21** and **1.22**

are currently believed to exist as mixtures of exo/endo chloride diastereomers. Addition of cocatalyst leads to an active anionic complex as shown in Scheme 1.21 where X can be either a chloride or carboxylate. These bimetallic cobalt catalysts display induction periods and poor agreement between theoretical and experimental M_n values likely due to slow initiation relative to propagation. Molecular weight distributions were approximately two, consistent with a single site mechanism.[85]

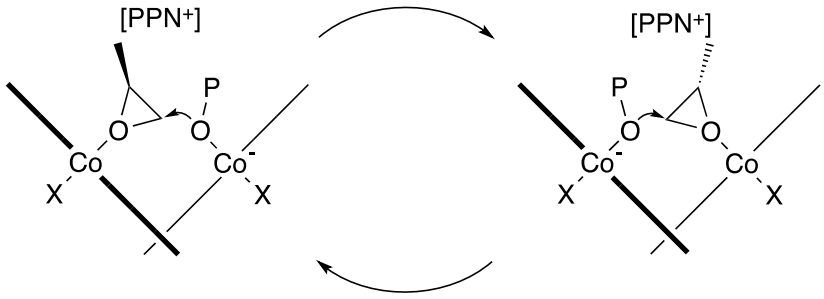

Scheme 1.21. Proposed Mechanism of Polymerization for **1.21** and **1.22**.

1.3.4. Tin-Based Catalysts

In 1993, Nakata and coworkers studied the use of organotin-alkyl phosphate condensates derived from dibutyltin oxide and tributyl phosphate to catalyze the polymerization of PO.[88] They observed that the polymeric product could be fractionated into benzene-hexane soluble and insoluble fractions. On studying the stereoerrors of the product by ^{13}C NMR spectroscopy, they determined that the insoluble fraction was isotactic PPO with 94% *m*-dyads (91% *mm*-triads). A direct correlation was found between increasing the molecular weights of the tin condensate initiators with increasing molecular weight and stereoregularity of the polyethers synthesized. Kragl and coworkers later demonstrated the further use of organotin phosphate coordination polymers to synthesize isotactic PPO.[89] The tin phospate polymers were made by the condensation of tributyl phosphate and butyl tin trichloride (Figure 1.4). PO was polymerized with high activity (TOF = 100 h^{-1}). After fractionation of the polymeric product, 10% was found to be insoluble in acetone and highly isotactic with 88% *m*-dyads. No allyl end groups were detected; these polymerizations have been proposed to undergo a bimetallic mechanism for enchainment.

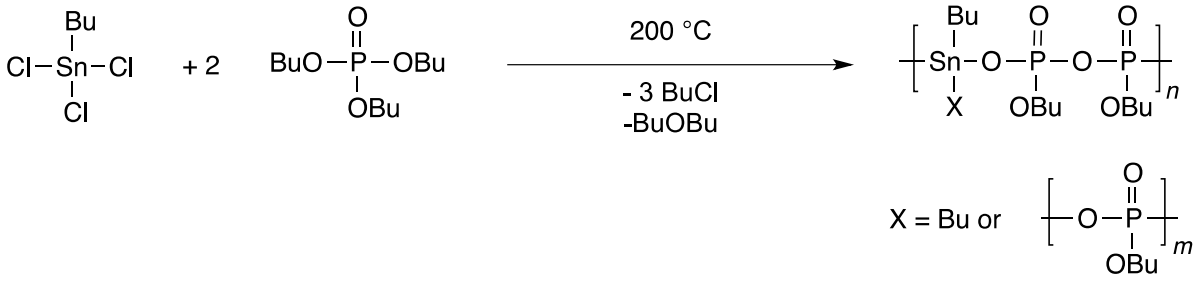

Figure 1.4. Preparation of organotin phosphate condensate catalysts.

1.3.5. Chromium-Based Catalysts

A significant contribution towards developing regioregular polycarbonates has been made by the Lu research group, including developing a saturated salicylaldamine chromium(III) catalyst ([SalanCr(III)], Figure 1.5), which in conjunction with quaternary ammonium salts can produce high molecular weight poly(propylene carbonate) with regiochemical control (>95% head-to-tail linkages) while also displaying moderate enantioselectivity ($2 < s < 8$) depending on the quaternary ammonium cocatalyst used.[90]

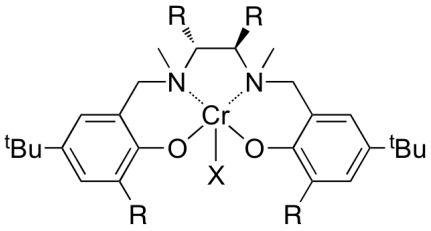

(Salan)Cr(III)

Figure 1.5. Structure of SalanCr(III) complex.

1.4. Outlook and Conclusions

Although significant advances in stereoselective epoxide polymerization have been achieved over the last half-century, only recently have catalysts been developed that are capable of high levels of stereocontrol. Historically, most catalysts for stereoselective epoxide polymerization have been heterogeneous and have exhibited poor selectivity. The current work in the development of well-defined, homogeneous, multimetallic catalysts with controlled spatial orientation of the active catalyst centers could lead to new generations of improved stereoselective epoxide polymerization catalysts. Major frontiers in stereoselective epoxide polymerization have yet to be explored, these include the development of new systems that are: highly stereoselective for epoxide/CO_2 copolymerization, highly selective for polysubstituted epoxide polymerization, stereoselective as well as living allowing for the formation of block copolymers. New catalysts are still needed to accomplish the challenge of synthesizing precisely defined highly tactic polyethers and polycarbonates.

1.5. References

(1) Pruitt, M. E.; Baggett, J. M. US Patent 2706181, 1955.

(2) Pruitt, M. E.; Baggett, J. M.; Bloomfield, R. J.; Templeton, J. H. US Patent 2706182, 1955.

(3) Pruitt, M. E.; Baggett, J. M. US Patent 2706189, 1955.

(4) Booth, C.; Jones, M. N.; Powell, E. *Nature* **1962**, *196*, 772-773.

(5) Natta, G.; Corradini, P.; Dall'Asta, G. *Atti Accad. Naz. Lincei Cl. Sci. Fis. Mat. Nat.* **1956**, *20*, 408-413.

(6) Price, C. C.; Osgan, M. *J. Am. Chem. Soc.* **1956**, *78*, 4787-4792.

(7) Price, C. C.; Osgan, M.; Hughes, R. E.; Shambelan, C. *J. Am. Chem. Soc.* **1956**, *78*, 690-691.

(8) Vandenberg, E. J. *Polymer* **1994**, *35*, 4933-4939.

(9) Spassky, N.; Dumas, P.; Le Borgne, A.; Momtaz, A.; Sepulchre, M. *Bull. Soc. Chim. Fr.* **1994**, *131*, 504-514.

(10) Spassky, N.; Momtaz, A.; Kassamaly, A.; Sepulchre, M. *Chirality* **1992**, *4*, 295-299.

(11) Spassky, N. *Makromol. Chem., Macromol. Symp.* **1991**, *42/43*, 15-49.

(12) Vandenberg, E. J. In *Coordination Polymerization*; Vandenberg, E. J., Price, C. C., Eds.; Plenum Publishing Corp.: New York, 1983, p 11-44.

(13) Tsuruta, T. *Pure Appl. Chem.* **1981**, *53*, 1745-1751.

(14) Spassky, N.; Leborgne, A.; Sepulchre, M. *Pure Appl. Chem.* **1981**, *53*, 1735-1744.

(15) Spassky, N. *ACS Symp. Ser.* **1977**, *59*, 191-209.

(16) Sigwalt, P. *Pure Appl. Chem.* **1976**, *48*, 257-266.

(17) Price, C. C. *Acc. Chem. Res.* **1974**, *7*, 294-301.

(18) Tsuruta, T. *J. Polym. Sci., Part D: Macromol. Rev.* **1972**, *6*, 179-250.

(19) Duda, A. *Polimery* **2004**, *49*, 469-478.

(20) Vandenberg, E. J. *J. Polym. Sci., Polym. Chem. Ed.* **1969**, *7*, 525-567.

(21) Coates, G.; Allen, S.; Ajiro, H. In *Stereoselective Polymerization with Single-Site Catalysts*; CRC Press: Boca Raton, FL, 2007, p 627-644.

(22) Farina, M. *Top. Stereochem.* **1987**, *17*, 1-111.

(23) Schilling, F. C.; Tonelli, A. E. *Macromolecules* **1986**, *19*, 1337-1343.

(24) Le Borgne, A.; Spassky, N.; Jun, C. L.; Momtaz, A. *Makromol. Chem.* **1988**, *189*, 637-650.

(25) Ugur, N.; Alyuruk, K. *J. Polym. Sci., Part A: Polym. Chem.* **1989**, *27*, 1749-1761.

(26) Cheng, H. N. In *Modern Methods of Polymer Characterization*; Barth, H. G., Mays, J. W., Eds.; John Wiley & Sons: New York, 1991, p 409-493.

(27) Bovey, F. A.; Mirau, P. A. *NMR of Polymers*; Academic Press: San Diego, 1996.

(28) Chisholm, M. H.; Navarro-Llobet, D. *Macromolecules* **2002**, *35*, 2389-2392.

(29) Gawley, R. E. *J. Org. Chem.* **2006**, *71*, 2411-2416.

(30) Wu, B.; Harlan, C. J.; Lenz, R. W.; Barron, A. R. *Macromolecules* **1997**, *30*, 316-318.

(31) Vandenberg, E. J. *J. Polym. Sci.* **1960**, *47*, 486-489.

(32) Vandenberg, E. J. US Patent 3135705, 1964.

(33) Vandenberg, E. J. US Patent 3219591, 1965.

(34) Vandenberg, E. J. *J. Polym. Sci., Part B: Polym. Lett.* **1964**, *2*, 1085-1088.

(35) Vandenberg, E. J. *J. Am. Chem. Soc.* **1961**, *83*, 3538-3539.

(36) Vandenberg, E. J. *J. Polym. Sci.* **1960**, *47*, 489-491.

(37) Braune, W.; Okuda, J. *Angew. Chem., Int. Ed.* **2003**, *42*, 64-68.

(38) Moore, D. R.; Cheng, M.; Lobkovsky, E. B.; Coates, G. W. *J. Am. Chem. Soc.* **2003**, *125*, 11911-11924.

(39) Tokunaga, M.; Larrow, J. F.; Kakiuchi, F.; Jacobsen, E. N. *Science* **1997**, *277*, 936-938.

(40) Haubenstock, H.; Panchalingam, V.; Odian, G. *Makromol. Chem.* **1987**, *188*, 2789-2799.

(41) Osgan, M.; Price, C. C. *J. Polym. Sci.* **1959**, *34*, 153-156.

(42) Kasperczyk, J.; Dworak, A.; Jedlinski, Z. *Makromol. Chem., Rapid Commun.* **1981**, *2*, 663-666.

(43) Dworak, A.; Jedlinski, Z. *Polymer* **1980**, *21*, 93-96.

(44) Takeda, N.; Inoue, S. *Makromol. Chem.* **1978**, *179*, 1377-1381.

(45) Aida, T.; Inoue, S. *Macromolecules* **1981**, *14*, 1166-1169.

(46) Aida, T.; Inoue, S. *Macromolecules* **1981**, *14*, 1162-1166.

(47) Vincens, V.; Le Borgne, A.; Spassky, N. *Makromol. Chem., Rapid Commun.* **1989**, *10*, 623-628.

(48) Vincens, V.; Le Borgne, A.; Spassky, N. *Makromol. Chem., Macromol. Symp.* **1991**, *47*, 285-291.

(49) Le Borgne, A.; Vincens, V.; Jouglard, M.; Spassky, N. *Makromol. Chem., Macromol. Symp.* **1993**, *73*, 37-46.

(50) Matsuura, K.; Inoue, S.; Tsuruta, T. *Makromol. Chem.* **1965**, *86*, 316-319.

(51) Kuran, W.; Listos, T.; Abramczyk, M.; Dawidek, A. *J. Macromol. Sci., Pure Appl. Chem.* **1998**, *A35*, 427-437.

(52) Emig, N.; Nguyen, H.; Krautscheid, H.; Reau, R.; Cazaux, J.-B.; Bertrand, G. *Organometallics* **1998**, *17*, 3599-3608.

(53) Furukawa, J.; Tsuruta, T.; Sakata, R.; Saigusa, T.; Kawasaki, A. *Makromol. Chem.* **1959**, *32*, 90-94.

(54) Kuran, W.; Listos, T. *Macromol. Chem. Phys.* **1994**, *195*, 401-411.

(55) Coulon, C.; Spassky, N.; Sigwalt, P. *Polymer* **1976**, *17*, 821-827.

(56) Kassamaly, A.; Sepulchre, M.; Spassky, N. *Polym. Bull. (Berlin)* **1988**, *19*, 119-122.

(57) Sepulchre, M.; Kassamaly, A.; Spassky, N. *Polym. Prepr. (Am. Chem. Soc., Div. Polym. Chem.)* **1990**, *31*, 91-92.

(58) Sepulchre, M.; Kassamaly, A.; Spassky, N. *Makromol. Chem., Macromol. Symp.* **1991**, *42/43*, 489-500.

(59) Ishimori, M.; Hagiwara, T.; Tsuruta, T.; Kai, Y.; Yasuoka, N.; Kasai, N. *Bull. Chem. Soc. Jpn.* **1976**, *49*, 1165-1166.

(60) Tsuruta, T. *J. Polym. Sci., Polym. Symp.* **1980**, *67*, 73-82.

(61) Tsuruta, T. *Macrmol. Chem. Phys., Supp.* **1981**, *5*, 230-233.

(62) Kageyama, H.; Miki, K.; Tanaka, N.; Kasai, N.; Ishimori, M.; Heki, T.; Tsuruta, T. *Makromol. Chem., Rapid Commun.* **1982**, *3*, 947-951.

(63) Hasebe, Y.; Tsuruta, T. *Makromol. Chem.* **1988**, *189*, 1915-1926.

(64) Yoshino, N.; Suzuki, C.; Kobayashi, H.; Tsuruta, T. *Makromol. Chem.* **1988**, *189*, 1903-1913.

(65) Tsuruta, T. *Makromol. Chem., Macromol. Symp.* **1991**, *47*, 277-283.

(66) Tsuruta, T.; Hasebe, Y. *Macromol. Chem. Phys.* **1994**, *195*, 427-438.

(67) Tsuruta, T. *Makromol. Chem., Macromol. Symp.* **1986**, *6*, 23-31.

(68) Kageyama, H.; Kai, Y.; Kasai, N.; Suzuki, C.; Yoshino, N.; Tsuruta, T. *Makromol. Chem., Rapid Commun.* **1984**, *5*, 89-93.

(69) Hasebe, Y.; Tsuruta, T. *Makromol. Chem.* **1987**, *188*, 1403-1414.

(70) Hasebe, Y.; Izumitani, K.; Torii, M.; Tsuruta, T. *Makromol. Chem.* **1990**, *191*, 107-119.

(71) Nozaki, K.; Nakano, K.; Hiyama, T. *J. Am. Chem. Soc.* **1999**, *121*, 11008-11009.

(72) Nakano, K.; Nozaki, K.; Hiyama, T. *Macromolecules* **2001**, *34*, 6325-6332.

(73) Cheng, M.; Darling, N. A.; Lobkovsky, E. B.; Coates, G. W. *Chem. Commun.* **2000**, 2007-2008.

(74) Nakano, K.; Nozaki, K.; Hiyama, T. *J. Am. Chem. Soc.* **2003**, *125*, 5501-5510.

(75) Tezuka, Y.; Ishimori, M.; Tsuruta, T. *Makromol. Chem.* **1983**, *184*, 895-906.

(76) Qin, Z. Q.; Thomas, C. M.; Lee, S.; Coates, G. W. *Angew. Chem., Int. Ed.* **2003**, *42*, 5484-5487.

(77) Lu, X. B.; Wang, Y. *Angew. Chem., Int. Ed.* **2004**, *43*, 3574-3577.

(78) Lu, X.-B.; Shi, L.; Wang, Y.-M.; Zhang, R.; Zhang, Y.-J.; Peng, X.-J.; Zhang, Z.-C.; Li, B. *J. Am. Chem. Soc.* **2006**, *128*, 1664-1674.

(79) Cohen, C.; Coates, G. W. *J. Poly. Sci. Part A* **2006**, *44*, 5182-5191.

(80) Cohen, C.; Thomas, C.; Peretti, K.; Lobkovsky, E.; Coates, G. *Dalton Trans.* **2006**, 237-249.

(81) Nakano, K.; Hashimoto, S.; Nakamura, M.; Kamada, T.; Nozaki, K. *Angew. Chem., Int. Ed.* **2011**, *50*, 4868-4871.

(82) Peretti, K.; Ajiro, H.; Cohen, C.; Lobkovsky, E.; Coates, G. *J. Am. Chem. Soc.* **2005**, *127*, 11566-11567.

(83) Ajiro, H.; Peretti, K. L.; Lobkovsky, E. B.; Coates, G. W. *Dalton Trans.* **2009**, 8828-8830.

(84) Hirahata, W.; Thomas, R. M.; Lobkovsky, E. B.; Coates, G. W. *J. Am. Chem. Soc.* **2008**, *130*, 17658-17659.

(85) Thomas, R. M.; Widger, P. C. B.; Ahmed, S. M.; Jeske, R. C.; Hirahata, W.; Lobkovsky, E. B.; Coates, G. W. *J. Am. Chem. Soc.* **2010**, *132*, 16520-16525.

(86) Widger, P. C. B.; Ahmed, S. M.; Hirahata, W.; Thomas, R. M.; Lobkovsky, E. B.; Coates, G. W. *Chem. Commun.* **2010**, *46*, 2935-2937.

(87) Cohen, C. T.; Coates, G. W. *J. Polym. Sci., Part A: Polym. Chem.* **2006**, *44*, 5182-5191.

(88) Miura, K.; Kitayama, T.; Hatada, K.; Nakata, T. *Polym. J.* **1993**, *25*, 685-696.

(89) Schütz, C.; Dwars, T.; Schnorpfeil, C.; Radnik, J.; Menzel, M.; Kragl, U. *J. Polym. Sci., Part A: Polym. Chem.* **2007**, *45*, 3032-3041.

(90) Li, B.; Wu, G.-P.; Ren, W.-M.; Wang, Y.-M.; Rao, D.-Y.; Lu, X.-B. *J. Polym. Sci., Part A: Polym. Chem.* **2008**, *46*, 6102-6113.

Chapter 2

Mechanistic Insight into the Enantioselective Polymerization of Epoxides Using a Bimetallic Cobalt Catalyst

2.1. Introduction

Polyethers are an important class of polymers used in various commodity materials such as foams, sealants, elastomers, surfactants, and biomedical components.[1] The development of advanced products using these polymers necessitates new and improved methods to control their thermal and mechanical properties. This challenge requires precise control over the regio- and stereoselective manner in which monomers are enchained during polymerization. Unfortunately, little to no regio- or stereocontrol is attained using traditional anionic, cationic and metal-mediated methods for polyether synthesis.[2]

In 1955, Pruitt and Baggett reported that iron (III) chloride catalyzes the polymerization of propylene oxide (PO) to form small amounts of stereoregular (isotactic) polypropylene oxide (PPO).[3] This important discovery led to the development of various catalysts that produced mixtures of isotactic and atactic polyethers.[4,5] The isotacticity was traditionally induced by the chiral environment around the propagating metal center, or with the use of chiral reagents.[2] Tsuruta was the first to postulate the idea that stereocontrol could be achieved using catalysts with enantiomorphic catalytic sites that reacted with only one enantiomer of epoxide for enchainment.[6] The use of well-defined zinc catalysts with *R* and *S* catalytic sites prepared moderately isotactic PPO, supporting Tsuruta's hypothesis for the source of stereocontrol.[7] Studies conducted by Vandenberg and Teyssie on bimetallic aluminum-zinc μ–oxoalkoxide catalysts led to a conjecture that stereoselective epoxide enchainment involved at least two metal centers.[8,9] The proposed bimetallic mechanism required an epoxide molecule to coordinate to one of the metal centers prior to nucleophilic attack by the propagating polyether chain bound to the adjacent metal. Okuda *et al*. later tested this mechanistic hypothesis by using a discrete

catalyst comprising a bisphenolatoaluminum and a corresponding aluminate complex to synthesize highly regioregular PPO.[10] Despite the many advances in this field, the scope of useful substrates remained limited, and it was still not possible to synthesize highly isotactic polyethers without stereoerrors.[2b]

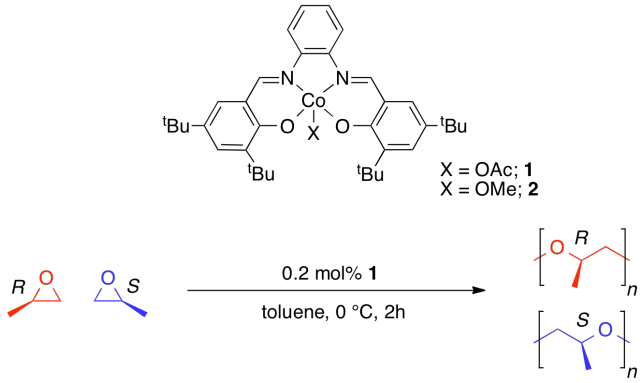

Figure 2.1. Stereoselective polymerization of propylene oxide using a highly active *salen*-based cobalt catalyst, **1**.

In 2005, we reported a highly active cobalt catalyst (**1**; Figure 2.1) for the stereoselective polymerization of racemic PO, exclusively producing regioregular and highly isotactic PPO with triad content (*mm*) >99%.[11] Complex **1** was limited in substrate scope, but polymerized butene oxide in high yields (*mm* >99%), and yielded trace amounts of isotactic poly(hexene oxide). X-ray analysis of single crystals of the methoxide derivative (**2**; Figure 2.1) revealed the presence of chiral clefts that we postulate are responsible for the stereoselective nature of the catalyst.[12] The Co centers were separated by an average distance of 7.13Å and were locked in a rigid geometry by the orientation of the *salen* planes. The heterogenous nature of the catalyst, and inability to predict the solid-state packing of complexes made it difficult to improve catalyst performance by rational ligand modification, thus leading to the development of a discrete

bimetallic complex mimicking the structural features seen in the unit cell of the crystal structure of **2**.

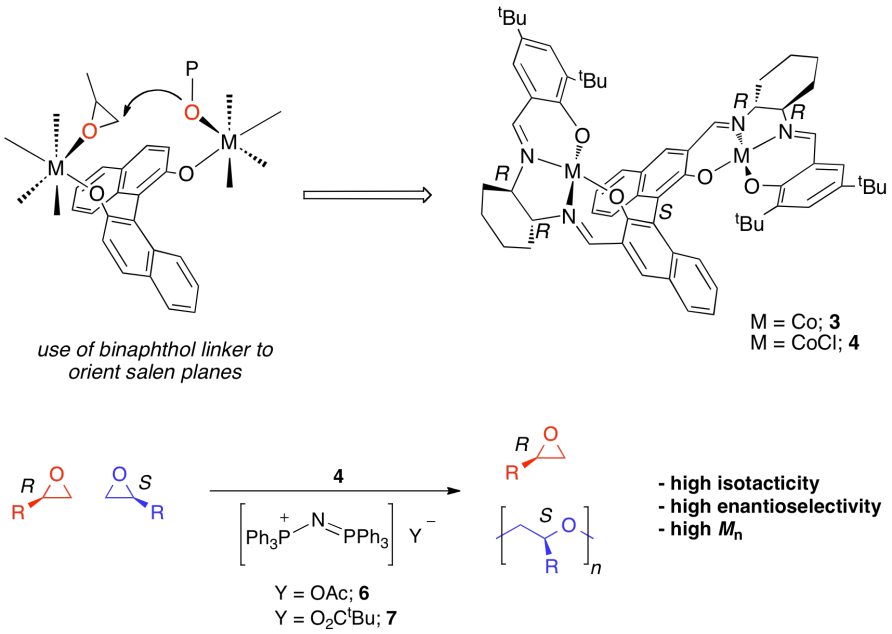

Figure 2.2. Enantioselective polymerization of epoxides using a bimetallic cobalt (III) catalyst.

The bimetallic cobalt (III) complex (**4**; Figure 2.2) was prepared by tethering optically pure *salen* moieties with a chiral binaphthol, achieving a favorable Co—Co distance for epoxide enchainment[12] and almost perpendicular orientation of the *salen* planes.[13] In the presence of a cocatalyst, **4** enantioselectively polymerizes racemic epoxides to prepare highly isotactic polyethers and enantiopure epoxides.[13-14] The catalyst selectively enchains the *S* enantiomer of monosubstituted epoxides by an enantiomorphic site control mechanism, enriching the starting material in the unreacted *R* enantiomer. Therefore, the use of **4** not only allows access to a variety of novel stereoregular macromolecules with potential commercial applications,[1] but also prepares important chiral building blocks.[15] Complex **4** was subsequently used to

enantioselectively polymerize a series of monosubstituted epoxides with high selectivity factors (*s*-factor) that ranged from 50 to 300.[14]

Synthesis of the diastereomer of **4** with all *S* chirality (**5**; Figure 2.3) showed that enantioselectivity was predominantly determined by the axial chirality of the binaphthol linker.[16] Crystal structures of the tetrapyridine adducts of **4**[14] and **5** were obtained, exhibiting similar catalytic clefts and Co—Co distances.

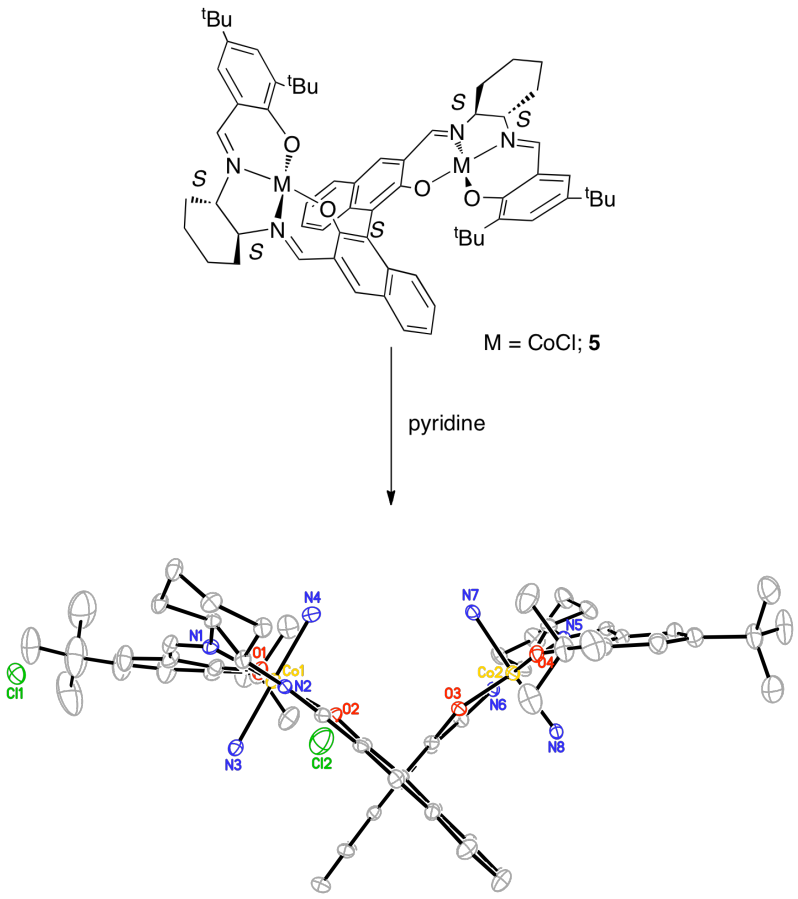

Figure 2.3. Complex **5** and corresponding crystal structure of its tetrapyridine adduct (hydrogen atoms were omitted and pyridine ligands truncated for clarity; thermal ellipsoids are at 30% probability level; Co—Co distance = 6.94Å).

Complex **4** displays high activity for enantioselective polyether synthesis in the presence of a bis(triphenylphosphine)iminium (PPN), phosphonium or phosphazenium cocatalyst salt.[13-14,16-17] Previous reports show that phosphazenium and PPN salts with a pivalate anion display the highest activity and selectivity for epoxide polymerization to date.[17] Since the cocatalyst used

drastically affects the reactivity of the catalyst, we propose it plays a major role in epoxide enchainment and catalyst activation.

As **4** was the first catalyst that polymerized a variety of racemic epoxides to form highly isotactic polyethers, we were interested in elucidating the mechanism of polyether formation in this system. The paramagnetism of the catalyst, short reaction times, exothermic nature of the reactions, observed induction periods, and precipitation of polyether during polymerization made it extremely difficult to attain reliable kinetic data or observe intermediates.[13-14,16-17] In this report, we propose a mechanistic hypothesis for the polymerization of monosubstituted epoxides by **4** based on experimental observations and theoretical calculations. Considering the complex and multi-faceted nature of the catalyst system, we attempt to elucidate the mechanism of polyether synthesis by focusing on four key aspects: (1) structural features of the catalyst, (2) the probable oxidation state of Co during the polymerization, (3) the role of the cocatalyst, and (4) calculated energy profiles for the polymerization.

2.2. Results and Discussion

2.2.1. Structural Features of the Catalyst

The architecture of complex **4** emphasized the simulation of a chiral cleft via careful orientation of *salen* planes, while maintaining Co—Co distances that would be favorable for epoxide polymerization. X-ray crystal structure analysis of a tetrapyridine adduct of **4** exhibited an endo naphthol-naphthol dihedral angle of 79° and Co—Co distances of approximately 6.45Å.[14] This arrangement potentially encourages polyether synthesis by coordination of an epoxide to one Co center inside the cleft, while the neighboring Co provides a propagating polyether alkoxide.[12] We believe these structural features are important for epoxide polymerization since the monometallic *salen*-Co(III) complex (**8**; Figure 2.4) does not polymerize PO under our standard polymerization conditions.[18]

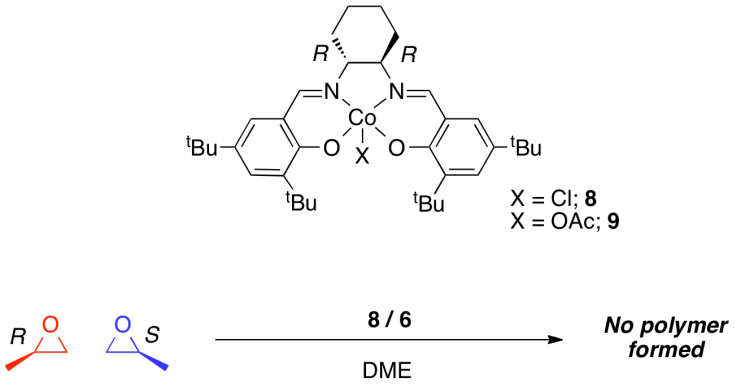

Figure 2.4. Polymerization of racemic PO with *salen*-Co(III) complex.

We hypothesize that in solution, **8** does not achieve the correct geometry to facilitate enchainment of epoxide from the Co centers due to steric hindrance caused by the polyether

alkoxide. To support the hypothesis that the *salen* moieties must be in close proximity and in the correct orientation for polymerization to take place, we synthesized complex **10** (Figure 2.5) by linking two *salen* moieties with an achiral biphenol. The use of a biphenol linker maintains Co adjacency and permits formation of *R* or *S* catalytic clefts via rotation about the biphenol bond. In agreement with our hypothesis, the use of **10** with **6** (from Figure 2.2) resulted in the formation of isotactic PPO (*mm* >87%). DFT calculations were then conducted to further investigate the importance of having two metal centers, the effect of the catalytic cleft, and their subsequent influences on regio- and stereoselectivity in the catalyst system.

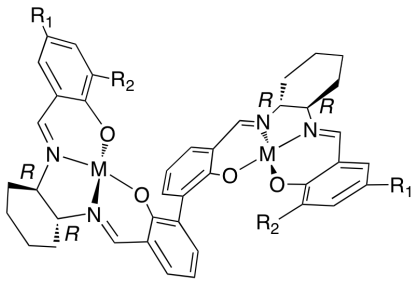

M = CoCl, $R_1 = R_2 = {}^t$Bu; **10**
M = CoCl, R_1 = H, $R_2 = {}^t$Bu, *S* axial chirality; **11***
M = CoCl, $R_1 = R_2$ = H, *S* axial chirality; **12***

Figure 2.5. Bimetallic Co(III) complexes with biphenol linkers. (*model complexes used for calculation purposes).

The model catalyst used for DFT calculations was similar to **10**, but had *S* axial chirality and no *para*–salicyl substituent (R_1= H, $R_2 = {}^t$Bu, **11**; Figure 2.5). In the model, a PO molecule is coordinated to one of the Co centers inside the catalytic cleft of **11**, and ring opened by a methoxide (OMe) molecule coordinated to the adjacent Co. The four transition states shown in Figure 2.6 display the different possibilities for nucleophilic attack at the methylene (1,2-addition) or methine carbon (2,1-addition) of each PO enantiomer.[19] Calculations show that the

favored transition state corresponds to 1,2-addition of the *S*-PO molecule (**TS-1,2-*S***; Figure 2.6A). This agrees with experimental findings using **4**, where *S*-epoxide is preferentially enchained with conservation of stereochemistry at the chiral methine carbon.[13-14,16] The transition state corresponding to the 1,2-addition of *R*-PO (**TS-1,2-*R***; Figure 2.6B) is 4.6 kcal/mol higher in energy relative to **TS-1,2-*S***, in agreement with the exceptional stereoselectivity of the catalyst. The energy difference between **TS-1,2-*R*** and the favored **TS-1,2-*S*** is represented by the term ΔE_{Stereo}. Similarly, ΔE_{Regio} represents the energy difference between transition states for the 2,1-addition of *S*- or *R*-PO (**TS-2,1-*S*** and **TS-2,1-*R***; Figure 2.6C and 2.6D) and the favored **TS-1,2-*S***. ΔE_{Regio} values for **TS-2,1-*S*** and **TS-2,1-*R*** are 3 and 4.5 kcal/mol respectively.

Calculations were also conducted using **4** as a model, and revealed that ΔE_{Stereo}(**TS-1,2-*R***) = 4.7 kcal/mol while ΔE_{Regio}(**TS-2,1-*S***) = 3.2 kcal/mol. Although the calculations imply that **4** should be less regioselective than stereoselective (ΔE_{Regio}(**TS-2,1-*S***) < ΔE_{Stereo}(**TS-1,2-*R***)), no regioerrors are observed by ^{13}C NMR spectroscopy of synthesized polyethers.[13-14] Since the calculated energy differences between **4** and **11** were fairly small, the model system **11** was used in the remaining calculations.

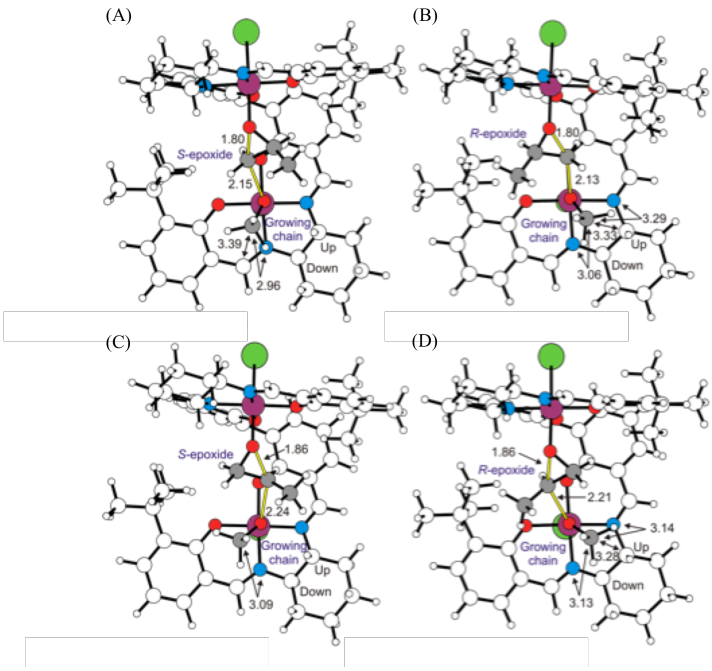

Figure 2.6. Four possible transition states for the ring opening of a PO molecule by methoxide in complex **11**: (A) **TS-1,2-*S***: ring opening of *S*-PO at the methylene carbon; (B) **TS-1,2-*R***: ring opening of *R*-PO at the methylene carbon; (C) **TS-2,1-*S***: ring opening of *S*-PO at the methine carbon; (D) **TS-2,1-*R***: ring opening of *R*-PO at the methine carbon.

In the transition states shown (Figure 2.6), no steric interactions were observed between the PO coordinated to the Co center and the ligand framework. Rather, large steric interactions were found between the catalyst ligand and growing polymer chain, represented here by the methyl group of OMe. In **TS-1,2-*S*** and **TS-2,1-*S***, the methyl group of OMe orients itself such that interactions with the ligand are minimized, whereas in **TS-1,2-*R*** and **TS-2,1-*R***, the methyl group experiences large steric interactions with the ligand *salen* moiety. These steric interactions between the propagating chain and ligand framework potentially explain the difference in selectivities and activities observed when (1*S*, 2*S*)-diaminocyclohexane or ethylenediamine are used to substitute (1*R*, 2*R*)-diaminocyclohexane in the ligand framework.[16]

The importance of the catalyst cleft was also studied using complex **11**. The dihedral angle (ϕ) of the biphenyl unit was varied, and corresponding energy values for **TS-1,2-*S*** and **TS-1,2-*R*** (Figure 2.6A and 2.6B) were calculated. Figure 2.7A indicates that the ideal ϕ value for epoxide polymerization is approximately 70°. Further calculations show that variations between 60° to 80° cost a penalty lower than 1 kcal/mol, implying that some flexibility of rotation is permitted about the bridging naphthol bond to accomodate coordination of epoxide, and polyether propagation (*vide infra*). The ΔE_{Stereo} values reported (Figure 2.7A) were normalized with respect to the energy of the most favored transition state, **TS-1,2-*S*** at ϕ = 70°. Similar ΔE_{Stereo} trends are observed for **TS-1,2-*S*** and **TS-1,2-*R***, with energy levels for the latter being relatively higher. The fall and rise of energy levels for the transition states upon adjusting ϕ highlights the importance of the catalyst cleft and the orientation of *salen* planes.

Further calculations were conducted using **4** as a model and showed that at the most favorable transition state **TS-1,2-*S***, ϕ = 75.8° and Co—Co distance was calculated to be 6.29Å (Figure 2.7B). These measurements are similar to those attained for the crystal structure of the tetrapyridine adduct of **4**.[14]

Overall, the experimental and theoretical results highlight the importance of the structural features of the catalyst, and also help explain the high stereoselectivity observed in the system.

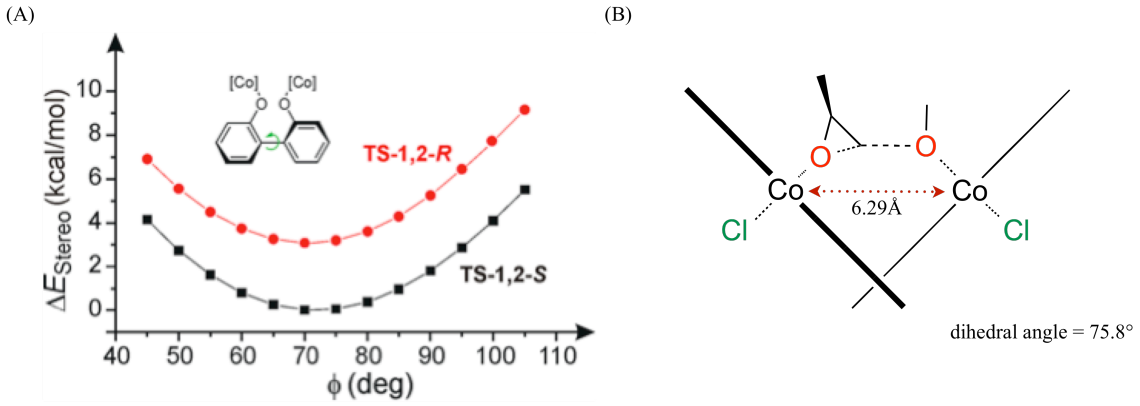

Figure 2.7. (A) Effect of varying dihedral angle; (ϕ) on ΔE_{Stereo} values, normalized with respect to lowest energy for favored **TS-1,2-*S*** at ϕ = 70°; (B) Side view of **TS-1,2-*S*** for catalyst **4**.

2.2.2. The Oxidation State of Co in the Catalyst

In order to elucidate the mechanism of epoxide enchainment, we considered the possible oxidation states of Co during polymerization. The crystal structures of the tetrapyridine adducts of **4** and **5** display two pyridine molecules coordinated to each Co and a respective chloride anion in close proximity of the metal centers.[14] The complexes were also diamagnetic in pyridine-d_5,[14,16] consistent with a bimetallic Co(III)-Co(III) complex. Although this data suggested +3 oxidation states of Co in the starting material, it did not eliminate the possibilities of having a Co(II)-Co(II) species generated by the reduction of the starting material (Figure 2.8) or a Co(II)-Co(III) species generated via radical mechanism during the course of the polymerization.

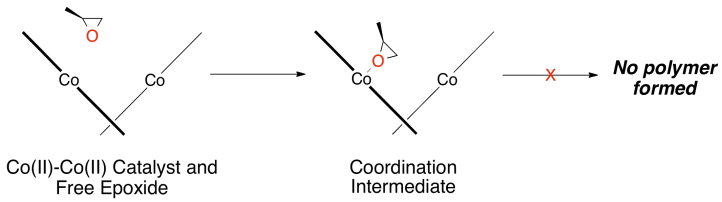

Figure 2.8. Reaction of PO with a Co(II)-Co(II) bimetallic catalyst, **3**.

The bimetallic Co(II) catalyst (**3**; Figure 2.2) was inactive for the polymerization of PO under standard reaction conditions. As shown in Figure 2.8, a PO molecule can coordinate to a Co center of **3**, but the absence of eligible alkoxide or halide nucleophiles on the adjacent metal center eliminates possibilities for propagation. Therefore, it seems unlikely that Co(II)-Co(II) oxidation states are involved in the polymerization.

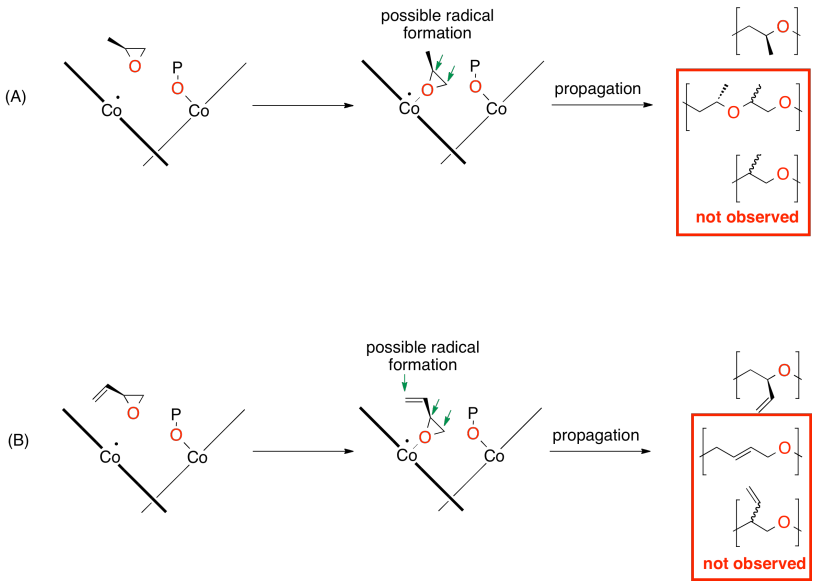

Figure 2.9. Possible mechanisms of epoxide polymerization using a Co(II)-Co(III) complex: (A) Polymerization of PO; (B) Polymerization of 3,4-epoxy-1-butene and potential polyether products.

The possibility of a mixed valence Co(II)-Co(III) species catalyzing the polymerization was also explored. This mechanism requires generation of a Co radical and enchainment of epoxide through a radical mechanism.[20,21] As shown in Figure 2.9A, radical formation in PO is possible at the methine and methylene carbons, resulting in enchainment at both positions producing regio- and stereoirregular PPO. Furthermore, the polymerization of 3,4-epoxy-1-butene by a Co(II)-Co(III) species would produce different regio/stereoisomers of poly-3,4-epoxy-1-butene (Figure 2.9B). ^{13}C NMR spectroscopy of PPO and poly-3,4-epoxy-1-butene synthesized using **4** provided no evidence for regioerrors or regio/stereoisomers,[14] thus eliminating the possibility of Co(II)-Co(III) oxidation states in the catalyst.

Since the intermediacy of Co(II)-Co(II) and Co(II)-Co(III) oxidation states appears unlikely based on the experimental findings, we propose that the catalyst exists as a Co(III)-Co(III) species throughout the reaction as observed in the starting material.

2.2.3. Role of the Cocatalyst

Cocatalysts have historically played an important role in the polymerization and copolymerization of epoxides by enhancing catalyst activity and enabling milder reaction conditions.[22] It is only in the presence of an ionic cocatalyst that complex **4** displays exceptional activity for the formation of highly isotactic polyethers. The ionic cocatalyst preferably contains a noncoordinating and unreactive cation, and an anion that can serve as a strong axial donor.[16-17] Previous reports show that axial donors drastically influence the rate and reactivity of related Co(III) *salen* complexes for epoxide hydrolysis and polymerization.[22a-b,23-24]

Based on previous success using PPN salts as cocatalysts for epoxide/CO_2 copolymerization,[22a] we used PPN acetate (**6**; Figure 2.2) with **4** for epoxide polymerization. Matrix-assisted laser desorption ionization (MALDI) mass spectrometry identified chloride and acetate functionalities on the polyether end groups, suggesting that the end groups can come from either catalyst or cocatalyst. The activity and selectivity of the catalyst was later enhanced using PPN pivalate (**7**; Figure 2.2),[16] and phosphazenium cocatalyst salts.[17] When combined with **4**, the phosphazenium cocatalysts generally displayed activities and selectivities much higher than those attained using PPN salts, but their use makes it difficult to stop reactions at reasonable conversions, increasing the errors associated with measuring conversion of epoxides and

calculating *s*-factors.[25] Therefore, we used **6** and **7** as cocatalysts while investigating their role in the polymerization system.

In order to understand the interaction of the cocatalyst with **4**, we used model Co complexes, *salen*-Co(III) chloride and *salen*-Co(III) acetate (**8** and **9** respectively; Figure 2.4). Complexes **8** and **9** are distinguishable by UV-Vis spectrometry[26] and have maximum absorbances at 362nm and 420nm respectively. **6** was titrated into a solution of **8**, and the maximum absorbance shifted from 362nm to 420nm (Figure 2.10). These results indicate that anion exchange is taking place in the presence of **6**, which is in agreement with previous reports for preparing *salen*-Co(III) complexes.[23]

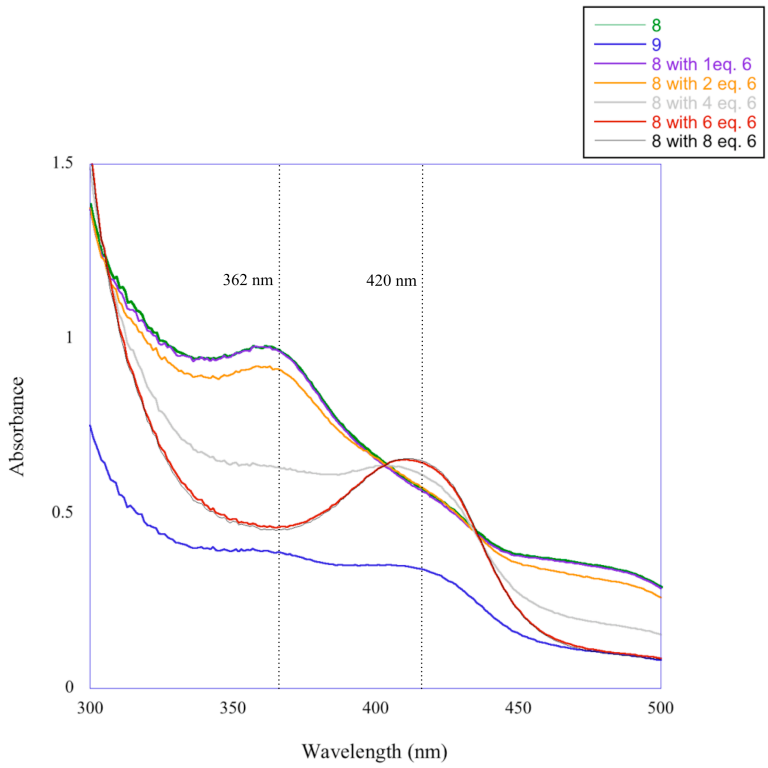

Figure 2.10. UV-Vis spectra attained from titration of **6** with **8** in methylene chloride.

After confirming that anion exchange occurs between **8** and the cocatalyst under conditions similar to those of the polymerization, we investigated the influence of the cocatalyst on the polymerization by varying the catalyst to cocatalyst ratio used in the polymerization system. The more active cocatalyst **7** was used with **4** for this study.[16] The results are shown in Table 2.1.

Table 2.1. Polymerization of PO varying catalyst to cocatalyst ratios.

entry	**4**:**7**	conv.[b] (%)	*mm*[c] (%)	$ee_{(P)}$[d] (%)	M_n[e] (kg/mol)	M_w/M_n[e]	*s*-factor[f]
1	1:1	10	99.1	99.4	43.6	3.5	>300
2	1:2	25	98.8	99.1	126	2.3	>300
3	1:4	30	98.6	99.1	106	2.4	>300
4[g]	1:4	21	97.0	98.0	270	2.2	120

[a] Polymerization conditions: [PO] = 1 M in DME; PO:**4** = 20,000:1; t_{rxn}= 10 mins; T_{rxn} = 0 °C. [b] Determined gravimetrically. [c] Determined by ^{13}C NMR spectroscopy. [d] Calculated using: $ee_{(P)} = (2[mm] + [mr] + [rm] - 1)^{1/2}$. [e] Determined by gel-permeation chromatography calibrated with polystyrene standards in tetrahydrofuran at 30 °C. [f] Calculated using: *s*-factor = $\ln[1 - c(1 + ee_{(P)})]/\ln[1 - c(1 - ee_{(P)})]$, where *c* is conversion of PO. [g] Reaction was conducted in neat PO; PO:**4** = 160,000:1; t_{rxn} = 5 mins.

The change in catalyst to cocatalyst ratio does not have a drastic effect on the isotacticity of the polyether product or the selectivity of the catalyst (Table 2.1, entry 1-3). Greater than 1 eq. of cocatalyst achieved higher turnovers, producing polyethers with higher average molecular weights (M_n) and narrower molecular weight distributions (M_w/M_n). This suggests that the presence of excess cocatalyst facilitates faster initiation, producing greater amounts of product with lower M_w/M_n values.

To test the limits of the polymerization, PO was polymerized at extremely low catalyst loadings (PO:**4** = 160,000:1; run in neat PO) in the presence of 4 eq. cocatalyst, producing highly

isotactic PPO with high M_n values and *s*-factors >100 (Table 2.1, entry 4). The TOF is estimated to be 7200 min^{-1}, which we believe is a lower limit of the calculated value. Attaining accurate TOF data is difficult due to the induction period, viscosity changes during polymerization, decrease in the concentration of *S*-PO, and deactivation of catalyst by trace impurities at very low catalyst loadings.

We propose that in solution, complex **4** exists as exo-exo, exo-endo, and endo-endo diastereomers that are in dynamic equilibrium (Figure 2.11). Calculations predict that the exo-endo species is 1.4 kcal/mol higher in free-energy (ΔG) relative to the exo-exo, whereas the endo-endo is 2.8 kcal/mol higher. Considering the anion-exchange experiments, the cocatalyst may facilitate exchange of axial ligands inside and outside the cleft, resulting in faster interconversion of the three diastereomers, as shown in Figure 2.11. Only two of the three conformations, the exo-exo and exo-endo, are potentially active catalyst species as they have open coordination sites for epoxide inside the catalyst cleft. Once an epoxide coordinates to a Lewis acidic cobalt center inside the cleft, the cocatalyst anion can facilitate initiation to form an alkoxide. In correlation to the results seen in Table 2.1, where increasing the amount of cocatalyst increases turnovers and decreases M_w/M_n, we hypothesize that anion exchange between catalyst and cocatalyst facilitates generation of a potentially active diastereomer of the catalyst and initial ring opening, thus increasing the rate of initiation.

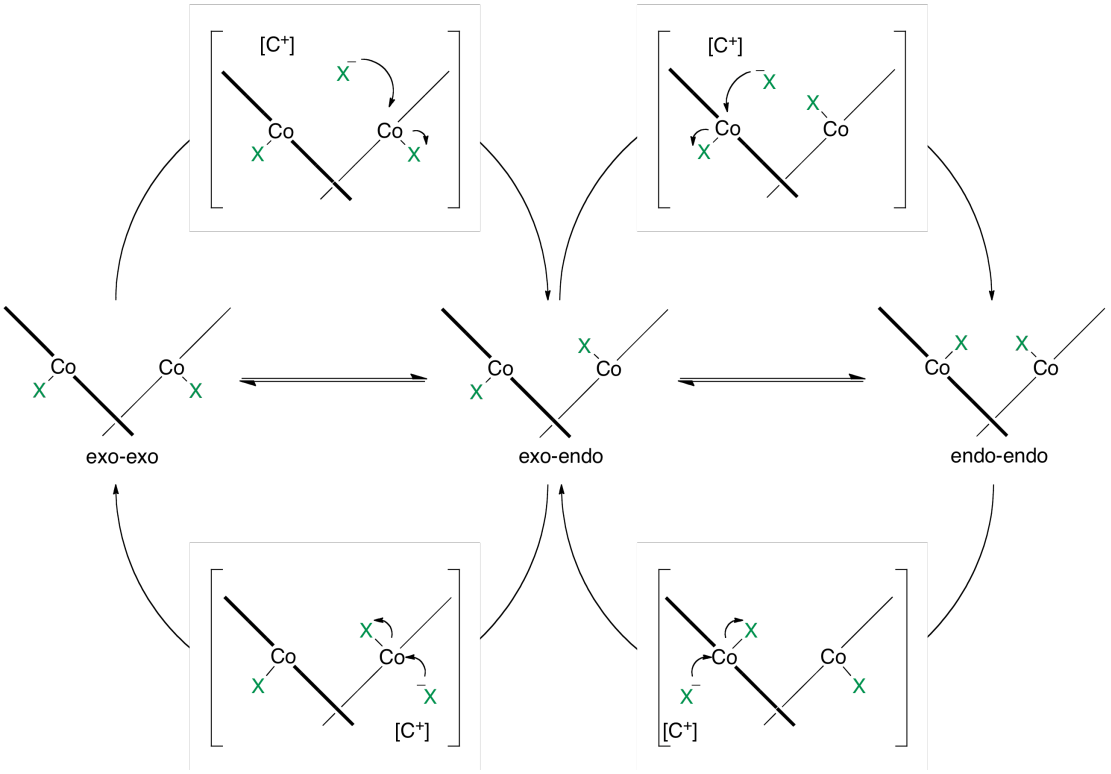

Figure 2.11. Interconversion of diastereomers of **4** in the presence of cocatalyst (X= halide or carboxylate).

Once the epoxide has been ring-opened, the alkoxide formed could either cause the dissociation of the axial ligand at the Co center, or generate an anionic species (cobaltate species). By modeling the two scenarios using **12** (R_1=H, R_2=H; Figure 2.5), DFT calculations revealed that the formation of the cobaltate species was thermodynamically favored.[27] The formation of cobaltate as the active catalyst is reminiscent of elegant work done by Okuda *et al.*, who showed that an aluminate complex was necessary for the bimetallic ring opening of epoxide.[10] Though calculations suggest the cobaltate is favored as the active catalyst species, it is still possible to dissociate the axial ligand outside of the cleft. As shown in Figure 2.12A, we propose that the two are in equilibrium – the complex formed from the dissociation of the axial ligand outside the cleft is a non-productive resting state that re-enters the catalytic cycle once an axial ligand reassociates. The presence of excess cocatalyst could be used to shift the equilibrium to favor formation of cobaltate and propagate polyether. This hypothesis is consistent with the observations from Table 2.1 (entry 2-4), where the use of excess cocatalyst produces polymers with narrower M_w/M_n values, which is a result of faster initiation relative to propagation.

As shown in Figure 2.12B, after the active cobaltate species is formed, an epoxide can coordinate to a cobalt center and be ring opened via nucleophilic attack by a propagating alkoxide. The ring opening of epoxides could continue in an alternating fashion, oscillating between adjacent Co centers in the cleft yielding polyether (Figure 2.12C).

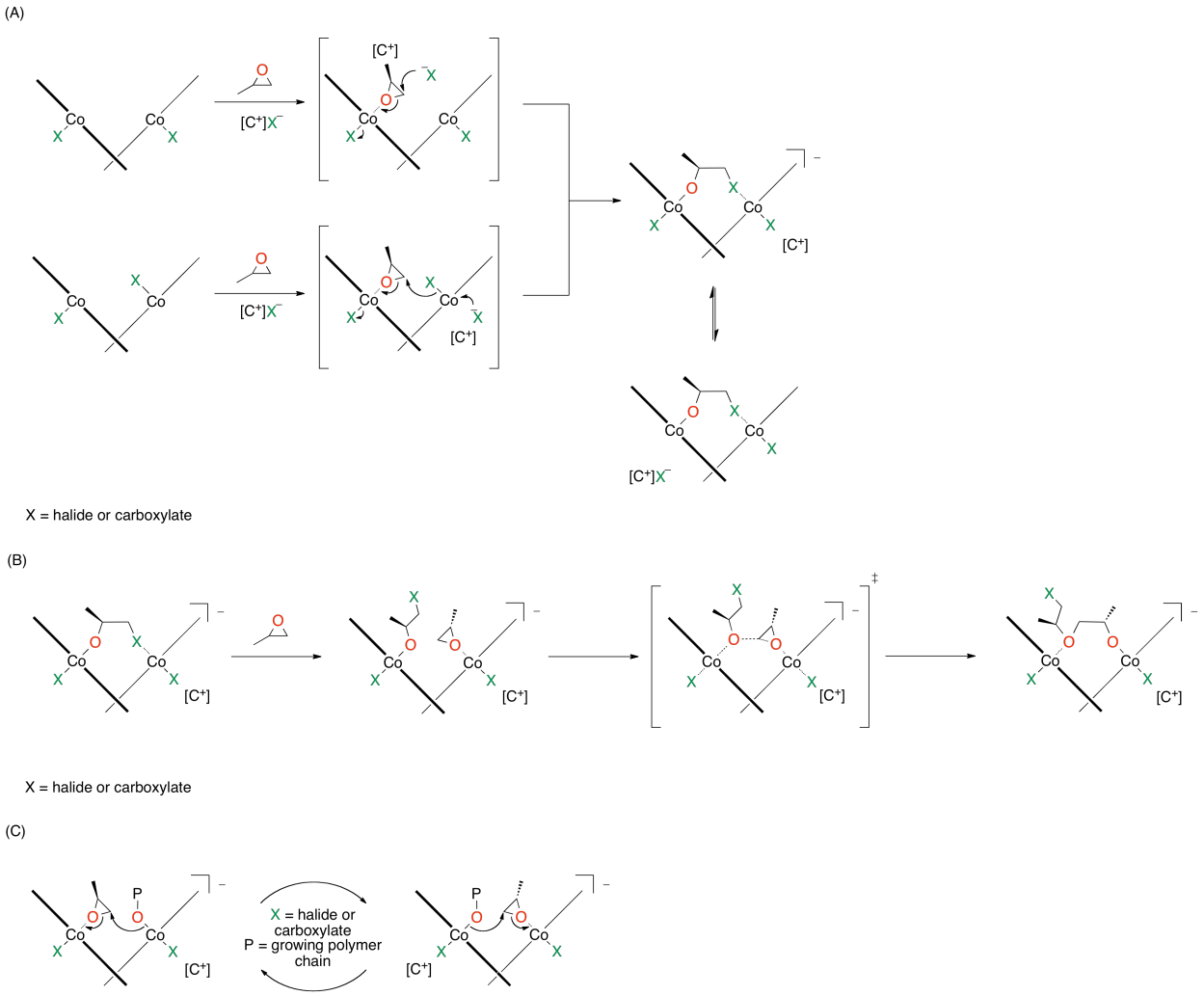

Figure 2.12. (A) Initiation of polymerization to form active cobaltate species; (B) Enchainment of epoxide monomer with cobaltate species; (C) Propagation of polyether.

The experimental and theoretical results reflect the importance of the cocatalyst in the polymerization system. The cocatalyst helps interconversion of catalyst diastereomers, initiates the polymerization to form the active cobaltate species, and shifts equilibrium towards active species during the catalytic cycle.

2.2.4. Energy Profiles for Epoxide Polymerization

After establishing a hypothesis for the role of the cocatalyst, we began to investigate the enchainment of epoxide using the active cobaltate species. Calculations were conducted using the cobaltate species of **4**, where the propagating polyether chain was represented by a methoxide molecule coordinated to one of the Co centers inside the catalyst cleft (Figure 2.13). An epoxide molecule then coordinates to the adjacent Co to form the coordination intermediate (**CI**), and is ring opened via nucleophilic attack at the methylene carbon by the methoxide (transition state, **TS**). Once the epoxide is ring opened, the cobaltate is maintained, and the oxygen at the β-position of the propagating chain coordinates to a Co until it is displaced by epoxide (resting state, **RS**). The free-energy changes corresponding to each state of the enchainment are reported in Table 2.2.

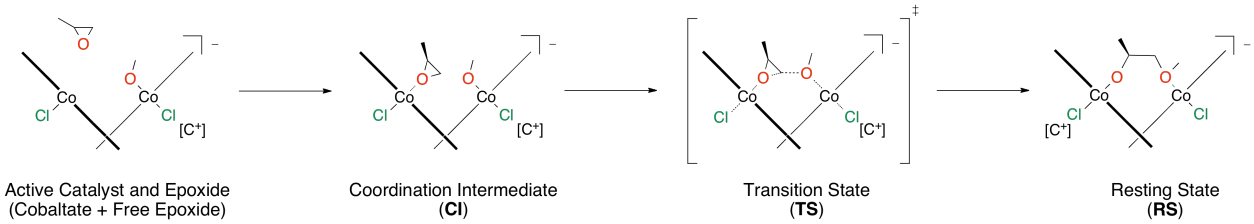

Figure 2.13. Enchainment of epoxide after generation of a cobaltate species.

Table 2.2. Free-energy changes for enchainment of epoxide using cobaltate species of **4.**

State	ΔG (kcal/mol)	Dihedral Angle (ϕ)	Co—Co Distance (Å)
CI	6.40	82.1	6.59
TS	15.8	75.8	6.29
RS	-7.20	75.0	6.23

All ΔG values are relative to the active catalyst and epoxide in Figure 2.13, for which $\Delta G = 0$.

The calculated ΔG values indicate that the formation of the **CI** and **TS** are relatively uphill in energy, but the formation of **RS** after enchainment of epoxide is thermodynamically favorable (Figure 2.14). The large energy transition from **CI** to **TS** suggests that the ring-opening of epoxide is possibly the rate determining step of the process.

Table 2.2 also shows the calculated dihedral angles and Co—Co distances during the process of propagation. The **CI** has the largest dihedral angle and largest Co—Co distance in order to accommodate both the epoxide and the methoxide in the catalyst cleft. The **TS** displays smaller values for both parameters as the epoxide and methoxide are brought closer for ring opening to take place, while **RS** has the smallest values for both due to the penultimate oxygen of the bound propagating polyether chain coordinating to the adjacent Co. Based on reports of related monomeric *salen*-Co(III) complexes,[23] the effects of the axial ligands on the enchainment of epoxide was then investigated computationally.

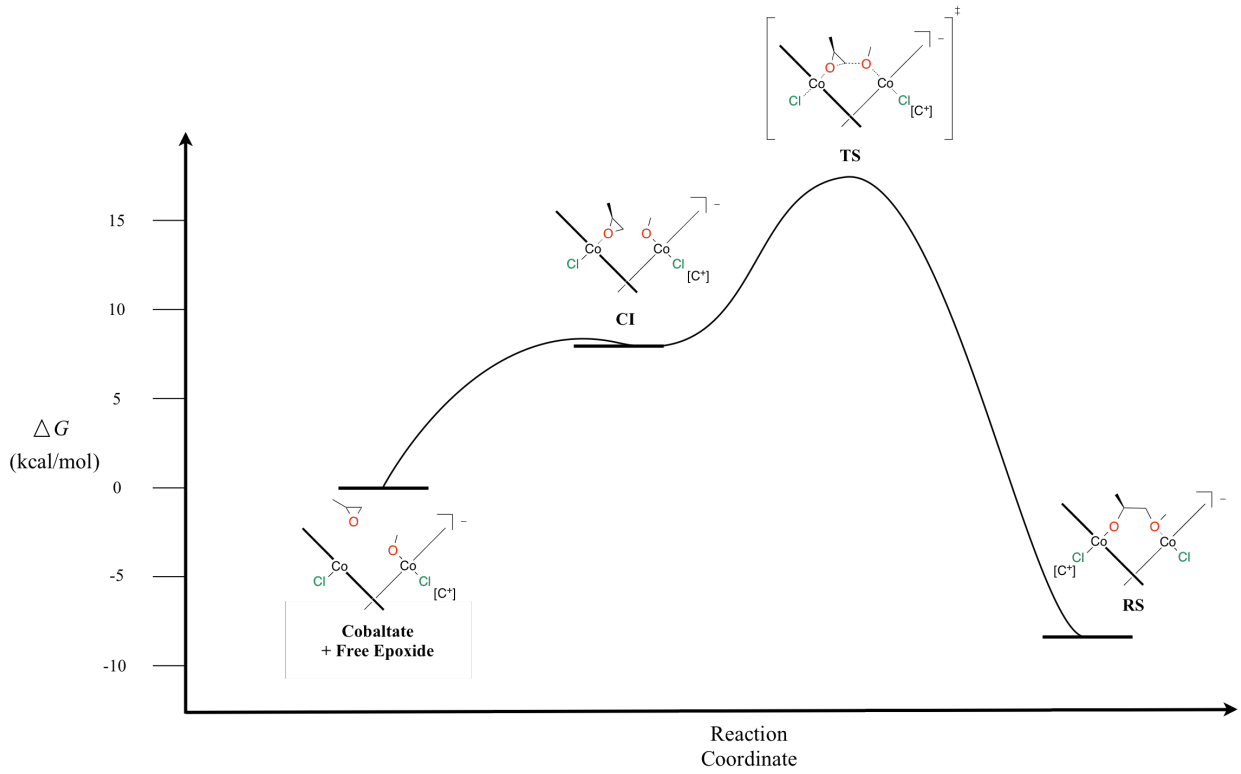

Figure 2.14. Free-energy diagram corresponding to results in Table 2.2.

Complex **11** was used for modeling the effects of the axial ligands on enchainment of epoxide. In order to simulate the highly active polymerization system of **4** with **6**,[13-14] only Cl and OAc were used as axial ligands in the model. The results are reported in Table 2.3.

Table 2.3. Free-energy changes for enchainment of epoxide varying axial ligands of the cobaltate species of **11**.

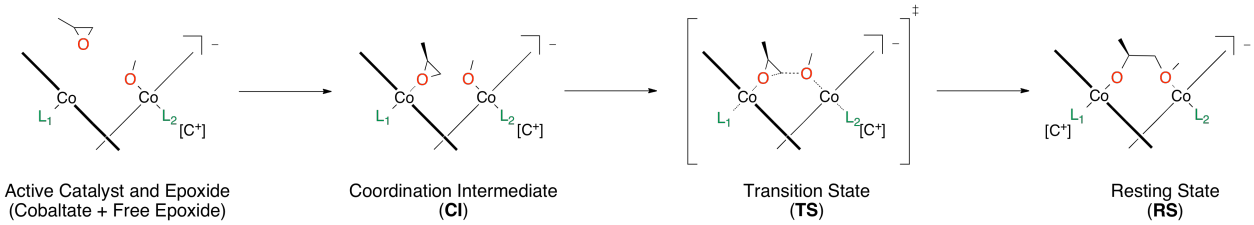

	Axial Ligands		ΔG (kcal/mol)		
entry	L_1	L_2	**CI**	**TS**	**RS**
1	Cl	Cl	7.6	16.6	-7.8
2	Cl	OAc	5.5	13.5	-8.1
3	OAc	Cl	4.1	12.9	-10.6
4	OAc	OAc	2.6	10.4	-12.3

All ΔG values are relative to the Active Catalyst and Epoxide, for which $\Delta G = 0$.

The calculations suggest that all combinations of the axial ligands (Cl and OAc) result in thermodynamically favorable enchainment pathways (Table 2.3 entry 1-4; Figure 2.15). The most energetically favorable pathway is observed when both axial ligands are OAc (Table 2.3, entry 4).[23b, 27]

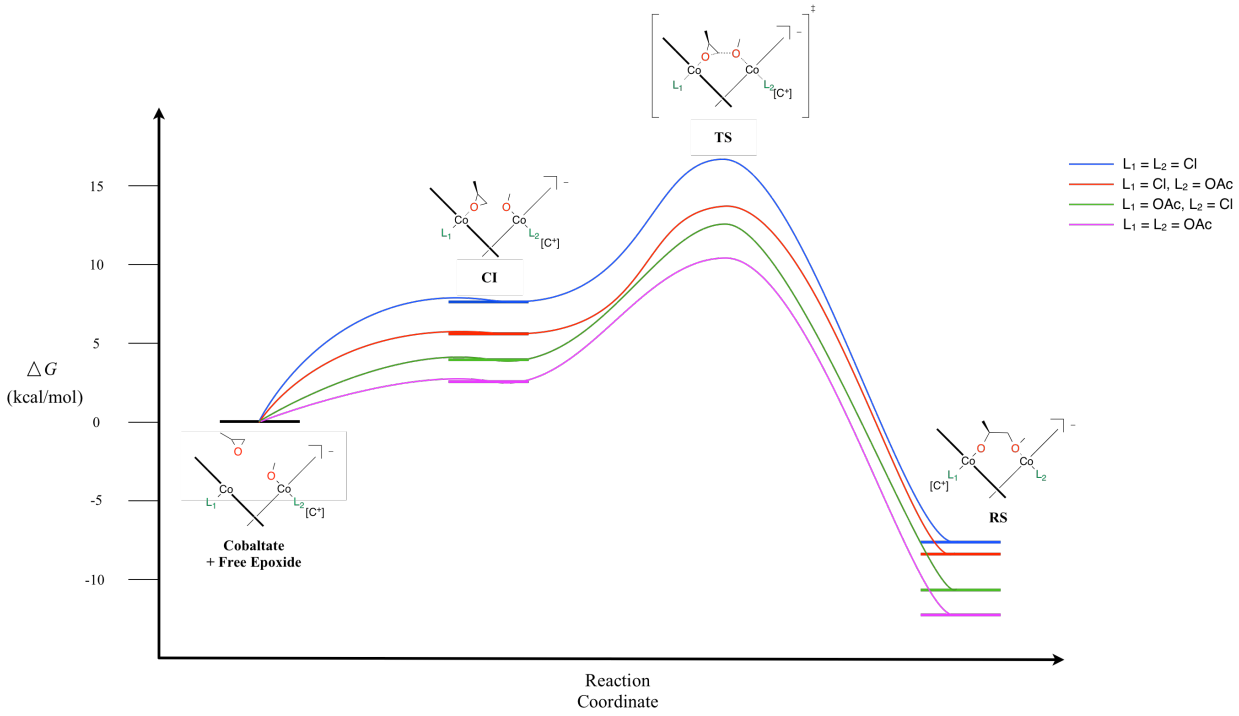

Figure 2.15. Free-energy diagram corresponding to results in Table 2.3.

The theoretical calculations provide insight into the enchainment of epoxide during the polymerization process. The results suggest that enchainment of epoxide is thermodynamically favorable and that the catalyst cleft may open and close slightly during the different steps of propagation.

2.3. Conclusion

The bimetallic cobalt (III) catalyst, **4** is highly active for the enantioselective polymerization of epoxides in the presence of a cocatalyst. Despite the complexities and multifaceted nature of the polymerization system, experimental observations and theoretical calculations led insight to (a) the necessity of the chiral catalyst cleft, (b) the Co—Co distances required for polyether synthesis, (c) predict the oxidation state of Co during the polymerization, (d) a better understanding of the role of the cocatalyst, and (e) the favorable free-energy changes occurring during epoxide enchainment.

Figure 2.16 shows our proposed catalytic cycle for epoxide enchainment – after formation of the cobaltate species (active catalyst), an epoxide molecule coordinates to a Co inside the catalytic cleft and is ring opened by a propagating alkoxide from the adjacent Co. The catalytic cycle repeats itself until dissociation of an axial ligand to revert to the inactive form of the catalyst. Chain growth resumes upon regeneration of the cobaltate species by association of the axial ligand.

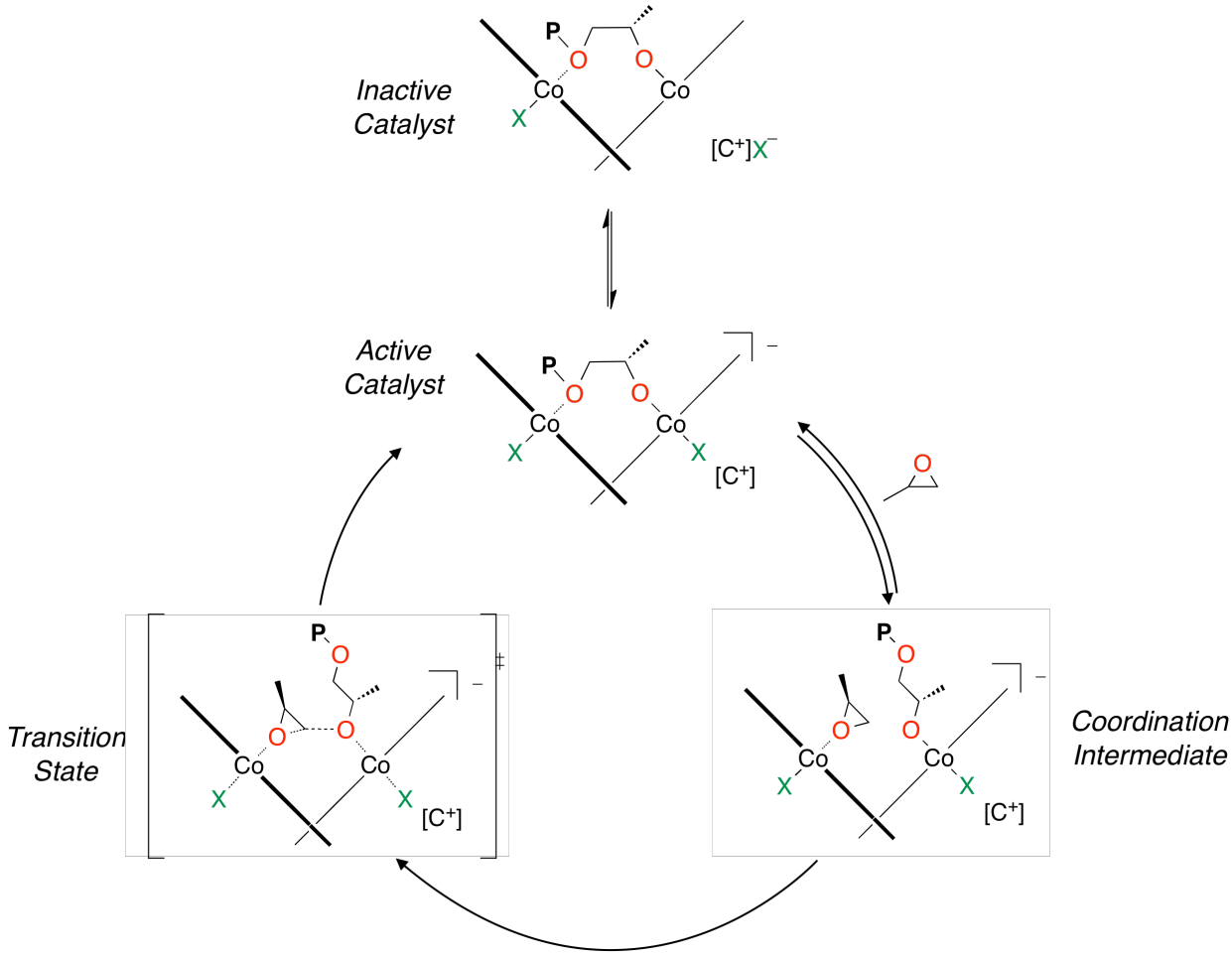

Figure 2.16. Catalytic cycle of epoxide enchainment (X= halide or carboxylate).

DFT calculations have provided valuable insight in regard to the individual steps of the catalytic cycle, particularly the rate-determining step of the reaction. As the ring-opening of epoxide is the slowest step of the polymerization, we plan to develop bimetallic catalysts that facilitate nucleophilic attack of the epoxide to provide more energetically favorable pathways, and thus more active catalysts.[28]

We anticipate that better understanding of the mechanism will allow the development of more optimized catalyst systems for polyether synthesis. Examples of new applications include the development of catalysts for the living polymerization of monosubstituted epoxides and for the polymerization of disubstituted epoxides.

2.4. Experimental

2.4.1. General Considerations

All manipulations of air or water sensitive compounds were carried out under dry nitrogen using a Braun Labmaster drybox or standard Schlenk line techniques. NMR spectra were recorded on Varian Unity spectrometers INOVA 500 (^{1}H, 500 MHz), or INOVA 600 (^{1}H, 600 MHz). ^{1}H NMR spectra were referenced with residual non- or partially-deuterated solvent shifts ($CHCl_3$ = 7.27 ppm, pyridine-d_4 = 8.74 ppm). ^{13}C NMR spectra were referenced to solvent signals ($CDCl_3$ = 77.23 ppm, pyridine-d_5 = 150.35 ppm). Mass spectrometry analyses were conducted at the School of Chemical Sciences Mass Spectrometry Laboratory at the University of Illinois at Urbana-Champaign.

2.4.2. Polymer Characterization

The polyethers synthesized were characterized using gel permeation chromatography (GPC) using an Agilent PL-GPC 50 integrated system, equipped with UV and refractive index detectors, and 2 PL gel Mini-MIX C columns (5 micron, 4.6 mm ID). The GPC columns were eluted with tetrahydrofuran at 30 °C at 0.3 mL/min and were calibrated with monodisperse polystyrene standards.

2.4.3. NMR Quantification of Polymer Tacticity

The polyethers synthesized display distinct resonances for the stereochemical defects in the polymer chain by ^{13}C NMR spectroscopy. The polyethers synthesized in this paper exhibit triad resolution of the methine carbon, which have been assigned previously. In all cases the methine resonances were used to quantify the triad integral values and to calculate [*mm*]. The *mr*

and *rm* triads are very small relative to the mm triad, and occur in the same area as the ^{13}C-^{13}C satellite signals of the *mm* triad. As *rr* triad resonances were very distinct, they were primarily used to calculate the tacticity of the polyether.

Representative calculation of polymer tacticity in PPO (From ^{13}C NMR integrations of the methine resonances, Figure 2.17; Table 2.1, entry 1)

$[mm]+[mr]+[rm]+[rr] = 1$

$[rr] = 3/1009 = 0.003$

$[mr + rm] = 2[rr] = 0.006$

$[mm] = 1 - [mr + rm + rr] = 1 - (0.003 + 0.006) = 0.991$

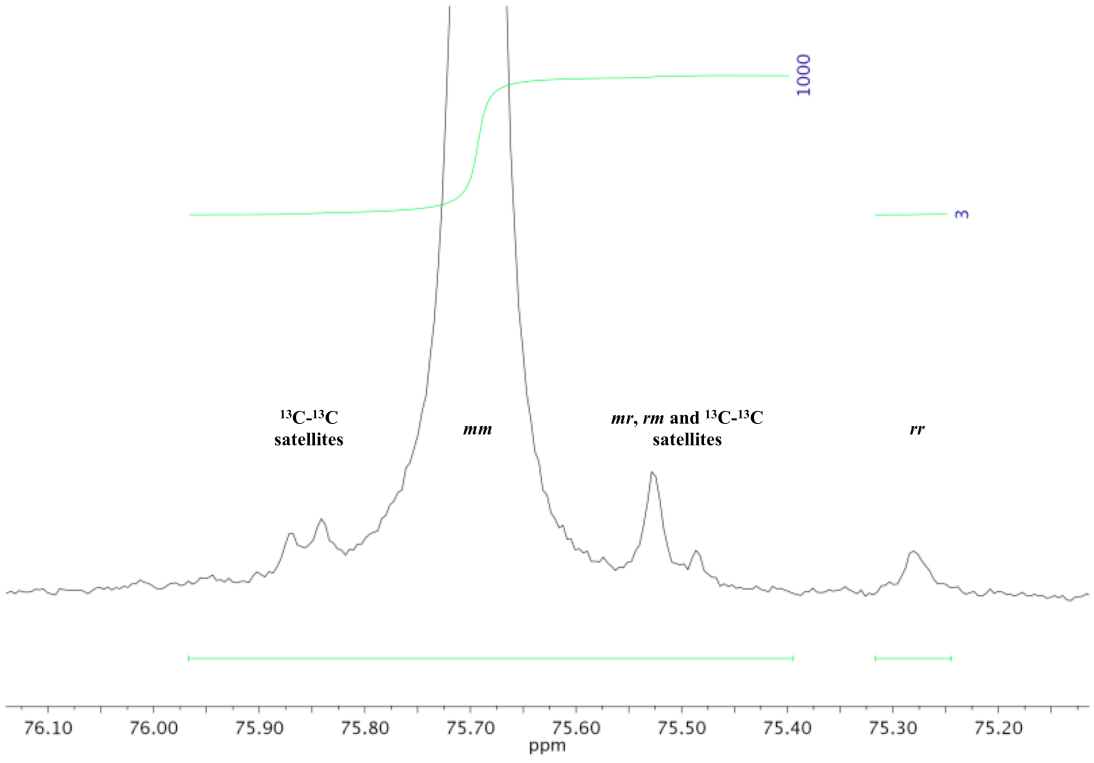

Figure 2.17. Calculation of polymer tacticity of PPO by ^{13}C NMR spectroscopy.

2.4.4. Calculating $ee_{(P)}$ and Selectivity factors (*s*-factor)

The values for [*mm*], [*mr*], [*rm*] and [*rr*], attained from the quantitative ^{13}C NMR spectroscopy of the polyethers were used in equation 1 to calculate polymer *ee*.

$$ee_{(P)} = (2[mm] + [mr] + [rr] - 1)^{1/2} \qquad (1)$$

Corresponding selectivity factors (*s*-factor) were calculated using equation 2, where *c* is conversion of epoxide to polymer. Equation 2 is only valid when $c < 50\%$.

$$s\text{-factor} = ln[1\text{-}c(1+ee_{(P)})]/ln[1\text{-}c(1\text{-}ee_{(P)})] \qquad (2)$$

2.4.5. Materials

HPLC grade methylene chloride and methanol were purchased from Fischer Scientific and purified over solvent columns. 3Å sieves were purchased from STREM, activated by heating at 165 °C under vacuum for 20 hours, and stored in a nitrogen filled glove box. Absolute ethanol was purchased from Koptec, dried over activated 4Å sieves and degassed by sparging with nitrogen for 2 hours. Dimethoxyethane (DME) was purchased from Sigma-Aldrich, dried over sodium, degassed through multiple freeze-pump-thaw cycles and vacuum transferred to a Straus flask that was stored in a nitrogen filled glove box. All epoxides were purchased from commercial sources, dried over calcium hydride, degassed through multiple freeze-pump-thaw cycles, and also stored in a nitrogen filled glove box. (1*R*, 2*R*)-diaminocyclohexane (99% *ee*), and cobalt acetate tetrahydrate were purchased from Sigma-Aldrich. (*S*)-1,1'-bi-2-naphthol and 1, 1'-biphenol-2,2'-diol were purchased from TCI. Cocatalysts bis(triphenylphosphine)iminium acetate and phosphazenium pivalate were prepared according to reported procedures.[16-17] Diformylated (*S*)-1,1'-bi-2-naphthol, and diformylated 1,1'-biphenol-2,2'-diol were also

synthesized from previous reports.[29] All other reagents were purchased from commercial sources and used as received.

2.4.6. Synthesis of Ligand Framework

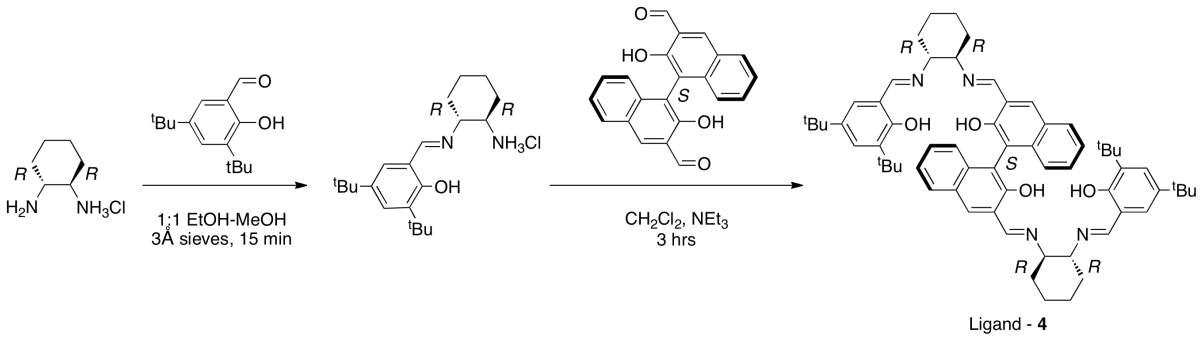

Figure 2.18. Synthesis of catalyst ligand.

Representative procedure to synthesize bimetallic ligand framework (Ligand – **4** as shown in Figure 2.18)

The HCl salt of (1*R*, 2*R*)-diaminocyclohexane (0.62g, 4.1mmol) and 3,5-di-(*tert*-butyl)-salicylaldehyde (0.96g, 4.1mmol) were taken in a 100 mL round bottom flask along with 3Å sieves and a teflon stir bar. A vacuum adaptor was attached to the flask and was placed under nitrogen while stirring. After stirring the solids together for 10 minutes, 20 mL of a 1:1 EtOH-MeOH mixture was canulated into the round bottom flask. On addition of solvent, the contents of the flask turn yellow. After 15 minutes of stirring, a distinct color change is observed from yellow to dark brown. At this point, a solution of diformylated (S)-1,1'-bi-2-napthol[1] (0.70g, 2.0 mmol) and triethylamine (1.1 mL, 7.9 mmol) in 15 mL anhydrous methylene chloride was added to the reaction mixture and allowed to stir. After 3 hours, a distinct color change from red to dark

brown is observed. The reaction mixture was then passed through a plug of celite, which was washed copiously with methylene chloride. After removal of solvent under reduced pressure, the brown solid was purified by column chromatography (12% ethyl acetate, 2% triethylamine, and 86% hexane) to attain a pure bright yellow solid, Ligand – **4**. Yield = 0.65 g (33%). Full characterization of Ligand – **3** was reported previously.[14]

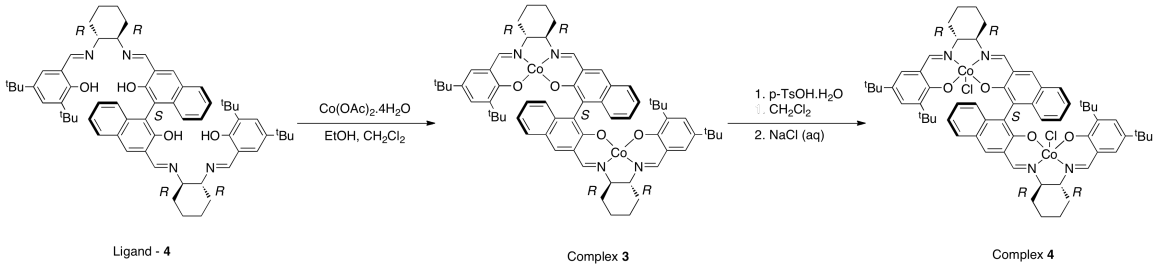

Figure 2.19. Synthesis of metallated ligand and catalyst.

Representative procedure to metallate ligands (Synthesis of complex **3**)

$Co(OAc)_2 \bullet 4H_2O$ (65 mg, 0.26 mmol) is taken in an oven dried Schlenk flask with a stir bar and placed under nitrogen conditions using Schlenk technique. The contents of the flask are heated carefully using a heat gun under vacuum to remove water from the cobalt salt (turns from pink to dark purple). After the flask cooled to room temperature, 5 mL of EtOH was canulated to the flask, and the contents were stirred to form a purple solution. A yellow solution of Ligand – **4** (120 mg, 0.12 mmol) in 10 mL of anhydrous methylene chloride was then canulated to the Schlenk flask, causing the cobalt solution to change from purple to dark reddish brown. The flask was closed and placed in an oil bath set at 60 °C. After heating for 2 hrs, solvent was removed by vacuum and a dark brown solid was attained. The solid was collected over a fine

glass frit, and washed with methanol (40 mL) and pentane (60ml x 3). The solid was dried under vacuum over night to yield 110 mg (84%) of **3**. Complex **3** was characterized earlier in previous reports.

Representative synthesis of complex **4**

3 (110 mg, 0.10 mmol) was taken in a 20 mL vial with a stir bar and dissolved in 12 mL of methylene chloride. *Para*-toluenesulfonic acid monohydrate (38 mg, 0.20 mmol) was added to the solution. The mixture was stirred and all the solvent was allowed to evaporate. A black solid was attained, and redissolved in 20 mL methylene chloride. The solution was washed with brine (40 mL x 4), and dried using Na_2SO_4. Solvent was removed under reduced pressure, and dried under vacuum overnight to yield **4** as a black crystalline solid (88 mg, 76%). Complex **4** was fully characterized in previous reports.

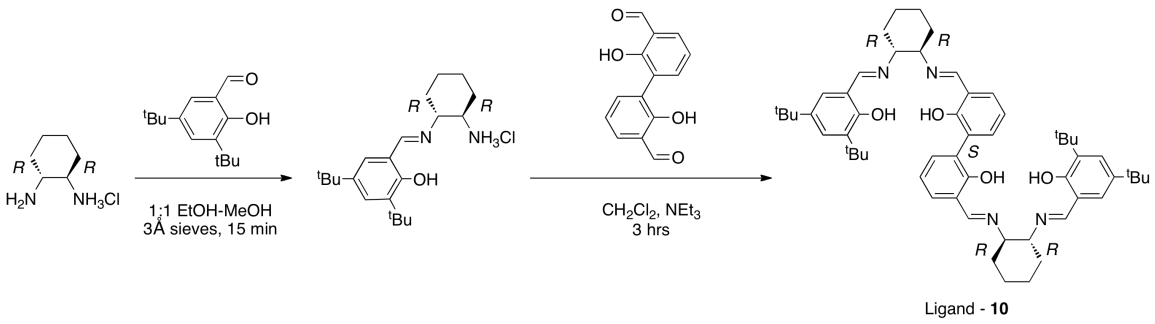

Figure 2.20. Synthesis of Ligand-**10.**

Representative procedure to synthesize Ligand - ***10***

The HCl salt of (1*R*, 2*R*)-diaminocyclohexane (0.93 g, 6.2 mmol) and 3,5-di-(*tert*-butyl)-salicyladehyde (1.45 g, 6.2 mmol) were placed in a 250 mL round bottom flask with 3Å sieves and a teflon stir bar. A vacuum adaptor was attached to the flask and the contents placed under

nitrogen with stirring. After stirring the solids together for 10 minutes, 35 mL of MeOH was canulated into the round bottom flask to give a yellow solution. After 15 minutes of stirring, the color had changed from yellow to dark brown and a solution of diformylated 1,1'-bi-2-phenol (0.75 g, 3.1 mmol) and triethylamine (1.7 mL, 12.4 mmol) in 30 mL of anhydrous methylene chloride was added to the reaction mixture and allowed to stir. After 2.5 hours the reaction mixture was passed through a plug of celite, which was rinsed copiously with methylene chloride, and washed with 30 mL of saturated aqueous ammonium chloride. The organic layer was separated, dried with $MgSO_4$, and filtered. After removal of solvent under reduced pressure, the brown solid was purified by column chromatography (5% diethylether, 94% pentane, 1% triethylamine, gradually increased in polarity to 20% diethylether, 79% pentane and 1% triethylamine) to give Ligand **- 10** as a pure bright yellow solid. Yield = 0.53 g (20.1%). R_f (20% EtOAc, 80% hexane) = 0.52.

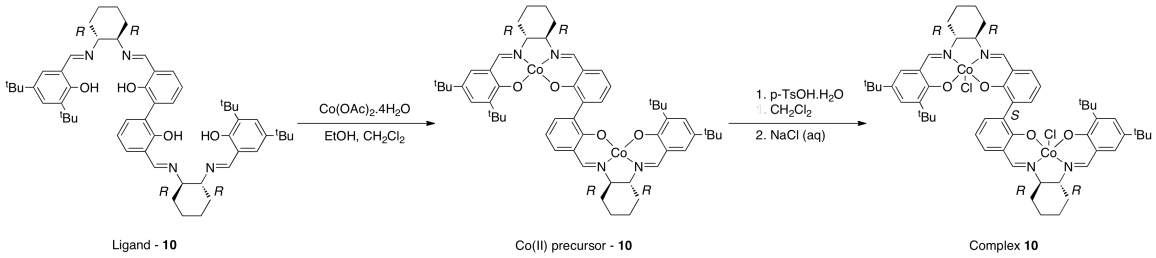

Figure 2.21. Synthesis of complex **10**.

*Metallation of Ligand-**10***

Under nitrogen, $Co(OAc)_2 \cdot 4H_2O$ (0.18 g, 0.73 mmol) was added to a 50 mL Schlenk tube and was heated under vacuum until the color had changed from pink to purple. Anhydrous methanol (10 mL) was added via canula. Ligand – **10** was dissolved in dichloromethane under nitrogen and the solution was canulated to the methanolic solution of cobalt acetate. The mixture

was heated at 40 °C for 3 hours, then cooled to room temperature and the solvent removed *in vacuo*. The resulting red solid was suspended in pentane, filtered over a fine glass frit, and washed with pentane to give the cobalt (II) precursor of **10** as a red solid. Yield = 0.30 g (87.8%).

Representative procedure for preparing Complex **10**

The cobalt (II) precursor of complex **10** (0.28 g, 0.29mmol) was dissolved in 15 mL of methylene chloride in a 20 mL vial and *para*-toluenesulfonic acid monohydrate (0.11 g, 0.60 mmol) was added. The solution was stirred open to air for 24 hours and the methylene chloride was allowed to evaporate. The resulting dark shiny solids were redissolved in methylene chloride and washed three times with brine, dried over $MgSO_4$ and filtered. Solvent was removed *in vacuo*, and the black solids were suspended in pentane, filtered over a fine glass frit, and washed with pentane to give **10** as a black solid in quantitative yield, 0.30g.

2.4.7. NMR Characterization Specifications

The ligands and complexes were characterized by 1-D and 2-D NMR spectroscopy in $CDCl_3$ or pyridine-d_5 at ambient temperature on a Varian Unity Inova 600 MHz spectrometer using a Varian 5 mm inverse ^{1}H-{^{13}C,^{15}N} triple-resonance probehead with triple-axis gradients, and/or Varian Unity Inova 500 MHz spectrometers using a Varian 5 mm inverse ^{1}H-{^{13}C,^{15}N} triple-resonance probehead with Z gradient or a Varian 5 mm dual broadband probehead with Z gradient. NMR data were acquired with the pulse sequences supplied in Vnmrj 2.2D/Chempack 4.1 (Agilent Inc.) and were processed and analyzed using the MestReNova 7.1 software package (2012, Mestrelab Research S. L.). All 2-D spectra were acquired with typical ^{1}H spectral widths

of 0.5 –14.5 ppm and 0.5 – 9.5 ppm for ligands and complexes, respectively. COSY spectra were acquired using the gCOSY sequence with 400 – 600 complex points in the indirectly detected dimension and 1 scan of 0.6 – 0.8 s acquisition time per increment. The resulting matrices were zero filled up to 4k and 8k complex data points in F1 and F2, respectively, and unshifted sine bell (F1), and simultaneous unshifted sine bell and Gaussian (F2) window functions were applied prior to Fourier transformation. TOCSY spectra were acquired with 80 ms mixing times using the TOCSY sequence with 200 – 400 complex points in the indirectly detected dimension and 2 or 4 scans of 0.4 s acquisition time per increment. The resulting matrices were zero filled up to 4k x 4k complex data points and Gaussian window functions were applied in both dimensions prior to Fourier transformation. NOESY spectra were acquired with 600 ms mixing times using the NOESY sequence with 200 – 300 complex points in the indirectly detected dimension and 4 or 8 scans of 0.4 s acquisition time per increment. The resulting matrices were zero filled up to 4k x 4k complex data points and Gaussian window functions were applied in both dimensions prior to Fourier transformation. ROESY spectra were acquired with 200 ms mixing times using the ROESYAD sequence with 200 – 600 complex points in the indirectly detected dimension and 4 or 8 scans of 0.4 s acquisition time per increment. The resulting matrices were zero filled up to 4k x 4k complex data points and Gaussian window functions were applied in both dimensions prior to Fourier transformation. Multiplicity-edited HSQC spectra were acquired using the HSQCAD sequence with a spectral window of -10 – 190 ppm and 400 – 800 complex points in the indirectly detected dimension, and 4 scans of 0.15 s acquisition time per increment. The resulting matrices were zero filled up to 4k x 2k complex data points in F1 and F2, respectively, and Gaussian window functions were applied in the ^{1}H dimension prior to Fourier transformation. HMBC spectra were acquired in phase sensitive mode and optimized for 8 Hz

couplings using the gHMBCAD sequence with a spectral window of -10 – 225 ppm and 600 – 1200 complex points in the indirectly detected dimension, and 4 scans of 0.3 s acquisition time per increment. The resulting matrices were zero filled up to 4k x 2k complex data points in F1 and F2, respectively, and simultaneous unshifted sine bell and Gaussian window functions were applied in the ^{1}H dimension prior to Fourier transformation.

2.4.8. Characterization Data for Ligands and Co Complexes

Ligand – **10**

HRMS-EI (m/z): calcd for $C_{56}H_{75}N_4O_4$, 867.5788; found, 867.5787. Ligand was characterized by ^{1}H, ^{13}C, COSY, ROESY, HSQC and HMBC NMR spectroscopy in $CDCl_3$.

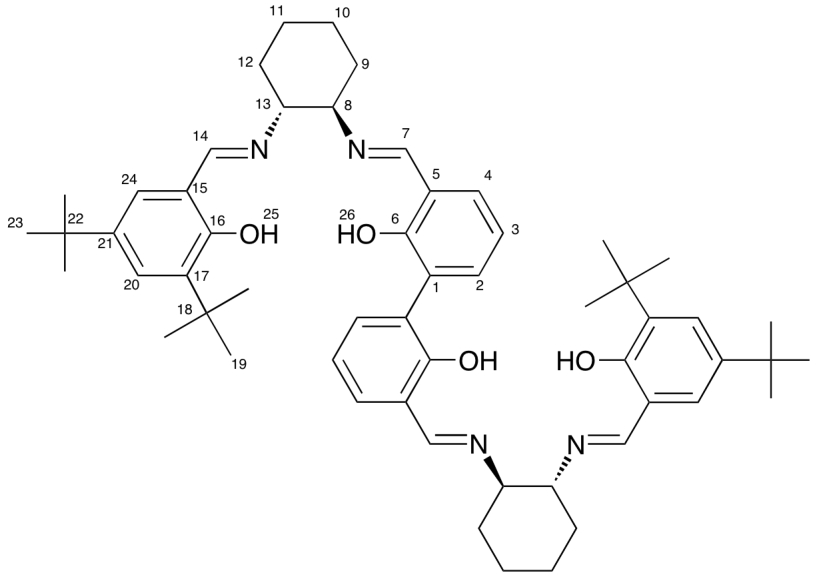

Atom No.	$^{13}C\{^{1}H\}$ NMR δ	^{1}H NMR δ
1	125.70	
2	134.32	7.29
3	118.14	6.84
4	131.21	7.14
5	118.99	

6	158.78	
7	165.05	8.33
8	72.78	3.35
9	33.18	1.94, 1.67
10	24.40	1.84, 1.42
11	24.34	1.84, 1.42
12	33.45	1.89, 1.69
13	72.44	3.20
14	165.94	8.22
15	117.88	
16	158.08	
17	136.47	
18	35.10	
19	29.55	1.42
20	126.95	7.31
21	140.02	
22	34.21	
23	31.61	1.25
24	126.20	6.96
25		13.68
26		13.82

Complex **10**

The Co(II) precursor of **10** was characterized by HRMS-EI. HRMS-EI (m/z): calcd for $C_{56}H_{71}Co_2N_4O_4$, 980.4061; found, 980.4069.

Complex **10** was characterized by ^{1}H, ^{13}C, COSY, ROESY, HSQC and HMBC NMR spectroscopy in pyridine-d_5.

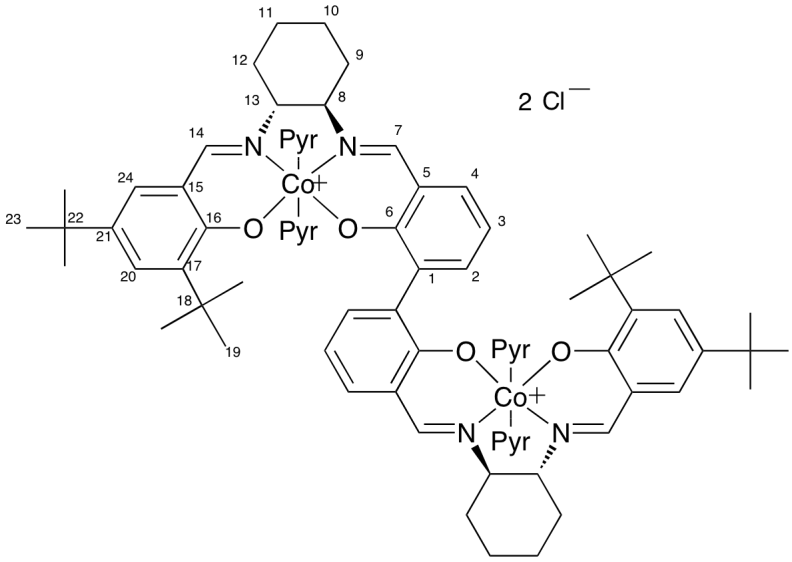

Atom No.	$^{13}C\{^{1}H\}$ NMR δ	^{1}H NMR δ
1	135.65	
2	137.31	7.20
3	115.95	6.68
4	135.41	7.71
5	120.05	
6	165.37	
7	166.15	8.73
8	73.16	2.94
9	29.44	2.76, 2.67
10	25.27	1.74, 1.14
11	25.05	2.00, 1.73
12	32.44	3.22, 1.54
13	68.30	5.04
14	168.85	8.81
15	117.29	
16	162.19	
17	143.23	
18	35.98	
19	30.62	1.50
20	131.39	7.67
21	136.92	
22	34.20	
23	31.58	1.25
24	130.39	7.60

2.4.9. Polymerizations

High Throughput Polymerizations: General procedure

The polymerizations were conducted on a Freeslate Core Module 3 robotic platform located inside a MBraun drybox equipped with a balance, liquid and solid dispense options, heated/cooled stirrers, and vortexers. The experiment was designed and executed using Library Studio(TM) and Automation Studio(TM) software. All solutions were dispensed robotically using a positive displacement dispense and disposable PDT tips. 24 8 mL vials each containing a stir bar were loaded into a Al reactor block and tared robotically. The reaction temperature was 0 °C and the stirring rate was 200 rpm. After 15 minutes, each reaction was quenched by addition of a solution of BHT. Volatiles were then removed from the reaction vials using a Speedvac vacuum centrifuge and the vials containing the products were weighed robotically.

Representative polymerization of propylene oxide using **4** *and* **7** (Table 2.1, entry 1)

Stock solutions (2 mg/mL) of **4** and **7** in dimethoxyethane (DME) were prepared in separate 20 mL vials inside a nitrogen filled glove box. Solutions were dispensed using a Freeslate Core Module 3 equipped with a PDT syringe and disposable PDT tips. The experiments were designed using Library Studio. 115 μL of the solution of **4** (0.230 mg, 0.200 μmol) and 63.9 μL of the solution of **7** (0.128 mg, 0.200 μmol) were dispensed into a tared 8 mL vial placed on a 6 x 4 aluminum vial plate. The temperature of the plate was set to 0 °C, and stir rate was set to 200 rpm. 3.45 mL of DME was dispensed into the reaction vial, and then 280 μL of propylene oxide (232 mg, 4.00 mmol) was added. After 15 minutes, the reaction was quenched with 300 μL of 5 mg/mL BHT in hexane solution (1.50 mg BHT, 6.82 mmol).

Volatiles were removed from the reaction vial using a vacuum centrifuge and then weighed. Mass of polypropylene oxide attained = 22.5 mg. Conversion = 9.72%. [*mm*]:[*mr* + *rm*]:[*rr*] = 0.991:0.006:0.003. $ee_{(P)}$ = 99.1%. *s*-factor >300. M_n = 43,600 g/mol, M_w/M_n = 3.5.

Effect of varying catalyst to cocatalyst ratio for PO polymerization (Table 2.1)

mass of **4** (mg)	moles of **4** (μmol)	mass of **7** (mg)	moles of **7** (μmol)	mass of Prod. (mg)	conv. (%)
0.230	0.200	0.128	0.200	22.5	9.72
0.230	0.200	0.256	0.400	57.1	24.6
0.230	0.200	0.511	0.800	69.4	29.9
0.0288	0.0250	0.0639	0.100	49.6	21.4

General conditions: Mass of PO added = 232 mg; Number of moles of PO added = 4 mmol; [PO]= 1 M in DME; PO:**4**:**7** = 20,000:1:1; T_{rxn}= 0 °C; t_{rxn}= 15 min; Conversions were determined gravimetrically.

Calculation of TOF (Table 1, entry 4):

No. of moles of polymer = 854 μmol

No. of moles of catalyst= 0.0250 μmol

t_{rxn}= 4.77 min

TOF = (854 μmol / 0.0250 μmol)/4.77 min = 7160 min^{-1}

Polymerization of PO with **8** *and* **6**

Complex **8** (4.6 mg, 7.0 μmol) and **6** (4.3 mg, 7.0 μmol) were taken in a 20 mL vial and dissolved in DME (6 mL) in a nitrogen filled glovebox. PO (83 mg, 14 mmol) was added to the contents of the vial and sealed. After stirring for 48 hours, the vial was removed from the

glovebox and an aliquot was taken for ^{1}H NMR analysis before volatiles were removed *in vacuo*. ^{1}H NMR and gravimetric analysis reveal no polymer formation.

Polymerization of PO with **10** *and* **7**

Complex **10** (3.8 mg, 3.6 μmol) and **7** (4.6 mg, 7.2 μmol) were taken in a 20 mL vial and dissolved in DME (6 mL) in a nitrogen filled glovebox. PO (83 mg, 14 mmol) was added to the contents of the vial, sealed and taken out of the box. After stirring for 5 hours, the reaction was quenched using 50 μL of 5% HCl in MeOH, and volatiles were removed *in vacuo*. Mass of PPO= 340 mg. Conv.= 41%. [*mm*]:[*mr* + *rm*]:[*rr*]= 0.880:0.008:0.004.

Polymerization of PO with **3** *and* **6**

Complex **3** (3.9 mg, 3.6 μmol) and **6** (4.3 mg, 7.0 μmol) were taken in a 20 mL vial and dissolved in DME (6 mL) in a nitrogen filled glovebox. PO (83 mg, 14 mmol) was added to the contents of the vial and sealed. After stirring for 5 hours, the vial was removed from the glovebox and an aliquot was taken for ^{1}H NMR analysis before volatiles were removed *in vacuo*. ^{1}H NMR and gravimetric analysis reveal no polymer formation.

2.4.10. UV-Vis Experimentation

UV-Vis absorbance spectra were recorded on a Cary 5000 UV-Vis-NIR spectrophotometer with a mercury lamp. Emission and excitation spectra were recorded on a Horiba Jobin Yvon Fluorolog-3 fluorescence spectrophotometer equipped with a 450 W Xe lamp, double excitation and double emission monochromators, a digital photon-counting photomultiplier and a secondary InGaAs detector for the NIR range.

UV-Vis sample preparation and titration procedure

Stock solutions (1 mg/mL) of **8** and **9** in anhydrous methylene chloride were prepared in a nitrogen filled glove box. 1.5 mL of the stock solution of **8** (1.5 mg, 2.4 μmol) was taken in a 50 mL volumetric flask and used to prepare a 0.12 mM solution. 3 mL of the solution was taken in a cuvette and sealed using a Teflon cap with an injectable top. 1.6 mL of the stock solution of **9** (1.6 mg, 2.4 μmol) was taken in a 50 mL volumetric flask to prepare a 0.12 mM solution. The diluted solution (3 mL) was taken in a cuvette and sealed with a teflon cap. A reference sample was prepared by adding 3 mL of anhydrous methylene chloride and also sealing it with a teflon cap. A 60 mM solution of **6** (5.2 mg, 8.7 μmol) was prepared and taken up in a 50 μL syringe (covered with a septa). The cuvettes were taken out of the glove box, and UV-Vis spectra collected.

The cuvette sample of **8** was fixed in the sample holder and the teflon cap was punctured with the syringe to add solution of **6**. After addition, the cap was covered with parafilm and the syringe tip covered with a septa to minimize any incorporation of air or water.

Equivalence of **6** with respect to **8**	Vol. of **6** added (μL)
1	5.0
2	10.0
4	20.0
6	30.0
8	40.0

2.4.11. MALDI Experimentation

MALDI-MS analysis was performed on a Bruker Biflex. The polymer samples were dissolved in THF at a concentration 5 mg/mL. The matrix used was CHCA (α-Cyano-4-hydroxycinnamic acid) dissolved in THF at a concentration of 0.25 M. Solutions of matrix, and polymer were mixed in a volume ratio of 10:1, respectively. The spectra were recorded in positive ion reflectron mode.

Polymer sample: PPO synthesized using **4** and **6**. M_n= 18,000 g/mol; M_w/M_n= 2.1.

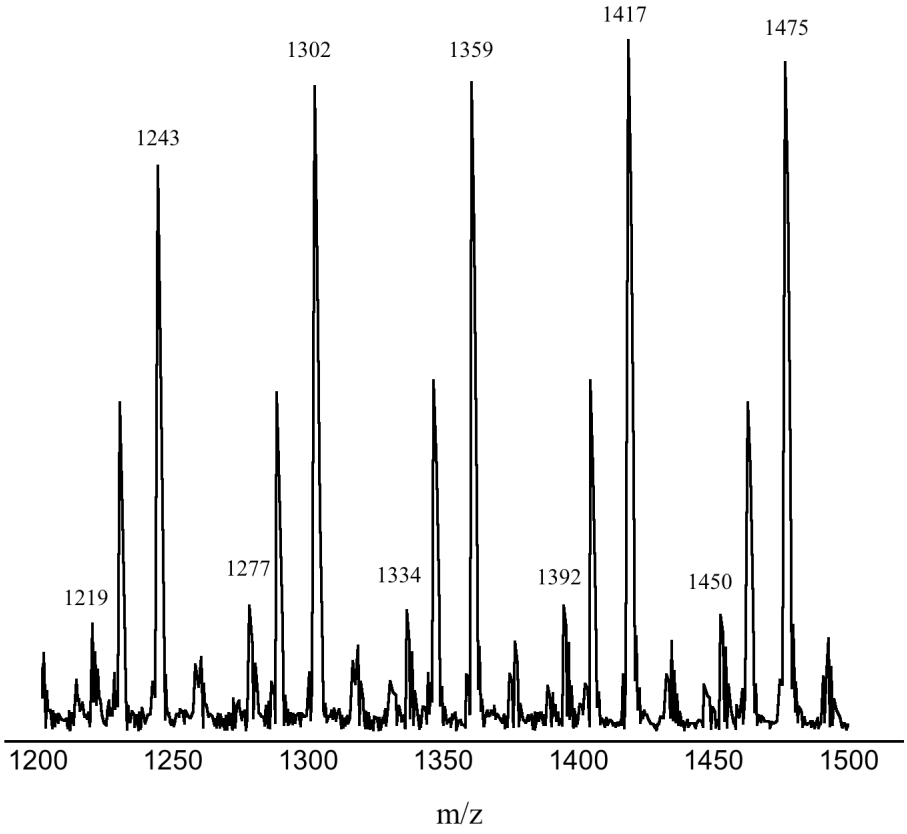

Figure 22. MALDI Spectrum of PPO with Cl and OAc end groups.

m/z	Proposed Assignment
1475	$Na(C_3H_6O)_{24}OAc$
1450	$Na(C_3H_6O)_{24}Cl$
1417	$Na(C_3H_6O)_{23}OAc$
1392	$Na(C_3H_6O)_{23}Cl$
1359	$Na(C_3H_6O)_{22}OAc$
1334	$Na(C_3H_6O)_{22}Cl$
1302	$Na(C_3H_6O)_{21}OAc$
1277	$Na(C_3H_6O)_{21}Cl$
1243	$Na(C_3H_6O)_{20}OAc$
1219	$Na(C_3H_6O)_{20}Cl$

2.4.12. Crystal Data and Refinement for tetrapyridine adduct of 5 (5-(pyr)$_2$).

Table 2.4. Crystal data and structure refinement for **5-(pyr)$_2$**.

Identification code	pw8	
Empirical formula	C104 H118 Cl2 Co2 N12 O4	
Formula weight	1788.86	
Temperature	173(2) K	
Wavelength	0.71073 Å	
Crystal system	Orthorhombic	
Space group	P2(1)2(1)2(1)	
Unit cell dimensions	a = 11.2391(5) Å	a= 90°
	b = 26.7837(14) Å	b= 90°
	c = 35.8843(17) Å	g = 90°
Volume	10802.1(9) Å^3	
Z	4	
Density (calculated)	1.100 Mg/m^3	
Absorption coefficient	0.408 mm^{-1}	
F(000)	3784	
Crystal size	0.60 x 0.15 x 0.05 mm^3	
Theta range for data collection	1.52 to 24.71°	
Index ranges	-13<=h<=11, -31<=k<=24, -41<=l<=42	
Reflections collected	46749	
Independent reflections	18418 [R(int) = 0.0579]	
Completeness to theta = 24.71°	100.0 %	
Absorption correction	Semi-empirical from equivalents	
Max. and min. transmission	0.9799 and 0.7920	
Refinement method	Full-matrix least-squares on F^2	
Data / restraints / parameters	18418 / 78 / 1117	
Goodness-of-fit on F^2	0.974	
Final R indices [I>2sigma(I)]	R1 = 0.0560, wR2 = 0.1280	
R indices (all data)	R1 = 0.0856, wR2 = 0.1399	
Absolute structure parameter	0.026(13)	
Largest diff. peak and hole	0.466 and -0.359 e•Å^{-3}	

Table 2.5. Atomic coordinates (x 10^4) and equivalent isotropic displacement parameters ($Å^2$x 10^3) for **5-(pyr)$_2$**. U(eq) is defined as one third of the trace of the orthogonalized U^{ij} tensor.

	x	y	z	U(eq)
Co(1)	278(1)	7294(1)	3184(1)	24(1)
Co(2)	3151(1)	9026(1)	2063(1)	25(1)
Cl(1)	1191(1)	9024(1)	6590(1)	57(1)
Cl(2)	-2277(1)	5950(1)	1960(1)	59(1)
O(1)	925(3)	7719(1)	3551(1)	30(1)
O(2)	207(3)	7850(1)	2860(1)	24(1)
O(3)	1746(3)	8750(1)	2282(1)	25(1)
O(4)	3140(3)	8499(1)	1712(1)	29(1)
N(1)	322(3)	6743(1)	3510(1)	26(1)
N(2)	-300(3)	6826(1)	2831(1)	22(1)
N(3)	-1333(3)	7462(1)	3367(1)	27(1)
N(4)	1909(3)	7160(1)	3013(1)	29(1)
N(5)	4553(3)	9306(1)	1860(1)	27(1)
N(6)	3233(3)	9567(1)	2403(1)	25(1)
N(7)	4108(3)	8583(1)	2376(1)	28(1)
N(8)	2177(3)	9388(1)	1697(1)	26(1)
C(1)	795(4)	7670(2)	3913(1)	31(1)
C(2)	1103(5)	8067(2)	4147(1)	40(1)
C(3)	907(6)	8001(2)	4527(2)	64(2)
C(4)	429(7)	7573(2)	4692(2)	72(2)
C(5)	205(5)	7192(2)	4460(1)	52(2)
C(6)	379(4)	7219(2)	4079(1)	35(1)
C(7)	270(4)	6769(2)	3870(1)	34(1)
C(8)	435(4)	6267(2)	3308(1)	28(1)
C(9)	159(5)	5786(2)	3512(1)	34(1)
C(10)	500(5)	5356(2)	3251(1)	39(1)
C(11)	-116(5)	5391(2)	2879(1)	36(1)
C(12)	29(4)	5903(2)	2694(1)	32(1)
C(13)	-346(4)	6298(1)	2964(1)	27(1)
C(14)	-734(4)	6938(2)	2509(1)	23(1)
C(15)	-848(4)	7432(2)	2360(1)	22(1)

C(16)	-1434(4)	7476(2)	2020(1)	27(1)
C(17)	-1640(4)	7942(2)	1861(1)	28(1)
C(18)	-2323(5)	7988(2)	1524(1)	38(1)
C(19)	-2529(5)	8434(2)	1366(1)	42(1)
C(20)	-2080(4)	8873(2)	1541(1)	40(1)
C(21)	-1436(4)	8846(2)	1869(1)	29(1)
C(22)	-1185(4)	8375(2)	2035(1)	25(1)
C(23)	-537(3)	8336(1)	2367(1)	19(1)
C(24)	-370(4)	7871(1)	2540(1)	20(1)
C(25)	1719(5)	8536(2)	3999(1)	45(1)
C(26)	906(6)	8816(2)	3714(2)	54(2)
C(27)	2888(5)	8381(2)	3806(2)	57(2)
C(28)	2029(6)	8910(2)	4307(2)	64(2)
C(29)	407(10)	7537(3)	5117(2)	123(4)
C(30)	1761(9)	7601(4)	5287(2)	137(4)
C(31)	5(8)	7020(3)	5244(2)	99(3)
C(32)	-182(11)	7943(3)	5292(2)	151(5)
C(33)	-1531(4)	7946(2)	3443(1)	32(1)
C(34)	-2572(5)	8096(2)	3620(1)	42(1)
C(35)	-3418(4)	7748(2)	3713(1)	42(1)
C(36)	-3215(5)	7255(2)	3622(1)	42(1)
C(37)	-2151(4)	7132(2)	3445(1)	28(1)
C(38)	2160(4)	7187(2)	2651(1)	32(1)
C(39)	3272(5)	7031(2)	2513(2)	47(1)
C(40)	4092(5)	6844(2)	2750(2)	50(2)
C(41)	3811(5)	6825(2)	3117(2)	47(1)
C(42)	2741(4)	6991(2)	3246(1)	33(1)
C(43)	3537(4)	8541(2)	1367(1)	30(1)
C(44)	3179(4)	8189(2)	1096(1)	34(1)
C(45)	3517(5)	8273(2)	731(1)	43(1)
C(46)	4249(5)	8670(2)	611(1)	43(1)
C(47)	4677(4)	8984(2)	881(1)	38(1)
C(48)	4334(4)	8925(2)	1254(1)	30(1)
C(49)	4883(4)	9255(2)	1522(1)	31(1)
C(50)	5187(4)	9608(2)	2136(1)	28(1)
C(51)	6174(4)	9962(2)	1990(1)	41(1)

C(52)	6740(5)	10216(2)	2333(2)	49(1)
C(53)	5808(5)	10489(2)	2576(2)	51(2)
C(54)	4803(4)	10141(2)	2691(1)	37(1)
C(55)	4270(4)	9909(2)	2345(1)	31(1)
C(56)	2436(4)	9693(2)	2636(1)	26(1)
C(57)	1340(4)	9438(2)	2700(1)	26(1)
C(58)	546(4)	9675(2)	2939(1)	29(1)
C(59)	-609(4)	9491(2)	2998(1)	27(1)
C(60)	-1432(4)	9739(2)	3227(1)	38(1)
C(61)	-2561(5)	9572(2)	3261(2)	43(1)
C(62)	-2904(4)	9138(2)	3067(1)	37(1)
C(63)	-2141(4)	8890(2)	2849(1)	27(1)
C(64)	-952(4)	9049(2)	2803(1)	25(1)
C(65)	-130(4)	8799(1)	2563(1)	21(1)
C(66)	1015(4)	8984(2)	2509(1)	23(1)
C(67)	2471(5)	7724(2)	1206(1)	47(1)
C(68)	3254(7)	7422(2)	1489(2)	72(2)
C(69)	1295(6)	7845(2)	1382(2)	62(2)
C(70)	2244(6)	7374(2)	872(2)	67(2)
C(71)	4519(6)	8733(2)	196(1)	52(2)
C(72)	3383(6)	8827(3)	-23(2)	78(2)
C(73)	5129(6)	8257(2)	45(2)	74(2)
C(74)	5376(7)	9180(3)	137(2)	84(2)
C(75)	5027(4)	8326(2)	2219(1)	39(1)
C(76)	5698(4)	7987(2)	2412(2)	39(1)
C(77)	5448(5)	7908(2)	2788(2)	41(1)
C(78)	4518(4)	8172(2)	2947(2)	40(1)
C(79)	3869(4)	8505(2)	2738(1)	31(1)
C(80)	1271(4)	9132(2)	1555(1)	28(1)
C(81)	733(5)	9273(2)	1217(1)	39(1)
C(82)	1129(5)	9697(2)	1034(1)	42(1)
C(83)	2027(4)	9977(2)	1202(1)	35(1)
C(84)	2513(4)	9821(2)	1528(1)	27(1)
N(1S)	6860(6)	10047(3)	999(2)	87(2)
C(1S)	6413(7)	10502(3)	1020(2)	88(2)
C(2S)	6895(10)	10888(4)	827(3)	112(3)

C(3S)	7766(10)	10803(4)	590(3)	132(4)
C(4S)	8233(8)	10333(5)	556(3)	131(4)
C(5S)	7747(7)	9964(3)	767(2)	87(2)
N(2S)	-1276(5)	6009(2)	4543(2)	72(2)
C(6S)	-2226(7)	6144(2)	4352(2)	72(2)
C(7S)	-3325(7)	5963(3)	4393(2)	81(2)
C(8S)	-3462(8)	5608(4)	4635(3)	102(3)
C(9S)	-2564(10)	5424(3)	4850(2)	92(3)
C(10S)	-1418(8)	5642(3)	4804(2)	92(3)
N(3S)	-1848(13)	11124(3)	3300(2)	134(3)
C(11S)	-2806(10)	11036(3)	3520(4)	120(3)
C(12S)	-2701(15)	10915(5)	3878(4)	164(6)
C(13S)	-1735(14)	10880(5)	4037(3)	133(5)
C(14S)	-671(11)	10915(5)	3850(5)	148(5)
C(15S)	-727(11)	11077(4)	3474(4)	125(4)
N(4S)	-1512(8)	8669(5)	-146(2)	145(3)
C(16S)	-1250(14)	8280(5)	73(5)	241(9)
C(17S)	-231(18)	8285(6)	286(6)	325(15)
C(18S)	339(9)	8694(5)	338(2)	119(4)
C(19S)	-107(12)	9113(4)	208(4)	196(7)
C(20S)	-974(13)	9097(4)	-46(4)	188(6)

Table 2.6. Bond lengths [Å] and angles [°] for **5-(pyr)$_2$**.

Co(1)-N(1)	1.882(3)	C(1)-C(6)	1.424(6)
Co(1)-O(1)	1.887(3)	C(2)-C(3)	1.392(7)
Co(1)-O(2)	1.891(3)	C(2)-C(25)	1.529(7)
Co(1)-N(2)	1.896(3)	C(3)-C(4)	1.397(8)
Co(1)-N(4)	1.967(4)	C(4)-C(5)	1.341(7)
Co(1)-N(3)	1.978(4)	C(4)-C(29)	1.529(9)
Co(2)-N(5)	1.892(4)	C(5)-C(6)	1.384(6)
Co(2)-O(4)	1.892(3)	C(6)-C(7)	1.424(6)
Co(2)-N(6)	1.897(4)	C(8)-C(13)	1.518(6)
Co(2)-O(3)	1.911(3)	C(8)-C(9)	1.515(6)
Co(2)-N(7)	1.957(4)	C(9)-C(10)	1.533(6)
Co(2)-N(8)	1.966(4)	C(10)-C(11)	1.506(6)
O(1)-C(1)	1.315(5)	C(11)-C(12)	1.534(6)
O(2)-C(24)	1.321(5)	C(12)-C(13)	1.495(6)
O(3)-C(66)	1.316(5)	C(14)-C(15)	1.434(6)
O(4)-C(43)	1.319(5)	C(15)-C(16)	1.393(6)
N(1)-C(7)	1.295(5)	C(15)-C(24)	1.444(5)
N(1)-C(8)	1.471(5)	C(16)-C(17)	1.390(6)
N(2)-C(14)	1.290(5)	C(17)-C(22)	1.414(6)
N(2)-C(13)	1.495(5)	C(17)-C(18)	1.439(6)
N(3)-C(37)	1.306(5)	C(18)-C(19)	1.342(6)
N(3)-C(33)	1.345(5)	C(19)-C(20)	1.426(7)
N(4)-C(38)	1.331(6)	C(20)-C(21)	1.385(6)
N(4)-C(42)	1.334(6)	C(21)-C(22)	1.424(6)
N(5)-C(49)	1.276(5)	C(22)-C(23)	1.400(6)
N(5)-C(50)	1.463(5)	C(23)-C(24)	1.404(5)
N(6)-C(56)	1.271(5)	C(23)-C(65)	1.495(5)
N(6)-C(55)	1.497(5)	C(25)-C(27)	1.542(7)
N(7)-C(79)	1.341(6)	C(25)-C(28)	1.531(6)
N(7)-C(75)	1.364(6)	C(25)-C(26)	1.564(7)
N(8)-C(80)	1.328(5)	C(29)-C(32)	1.420(10)
N(8)-C(84)	1.364(5)	C(29)-C(31)	1.524(9)
C(1)-C(2)	1.397(7)	C(29)-C(30)	1.648(11)

C(33)-C(34)	1.391(7)	C(67)-C(70)	1.540(7)
C(34)-C(35)	1.371(7)	C(67)-C(68)	1.569(8)
C(35)-C(36)	1.382(7)	C(71)-C(72)	1.521(9)
C(36)-C(37)	1.392(6)	C(71)-C(73)	1.545(8)
C(38)-C(39)	1.408(7)	C(71)-C(74)	1.553(8)
C(39)-C(40)	1.349(8)	C(75)-C(76)	1.369(6)
C(40)-C(41)	1.357(8)	C(76)-C(77)	1.392(7)
C(41)-C(42)	1.363(7)	C(77)-C(78)	1.386(7)
C(43)-C(44)	1.414(6)	C(78)-C(79)	1.376(6)
C(43)-C(48)	1.423(6)	C(80)-C(81)	1.406(6)
C(44)-C(45)	1.380(7)	C(81)-C(82)	1.385(7)
C(44)-C(67)	1.531(7)	C(82)-C(83)	1.394(7)
C(45)-C(46)	1.412(7)	C(83)-C(84)	1.356(6)
C(46)-C(47)	1.371(7)	N(1S)-C(5S)	1.317(8)
C(46)-C(71)	1.528(7)	N(1S)-C(1S)	1.320(8)
C(47)-C(48)	1.402(6)	C(1S)-C(2S)	1.357(10)
C(48)-C(49)	1.445(6)	C(2S)-C(3S)	1.316(11)
C(50)-C(55)	1.509(6)	C(3S)-C(4S)	1.369(11)
C(50)-C(51)	1.550(6)	C(4S)-C(5S)	1.359(9)
C(51)-C(52)	1.541(7)	N(2S)-C(6S)	1.321(7)
C(52)-C(53)	1.546(7)	N(2S)-C(10S)	1.366(8)
C(53)-C(54)	1.522(7)	C(6S)-C(7S)	1.335(9)
C(54)-C(55)	1.510(6)	C(7S)-C(8S)	1.296(9)
C(56)-C(57)	1.426(6)	C(8S)-C(9S)	1.363(10)
C(57)-C(58)	1.390(6)	C(9S)-C(10S)	1.425(10)
C(57)-C(66)	1.443(6)	N(3S)-C(11S)	1.356(10)
C(58)-C(59)	1.403(6)	N(3S)-C(15S)	1.412(11)
C(59)-C(60)	1.405(6)	C(11S)-C(12S)	1.328(11)
C(59)-C(64)	1.429(6)	C(12S)-C(13S)	1.230(12)
C(60)-C(61)	1.350(7)	C(13S)-C(14S)	1.374(12)
C(61)-C(62)	1.409(6)	C(14S)-C(15S)	1.421(11)
C(62)-C(63)	1.336(6)	N(4S)-C(16S)	1.338(11)
C(63)-C(64)	1.412(6)	N(4S)-C(20S)	1.345(10)
C(64)-C(65)	1.430(6)	C(16S)-C(17S)	1.377(12)
C(65)-C(66)	1.393(6)	C(17S)-C(18S)	1.283(12)
C(67)-C(69)	1.502(8)	C(18S)-C(19S)	1.313(11)

C(19S)-C(20S)	1.336(11)	C(7)-N(1)-Co(1)	125.1(3)
N(1)-Co(1)-O(1)	91.71(14)	C(8)-N(1)-Co(1)	112.0(3)
N(1)-Co(1)-O(2)	179.04(15)	C(14)-N(2)-C(13)	119.4(4)
O(1)-Co(1)-O(2)	88.25(12)	C(14)-N(2)-Co(1)	125.2(3)
N(1)-Co(1)-N(2)	84.69(15)	C(13)-N(2)-Co(1)	115.0(3)
O(1)-Co(1)-N(2)	175.62(14)	C(37)-N(3)-C(33)	119.6(4)
O(2)-Co(1)-N(2)	95.39(13)	C(37)-N(3)-Co(1)	124.2(3)
N(1)-Co(1)-N(4)	91.52(15)	C(33)-N(3)-Co(1)	116.0(3)
O(1)-Co(1)-N(4)	88.18(14)	C(38)-N(4)-C(42)	118.8(4)
O(2)-Co(1)-N(4)	89.44(14)	C(38)-N(4)-Co(1)	119.5(3)
N(2)-Co(1)-N(4)	89.42(15)	C(42)-N(4)-Co(1)	121.3(3)
N(1)-Co(1)-N(3)	89.80(15)	C(49)-N(5)-C(50)	124.1(4)
O(1)-Co(1)-N(3)	89.06(14)	C(49)-N(5)-Co(2)	124.5(3)
O(2)-Co(1)-N(3)	89.24(14)	C(50)-N(5)-Co(2)	111.3(3)
N(2)-Co(1)-N(3)	93.41(15)	C(56)-N(6)-C(55)	118.6(4)
N(4)-Co(1)-N(3)	176.98(15)	C(56)-N(6)-Co(2)	126.2(3)
N(5)-Co(2)-O(4)	92.51(15)	C(55)-N(6)-Co(2)	114.6(3)
N(5)-Co(2)-N(6)	84.48(16)	C(79)-N(7)-C(75)	118.4(4)
O(4)-Co(2)-N(6)	176.99(15)	C(79)-N(7)-Co(2)	122.6(3)
N(5)-Co(2)-O(3)	178.38(15)	C(75)-N(7)-Co(2)	118.9(3)
O(4)-Co(2)-O(3)	88.89(13)	C(80)-N(8)-C(84)	118.7(4)
N(6)-Co(2)-O(3)	94.12(14)	C(80)-N(8)-Co(2)	115.5(3)
N(5)-Co(2)-N(7)	90.20(15)	C(84)-N(8)-Co(2)	124.3(3)
O(4)-Co(2)-N(7)	86.24(14)	O(1)-C(1)-C(2)	119.2(4)
N(6)-Co(2)-N(7)	93.83(15)	O(1)-C(1)-C(6)	122.2(4)
O(3)-Co(2)-N(7)	89.08(14)	C(2)-C(1)-C(6)	118.5(4)
N(5)-Co(2)-N(8)	90.61(15)	C(3)-C(2)-C(1)	116.8(5)
O(4)-Co(2)-N(8)	85.31(14)	C(3)-C(2)-C(25)	121.0(5)
N(6)-Co(2)-N(8)	94.63(15)	C(1)-C(2)-C(25)	122.1(4)
O(3)-Co(2)-N(8)	90.31(14)	C(2)-C(3)-C(4)	125.6(6)
N(7)-Co(2)-N(8)	171.54(15)	C(5)-C(4)-C(3)	115.5(5)
C(1)-O(1)-Co(1)	125.9(3)	C(5)-C(4)-C(29)	124.7(6)
C(24)-O(2)-Co(1)	126.2(2)	C(3)-C(4)-C(29)	118.9(6)
C(66)-O(3)-Co(2)	125.8(3)	C(4)-C(5)-C(6)	123.3(5)
C(43)-O(4)-Co(2)	124.1(3)	C(5)-C(6)-C(1)	120.1(4)
C(7)-N(1)-C(8)	122.9(4)	C(5)-C(6)-C(7)	117.7(5)

C(1)-C(6)-C(7)	121.8(4)	C(2)-C(25)-C(26)	110.8(4)
N(1)-C(7)-C(6)	124.6(4)	C(27)-C(25)-C(26)	109.4(4)
N(1)-C(8)-C(13)	107.7(3)	C(28)-C(25)-C(26)	107.0(4)
N(1)-C(8)-C(9)	118.7(3)	C(32)-C(29)-C(31)	115.3(8)
C(13)-C(8)-C(9)	108.7(4)	C(32)-C(29)-C(4)	113.5(8)
C(8)-C(9)-C(10)	107.0(3)	C(31)-C(29)-C(4)	111.1(6)
C(11)-C(10)-C(9)	112.4(4)	C(32)-C(29)-C(30)	100.8(8)
C(10)-C(11)-C(12)	113.0(4)	C(31)-C(29)-C(30)	105.0(8)
C(13)-C(12)-C(11)	108.8(4)	C(4)-C(29)-C(30)	110.3(7)
N(2)-C(13)-C(12)	117.0(3)	N(3)-C(33)-C(34)	120.6(5)
N(2)-C(13)-C(8)	106.9(3)	C(35)-C(34)-C(33)	120.0(5)
C(12)-C(13)-C(8)	109.1(4)	C(34)-C(35)-C(36)	118.5(5)
N(2)-C(14)-C(15)	125.5(4)	C(35)-C(36)-C(37)	118.4(5)
C(16)-C(15)-C(14)	116.5(4)	N(3)-C(37)-C(36)	122.8(4)
C(16)-C(15)-C(24)	120.0(4)	N(4)-C(38)-C(39)	121.0(5)
C(14)-C(15)-C(24)	123.5(4)	C(40)-C(39)-C(38)	119.7(5)
C(17)-C(16)-C(15)	120.9(4)	C(39)-C(40)-C(41)	117.8(5)
C(16)-C(17)-C(22)	119.7(4)	C(40)-C(41)-C(42)	121.5(5)
C(16)-C(17)-C(18)	120.7(4)	N(4)-C(42)-C(41)	121.1(5)
C(22)-C(17)-C(18)	119.6(4)	O(4)-C(43)-C(44)	119.6(4)
C(19)-C(18)-C(17)	121.6(5)	O(4)-C(43)-C(48)	122.8(4)
C(18)-C(19)-C(20)	119.1(5)	C(44)-C(43)-C(48)	117.6(4)
C(21)-C(20)-C(19)	121.2(4)	C(45)-C(44)-C(43)	117.9(4)
C(20)-C(21)-C(22)	120.3(4)	C(45)-C(44)-C(67)	121.3(4)
C(23)-C(22)-C(17)	120.2(4)	C(43)-C(44)-C(67)	120.9(4)
C(23)-C(22)-C(21)	121.6(4)	C(44)-C(45)-C(46)	124.8(5)
C(17)-C(22)-C(21)	118.1(4)	C(47)-C(46)-C(45)	116.8(5)
C(22)-C(23)-C(24)	120.7(4)	C(47)-C(46)-C(71)	123.5(5)
C(22)-C(23)-C(65)	119.8(4)	C(45)-C(46)-C(71)	119.7(5)
C(24)-C(23)-C(65)	119.1(4)	C(46)-C(47)-C(48)	120.6(5)
O(2)-C(24)-C(23)	119.2(4)	C(47)-C(48)-C(43)	121.9(4)
O(2)-C(24)-C(15)	122.4(3)	C(47)-C(48)-C(49)	116.6(4)
C(23)-C(24)-C(15)	118.4(4)	C(43)-C(48)-C(49)	121.4(4)
C(2)-C(25)-C(27)	108.6(4)	N(5)-C(49)-C(48)	125.0(4)
C(2)-C(25)-C(28)	113.0(4)	N(5)-C(50)-C(55)	107.4(4)
C(27)-C(25)-C(28)	107.9(5)	N(5)-C(50)-C(51)	117.3(4)

C(55)-C(50)-C(51)	109.2(4)	C(72)-C(71)-C(73)	109.2(5)
C(52)-C(51)-C(50)	107.3(4)	C(46)-C(71)-C(73)	109.8(5)
C(51)-C(52)-C(53)	112.3(4)	C(72)-C(71)-C(74)	108.7(5)
C(54)-C(53)-C(52)	111.4(4)	C(46)-C(71)-C(74)	110.0(5)
C(55)-C(54)-C(53)	108.9(4)	C(73)-C(71)-C(74)	108.3(5)
N(6)-C(55)-C(50)	105.9(3)	N(7)-C(75)-C(76)	122.7(5)
N(6)-C(55)-C(54)	116.5(4)	C(75)-C(76)-C(77)	118.8(5)
C(50)-C(55)-C(54)	110.9(4)	C(78)-C(77)-C(76)	118.2(5)
N(6)-C(56)-C(57)	126.0(4)	C(79)-C(78)-C(77)	120.4(5)
C(58)-C(57)-C(56)	115.8(4)	N(7)-C(79)-C(78)	121.4(5)
C(58)-C(57)-C(66)	121.0(4)	N(8)-C(80)-C(81)	121.6(4)
C(56)-C(57)-C(66)	123.0(4)	C(82)-C(81)-C(80)	119.3(5)
C(57)-C(58)-C(59)	121.8(4)	C(81)-C(82)-C(83)	118.0(5)
C(58)-C(59)-C(60)	122.1(4)	C(84)-C(83)-C(82)	119.9(4)
C(58)-C(59)-C(64)	117.8(4)	C(83)-C(84)-N(8)	122.2(4)
C(60)-C(59)-C(64)	120.0(4)	C(5S)-N(1S)-C(1S)	118.7(7)
C(61)-C(60)-C(59)	121.0(5)	N(1S)-C(1S)-C(2S)	121.5(8)
C(60)-C(61)-C(62)	119.0(5)	C(3S)-C(2S)-C(1S)	119.7(9)
C(63)-C(62)-C(61)	121.6(4)	C(2S)-C(3S)-C(4S)	120.1(9)
C(62)-C(63)-C(64)	121.8(4)	C(5S)-C(4S)-C(3S)	117.7(9)
C(63)-C(64)-C(59)	116.6(4)	N(1S)-C(5S)-C(4S)	122.2(8)
C(63)-C(64)-C(65)	122.7(4)	C(6S)-N(2S)-C(10S)	117.3(6)
C(59)-C(64)-C(65)	120.6(4)	N(2S)-C(6S)-C(7S)	126.3(7)
C(66)-C(65)-C(64)	120.9(4)	C(8S)-C(7S)-C(6S)	116.7(8)
C(66)-C(65)-C(23)	120.8(4)	C(7S)-C(8S)-C(9S)	123.9(8)
C(64)-C(65)-C(23)	118.3(4)	C(8S)-C(9S)-C(10S)	117.0(7)
O(3)-C(66)-C(65)	119.5(4)	N(2S)-C(10S)-C(9S)	118.7(7)
O(3)-C(66)-C(57)	122.5(4)	C(11S)-N(3S)-C(15S)	115.8(9)
C(65)-C(66)-C(57)	117.9(4)	C(12S)-C(11S)-N(3S)	122.3(11)
C(69)-C(67)-C(44)	112.9(4)	C(13S)-C(12S)-C(11S)	123.1(13)
C(69)-C(67)-C(70)	108.2(5)	C(12S)-C(13S)-C(14S)	122.4(11)
C(44)-C(67)-C(70)	112.4(4)	C(13S)-C(14S)-C(15S)	116.5(10)
C(69)-C(67)-C(68)	109.4(5)	N(3S)-C(15S)-C(14S)	119.1(9)
C(44)-C(67)-C(68)	107.2(5)	C(16S)-N(4S)-C(20S)	114.1(9)
C(70)-C(67)-C(68)	106.5(4)	N(4S)-C(16S)-C(17S)	120.1(13)
C(72)-C(71)-C(46)	110.8(5)	C(18S)-C(17S)-C(16S)	120.2(13)

C(17S)-C(18S)-C(19S)	119.2(10)
C(18S)-C(19S)-C(20S)	119.6(10)
C(19S)-C(20S)-N(4S)	122.4(10)

Symmetry transformations used to generate equivalent atoms:

Table 2.7. Anisotropic displacement parameters ($Å^2 x\ 10^3$) for **5-(pyr)$_2$**. The anisotropic displacement factor exponent takes the form: $-2p^2[\ h^2\ a^{*2}U^{11} + ...\ + 2\ h\ k\ a^*\ b^*\ U^{12}\ ]$

	U^{11}	U^{22}	U^{33}	U^{23}	U^{13}	U^{12}
Co(1)	26(1)	19(1)	25(1)	1(1)	-1(1)	-1(1)
Co(2)	25(1)	20(1)	29(1)	2(1)	3(1)	-1(1)
Cl(1)	63(1)	35(1)	74(1)	-2(1)	14(1)	-11(1)
Cl(2)	64(1)	50(1)	62(1)	15(1)	-12(1)	-11(1)
O(1)	38(2)	26(2)	27(2)	2(2)	-4(2)	-5(2)
O(2)	28(2)	17(2)	27(2)	2(1)	-6(2)	-2(1)
O(3)	25(2)	17(2)	32(2)	0(1)	3(1)	1(1)
O(4)	37(2)	22(2)	27(2)	2(1)	6(2)	2(2)
N(1)	27(2)	20(2)	31(2)	-1(2)	0(2)	2(2)
N(2)	23(2)	16(2)	26(2)	2(2)	4(2)	2(2)
N(3)	32(2)	24(2)	26(2)	2(2)	0(2)	1(2)
N(4)	25(2)	21(2)	40(2)	1(2)	-6(2)	-3(2)
N(5)	25(2)	25(2)	29(2)	3(2)	3(2)	0(2)
N(6)	27(2)	22(2)	27(2)	4(2)	4(2)	-2(2)
N(7)	24(2)	29(2)	30(2)	2(2)	5(2)	-1(2)
N(8)	27(2)	27(2)	24(2)	2(2)	4(2)	-1(2)
C(1)	32(3)	33(3)	29(3)	3(2)	-8(2)	-3(2)
C(2)	51(3)	29(3)	40(3)	-5(2)	-4(3)	0(3)
C(3)	101(5)	59(4)	33(3)	-9(3)	-1(3)	-11(4)
C(4)	121(6)	58(4)	39(3)	-7(3)	0(4)	-28(4)
C(5)	80(4)	47(3)	29(3)	0(3)	9(3)	-7(3)
C(6)	43(3)	32(3)	29(3)	-2(2)	-7(2)	4(3)
C(7)	41(3)	33(3)	29(3)	8(2)	-1(3)	-1(2)
C(8)	32(3)	21(2)	30(2)	0(2)	4(2)	7(2)
C(9)	47(3)	20(2)	35(3)	4(2)	2(2)	0(2)
C(10)	58(3)	28(3)	33(3)	5(2)	6(3)	2(2)
C(11)	46(3)	19(2)	44(3)	-3(2)	-1(3)	2(2)
C(12)	44(3)	18(2)	35(3)	-3(2)	6(2)	2(2)
C(13)	37(3)	14(2)	30(2)	-1(2)	6(2)	0(2)

C(14)	20(2)	17(2)	31(3)	1(2)	0(2)	-2(2)
C(15)	13(2)	24(2)	29(2)	0(2)	0(2)	-1(2)
C(16)	33(3)	29(2)	19(2)	-8(2)	0(2)	-1(2)
C(17)	34(3)	25(2)	23(2)	2(2)	3(2)	5(2)
C(18)	47(3)	33(3)	32(3)	-5(2)	-9(2)	3(2)
C(19)	59(4)	37(3)	29(3)	3(2)	-13(3)	2(3)
C(20)	45(3)	40(3)	35(3)	7(2)	2(3)	8(3)
C(21)	35(3)	25(2)	27(2)	2(2)	1(2)	0(2)
C(22)	26(2)	23(2)	24(2)	-1(2)	2(2)	2(2)
C(23)	15(2)	17(2)	26(2)	-2(2)	4(2)	1(2)
C(24)	19(2)	15(2)	26(2)	-3(2)	3(2)	0(2)
C(25)	64(4)	39(3)	33(3)	-5(2)	-3(3)	-10(3)
C(26)	77(4)	34(3)	49(3)	4(3)	-19(3)	-7(3)
C(27)	56(4)	61(4)	56(4)	-6(3)	-5(3)	-17(3)
C(28)	91(5)	55(4)	46(3)	-14(3)	-10(3)	-23(4)
C(29)	216(12)	101(6)	51(5)	-13(5)	35(6)	-29(7)
C(30)	155(9)	174(10)	81(6)	17(6)	-32(7)	-45(8)
C(31)	140(8)	113(6)	45(4)	12(4)	9(5)	-44(6)
C(32)	224(12)	135(8)	94(6)	-45(6)	92(8)	-38(9)
C(33)	36(3)	27(3)	34(3)	-5(2)	6(2)	3(2)
C(34)	55(4)	33(3)	38(3)	-3(2)	-3(3)	8(3)
C(35)	36(3)	52(3)	38(3)	-5(3)	8(2)	9(3)
C(36)	45(3)	41(3)	39(3)	-1(3)	1(3)	-12(3)
C(37)	22(3)	30(3)	31(3)	-1(2)	5(2)	-1(2)
C(38)	33(3)	29(3)	34(3)	6(2)	2(2)	-4(2)
C(39)	43(3)	45(3)	55(3)	-11(3)	6(3)	-4(3)
C(40)	22(3)	36(3)	93(5)	-7(3)	2(3)	6(2)
C(41)	31(3)	36(3)	73(4)	8(3)	-7(3)	2(3)
C(42)	31(3)	24(2)	43(3)	5(2)	-8(2)	-1(2)
C(43)	33(3)	24(3)	33(3)	2(2)	6(2)	8(2)
C(44)	43(3)	25(3)	33(3)	0(2)	5(3)	4(2)
C(45)	49(3)	40(3)	41(3)	-1(3)	7(3)	5(3)
C(46)	47(3)	45(3)	36(3)	4(3)	9(3)	7(3)
C(47)	40(3)	42(3)	33(3)	2(2)	2(2)	-5(3)
C(48)	26(3)	33(3)	29(3)	5(2)	3(2)	2(2)
C(49)	25(3)	35(3)	33(3)	7(2)	-2(2)	2(2)

C(50)	21(2)	25(2)	38(3)	0(2)	-2(2)	-6(2)
C(51)	32(3)	41(3)	49(3)	-7(3)	7(3)	-9(2)
C(52)	34(3)	62(4)	51(3)	-6(3)	5(3)	-20(3)
C(53)	48(3)	47(3)	58(4)	-19(3)	3(3)	-12(3)
C(54)	33(3)	37(3)	40(3)	-6(2)	7(2)	-10(2)
C(55)	23(2)	30(3)	39(3)	3(2)	6(2)	-6(2)
C(56)	28(3)	20(2)	31(3)	-3(2)	2(2)	-4(2)
C(57)	22(2)	26(2)	30(3)	3(2)	1(2)	-2(2)
C(58)	36(3)	26(2)	24(2)	-4(2)	-1(2)	-1(2)
C(59)	27(3)	26(2)	28(3)	-2(2)	1(2)	-1(2)
C(60)	41(3)	30(3)	43(3)	-8(2)	3(3)	4(2)
C(61)	37(3)	34(3)	57(4)	-15(3)	19(3)	4(2)
C(62)	25(3)	39(3)	47(3)	-4(2)	2(2)	0(2)
C(63)	21(2)	25(2)	35(3)	-4(2)	-1(2)	-3(2)
C(64)	27(2)	21(2)	25(2)	3(2)	-3(2)	-1(2)
C(65)	23(2)	12(2)	28(2)	0(2)	-2(2)	4(2)
C(66)	22(2)	18(2)	28(2)	-2(2)	-1(2)	-1(2)
C(67)	69(4)	28(3)	43(3)	-6(3)	15(3)	-5(3)
C(68)	119(6)	37(3)	59(4)	9(3)	-2(4)	3(4)
C(69)	76(4)	46(4)	64(4)	-16(3)	16(4)	-26(3)
C(70)	86(5)	52(4)	62(4)	-22(3)	15(4)	-13(4)
C(71)	67(4)	58(4)	32(3)	-2(3)	12(3)	-2(3)
C(72)	88(5)	97(5)	48(4)	2(4)	7(4)	15(4)
C(73)	89(5)	83(5)	49(4)	-9(4)	15(4)	11(4)
C(74)	128(6)	83(5)	42(4)	4(3)	28(4)	-22(5)
C(75)	40(3)	34(3)	42(3)	6(2)	1(2)	0(2)
C(76)	33(3)	30(3)	53(3)	9(3)	0(3)	4(2)
C(77)	39(3)	33(3)	52(3)	7(2)	-10(3)	-1(2)
C(78)	37(3)	44(3)	37(3)	12(3)	-2(3)	2(3)
C(79)	30(3)	34(3)	28(3)	3(2)	6(2)	-4(2)
C(80)	32(3)	19(2)	33(3)	-6(2)	3(2)	-1(2)
C(81)	48(3)	31(3)	37(3)	0(2)	-1(3)	-2(2)
C(82)	44(3)	50(3)	30(3)	7(3)	3(3)	7(3)
C(83)	38(3)	31(3)	36(3)	7(2)	6(2)	-3(2)
C(84)	23(2)	21(2)	39(3)	5(2)	3(2)	2(2)
N(1S)	81(4)	88(5)	92(5)	29(4)	1(4)	-5(4)

C(1S)	92(6)	104(7)	67(5)	30(5)	5(4)	8(5)
C(2S)	136(9)	107(7)	93(7)	26(6)	-31(6)	10(7)
C(3S)	118(9)	141(10)	136(10)	81(9)	-22(8)	-40(8)
C(4S)	78(6)	214(12)	100(7)	70(8)	14(5)	-9(8)
C(5S)	72(5)	124(7)	66(5)	13(5)	1(4)	5(5)
N(2S)	74(4)	62(4)	81(4)	-2(3)	10(3)	-12(3)
C(6S)	71(5)	61(4)	83(5)	1(4)	7(4)	2(4)
C(7S)	87(6)	84(5)	73(5)	-21(5)	9(4)	6(5)
C(8S)	97(7)	102(7)	108(7)	-28(6)	21(6)	-20(6)
C(9S)	142(8)	71(5)	64(5)	2(4)	46(6)	-3(6)
C(10S)	123(8)	82(6)	71(5)	-22(5)	16(5)	19(6)
N(3S)	197(10)	94(6)	111(7)	-10(5)	38(8)	10(7)
C(11S)	139(9)	73(6)	148(10)	-40(7)	17(9)	13(6)
C(12S)	290(20)	112(9)	93(9)	7(8)	49(11)	-24(12)
C(13S)	159(12)	147(10)	92(8)	23(7)	-29(9)	32(10)
C(14S)	105(9)	167(11)	171(12)	-54(11)	-26(9)	-19(8)
C(15S)	119(10)	79(7)	178(13)	-72(8)	43(9)	-19(6)
N(4S)	139(8)	162(9)	135(7)	-17(7)	-29(6)	22(8)
C(16S)	280(20)	105(9)	340(20)	8(13)	-181(17)	31(11)
C(17S)	370(30)	194(17)	410(30)	-25(17)	-310(30)	13(18)
C(18S)	85(6)	187(11)	85(6)	-46(7)	-24(5)	34(8)
C(19S)	191(13)	120(10)	277(17)	-37(10)	-165(13)	0(9)
C(20S)	250(17)	82(8)	231(15)	39(9)	-93(13)	-14(9)

Table 2.8. Hydrogen coordinates (x 10^4) and isotropic displacement parameters (Å^{2}x 10^3) for **5-(pyr)$_2$**.

	x	y	z	U(eq)
H(3A)	1116	8269	4687	77
H(5A)	-88	6889	4562	63
H(7A)	152	6467	4004	41
H(8A)	1277	6244	3219	33
H(9A)	-698	5769	3574	41
H(9B)	623	5766	3746	41
H(10A)	1372	5360	3211	47
H(10B)	290	5035	3371	47
H(11A)	-974	5321	2913	43
H(11B)	210	5131	2711	43
H(12A)	869	5955	2621	39
H(12B)	-468	5921	2466	39
H(13A)	-1182	6225	3041	33
H(14A)	-1002	6669	2357	27
H(16A)	-1698	7184	1894	32
H(18A)	-2637	7696	1410	45
H(19A)	-2968	8457	1140	50
H(20A)	-2226	9189	1430	48
H(21A)	-1160	9144	1984	35
H(26A)	174	8924	3838	80
H(26B)	706	8590	3508	80
H(26C)	1329	9108	3616	80
H(27A)	3399	8206	3985	86
H(27B)	3299	8679	3714	86
H(27C)	2708	8158	3597	86
H(28A)	1298	9018	4432	96
H(28B)	2427	9200	4197	96
H(28C)	2559	8751	4489	96
H(30A)	1739	7565	5559	205
H(30B)	2068	7933	5223	205

H(30C)	2282	7345	5180	205
H(31A)	26	7003	5516	149
H(31B)	539	6767	5139	149
H(31C)	-808	6959	5156	149
H(32A)	-163	7899	5563	227
H(32B)	-1010	7956	5207	227
H(32C)	221	8256	5226	227
H(33A)	-954	8189	3375	39
H(34A)	-2699	8438	3676	50
H(35A)	-4126	7845	3838	50
H(36A)	-3788	7005	3678	50
H(37A)	-2015	6793	3379	34
H(38A)	1580	7313	2483	39
H(39A)	3445	7057	2255	57
H(40A)	4841	6728	2662	60
H(41A)	4374	6694	3289	56
H(42A)	2585	6986	3506	39
H(45A)	3237	8046	547	52
H(47A)	5210	9245	815	46
H(49A)	5541	9449	1440	37
H(50A)	5565	9373	2318	33
H(51A)	6782	9770	1851	49
H(51B)	5829	10216	1821	49
H(52A)	7344	10459	2247	59
H(52B)	7149	9961	2485	59
H(53A)	6201	10622	2802	61
H(53B)	5476	10774	2435	61
H(54A)	5114	9876	2857	44
H(54B)	4186	10330	2828	44
H(55A)	4003	10186	2178	37
H(56A)	2584	9983	2782	32
H(58A)	791	9969	3065	35
H(60A)	-1191	10028	3361	45
H(61A)	-3115	9744	3414	51
H(62A)	-3696	9019	3091	44
H(63A)	-2405	8599	2723	32

H(68A)	3429	7632	1706	108
H(68B)	4000	7323	1369	108
H(68C)	2821	7123	1570	108
H(69A)	1418	8075	1590	93
H(69B)	924	7537	1473	93
H(69C)	774	8002	1197	93
H(70A)	1748	7546	688	100
H(70B)	1835	7072	959	100
H(70C)	3005	7281	758	100
H(72A)	2837	8546	11	117
H(72B)	3575	8864	-288	117
H(72C)	3005	9134	68	117
H(73A)	4587	7972	71	110
H(73B)	5857	8192	187	110
H(73C)	5329	8304	-218	110
H(74A)	6122	9119	270	127
H(74B)	5005	9486	232	127
H(74C)	5541	9219	-130	127
H(75A)	5209	8384	1964	46
H(76A)	6323	7810	2293	47
H(77A)	5903	7678	2931	49
H(78A)	4329	8123	3202	47
H(79A)	3236	8684	2852	37
H(80A)	980	8848	1684	34
H(81A)	106	9078	1114	47
H(82A)	797	9795	802	50
H(83A)	2299	10276	1088	42
H(84A)	3107	10022	1643	33
H(1SA)	6571	9804	1137	105
H(1SB)	5739	10560	1173	105
H(2SA)	6605	11217	862	135
H(3SA)	8071	11068	442	158
H(4SA)	8875	10267	391	157
H(5SA)	8057	9635	746	105
H(2SB)	-578	6149	4504	87
H(6SA)	-2118	6394	4167	86

H(7SA)	-3975	6088	4252	98
H(8SA)	-4233	5469	4664	123
H(9SA)	-2697	5161	5023	111
H(10C)	-765	5535	4952	110
H(3SB)	-1921	11206	3064	161
H(11C)	-3580	11061	3415	144
H(12C)	-3404	10853	4017	196
H(13B)	-1725	10826	4299	159
H(14B)	64	10836	3967	177
H(15A)	-19	11152	3340	150
H(4SB)	-1993	8647	-339	175
H(16B)	-1769	8000	82	289
H(17A)	51	7984	395	390
H(18B)	1074	8694	469	143
H(19B)	186	9425	295	235
H(20B)	-1220	9400	-160	225

2.5. References and Notes

(1) (a) Stevens, M. P. *Polymer Chemistry*; Oxford University Press: New York, 1999; Chapter 11 (b) Wilms, D.; Stiriba, S.-E.; Frey, H. *Acc. Chem. Res.* **2009**, *43*, 129. (c) Odian, G. *Principles of Polymerization*, 4th Ed.; John Wiley and Sons: Hoboken, NJ, 2004.

(2) (a) Kuran, W. *Prog. Polym. Sci.* **1998**, *23*, 919 and references therein. (b) *Stereoselective Polymerization with Single Site Catalysts*; Baugh, L. S., Canich, J. M., Eds.; CRC Press: Boca Raton, 2008. (c) Okamoto, Y. *Prog. Polym. Sci.* **2005**, *25*, 159.

(3) Pruitt, M. E.; Baggett, J. M. (Dow Chemical Co.) U.S. Patent 2706181, 1955.

(4) (a) Price, C. C.; Osgan, M. *J. Am. Chem. Soc.* **1956**, *78*, 4787. (b) Osgan, M.; Price, C. C. *J. Polym. Sci.* **1959**, *34*, 153.

(5) (a) Vandenberg, E. J. (Hercules Powder Co.). U.S. Patent 3219591, 1965. (b) Vandenberg, E. *Polymer* **1994**, *35*, 4933. (c) Wu, B.; Harlan, C. J.; Lenz, R. W.; Barron, A. R. *Macromolecules* **1997**, *30*, 316. (d) Takeda, N.; Inoue, S. *Makromol. Chem.* **1978**, 179, 1377. (e) Le Borgne, A.; Spassky, N.; Jun, C. L.; Momtaz, A. *Makromol. Chem.* **1988**, *189*, 637.

(6) (a) Hasebe, Y.; Tsuruta, T. *Makromol. Chem.-Macromol. Chem. Phys.* **1988**, *189*, 1915. (b) Yoshino, N.; Suzuki, C.; Kobayashi, H.; Tsuruta, T. *Makromol. Chem.-Macromol. Chem. Phys.* **1988**, *189*, 1903.

(7) Tsuruta, T.; Kawakami, Y. *Comprehensive Polymer Science*, Vol. 3, Eds.; Allen, G.; Bevington, J. C. Pergamon Press, Oxford, 1989; pp. 489.

(8) (a) Vandenberg, E. J. *Pure Appl. Chem.* **1976**, *48*, 295. (b) Vandenberg, E. J. *J. Polym. Sci.* **1960**, *47*, 486. (c) Vandenberg, E. J. *J. Polym. Sci., Part A-1: Polym. Chem.*, **1969**, *7*, 525. (d) Osgan, M.; Teyssie, Ph. *J. Polym. Sci., Part B: Polym. Phys.*, **1967**, *5*, 789. (e) Kohler, N.;

Osgan, M.; Teyssie, Ph. *J. Polym. Sci., Part B: Polym. Phys.*, **1968**, *6*, 559. (f) Osgan, M.; Teyssie, Ph. *J. Polym. Sci., Part B: Polym. Phys.*, **1970**, *8*, 319.

(9) Vandenberg, E. J. *J. Polym. Sci., Part A: Polym. Chem.* **1986**, *24*, 1423.

(10) Braune, W.; Okuda, J. *Angew. Chem. Int. Ed.* **2003**, *42*, 64.

(11) Peretti, K. L.; Ajiro, H.; Cohen, C. T.; Lobkovsky, E. B.; Coates, G. W. *J. Am. Chem. Soc.* **2005**, *127*, 11566.

(12) Ajiro, H.; Peretti, K. L.; Lobkovsky, E. B.; Coates, G. W. *Dalton Trans.* **2009**, 8828.

(13) Hirahata, W.; Thomas, R. M.; Lobkovsky, E. B.; Coates, G. W. *J. Am. Chem. Soc.* **2008**, *130*, 17658.

(14) Thomas, R. M.; Widger, P. C. B.; Ahmed, S. M.; Jeske, R. C.; Hirahata, W.; Lobkovsky, E. B.; Coates, G. W. *J. Am. Chem. Soc.* **2010**, *132*, 16520.

(15) (a) *Comprehensive Asymmetric Catalysis*; Jacobsen, E. N.; Pfaltz, A.; Yamamoto, H. Eds.; Springer: Berlin, 1999. (b) Halpern, J.; Trost, B. M. *Proc. Nat. Acad. Sci. U. S. A.* **2004**, *101*, 5347.

(16) Widger, P. C. B.; Ahmed, S. M.; Hirahata, W.; Thomas, R. M.; Lobkovsky, E. B.; Coates, G. W. *Chem. Commun.* **2010**, *46*, 2935.

(17) Widger, P. C. B.; Ahmed, S. M.; Coates, G. W. *Macromolecules* **2011**, *44*, 5666.

(18) Standard polymerization conditions using **4**: [PO] = 2 M in DME; PO:catalyst:cocatalyst= 4000:1:2; T_{rxn}= 0 °C; t_{rxn}= 15min.

(19) For each transition state shown in Figure 2.6, the methyl group of the PO was modeled pointing away from the catalyst cleft, as the analogous transition states with the methyl pointing into the cleft were at least 2 kcal/mol higher in energy.

(20) (a) Debuigne, A.; Poli, R.; Jerome, C.; Jerome, R.; Detrembleur, C. *Prog. Polym. Sci.* **2009**, *34*, 211. (b) Gansauer, A.; Barchuk, A.; Keller, F.; Schmitt, M.; Grimme, S.; Gerenkamp, M.; Muck-Lichtenfeld, C.; Daasbjerg, K.; Svith, H. *J. Am. Chem. Soc.* **2007**, *129*, 1359.

(21) Percec, V.; Wang, J. H. *Makromol. Chem.-Macromol. Symp.* **1992**, *54*, 337.

(22) (a) Cohen, C. T.; Chu, T.; Coates, G. W. *J. Am. Chem. Soc.* **2005**, *127*, 10869. (b) Cohen, C. T.; Coates, G. W. *J. Polym. Sci., Part A: Polym. Chem.* **2006**, *44*, 5182. (c) Darensbourg, D. J.; Phelps, A. L. *Inorg. Chem.* **2005**, *44*, 4622. (d) Aida, T.; Inoue, S. *J. Am. Chem. Soc.* **1985**, *107*, 1358. (e) Lu, X.; Wang, Y. *Angew. Chem., Int. Ed.* **2004**, *43*, 3574. (f) Aida, T.; Inoue, S. *Acc. Chem. Res.* **1996**, *29*, 39. (g) Aida, T.; Ishikawa, M.; Inoue, S. *Macromolecules* **1986**, *19*, 8. (h) Darensbourg, D. J.; Billodeaux, D. R. *Inorg. Chem.* **2005**, *44*, 1433. (i) Nakano, K.; Hashimoto, S.; Nozaki, K. *Chem. Sci.* **2010**, *1*, 369. (j) Sugitomo, H.; Kuroda, K. *Macromolecules* **2008**, *41*, 312. (k) Hosseini Nejad, E.; van Melis, C. G. W.; Vermeer, T. J.; Koning, C. E.; Duchateau, R. *Macromolecules* **2012**, *45*, 1770.

(23) (a) Nielsen, L. P. C.; Stevenson, C. P.; Blackmond, D. G.; Jacobsen, E. N. *J. Am. Chem. Soc.* **2004**, *126*, 1360. (b) Nielsen, L. P. C.; Zuend, S. J.; Ford, D. D.; Jacobsen, E. N. *J. Org. Chem.* **2012**, *77*, 2486.

(24) Ajiro, H.; Allen, S. D.; Coates, G. W. "Discrete Catalysts for Stereoselective Epoxide Polymerization" in ref. 2b, Chapter 24; pp. 627.

(25) Schaus, S. E.; Brandes, B. D.; Larrow, J. F.; Tokunaga, M.; Hansen, K. B.; Gould, A. E.; Furrow, M. E.; Jacobsen, E. N. *J. Am. Chem. Soc.* **2002**, *124*, 1307.

(26) Kemper, S.; HrobaÃÅrik, P.; Kaupp, M.; SchloÃàrer, N. E. *J. Am. Chem. Soc.* **2009**, *131*, 4172.

(27) Calculations are still in progress and are being conducted by Prof. Luigi Cavallo and Dr. Albert Poater.

(28) See Chapter 3.

(29) (a) Nomura, N.; Ishii, R.; Yamamoto, Y.; Kondo, T. *Chem.Eur. J.* **2007**, *13*, 4433. (b) Casiraghi, G.; Casnati, G.; Puglia, G.; Sartori, G.; Terenghi, G. *J. Chem. Soc., Perkin Trans. 1* **1980**, 1862. (c) Zhang, H. C.; Huang, W. S.; Pu, L. *J. Org. Chem.* **2001**, *66*, 481.

Chapter 3

Systematic Ligand Variations to Enhance a Highly Active Bimetallic Catalyst for Enantioselective Epoxide Polymerization

3.1. Introduction

The growing demand for chiral building blocks and stereoregular macromolecules in commodity and advanced materials necessitates the development of new and efficient methods to obtain them.[1] Chiral catalysts are often used to prepare enantiopure compounds,[2] as well as isotactic polymers via stereoselective polymerization.[1b,3] We recently reported a chiral bimetallic cobalt (III) catalyst (**3**), which in the presence of a cocatalyst enantioselectively polymerizes racemic monosubstituted epoxides to yield highly isotactic polyethers and enantiopure epoxides, as shown in Scheme 3.1.[4,5] The enantiopure epoxides attained using **3** serve as important reagents and intermediates for the pharmaceutical industry.[1c] Prior to this work, isotactic polyethers were extremely difficult to synthesize from racemic epoxides, and like their atactic counterparts, may find use in commodity materials such as foams, sealants and biomedical components.[6]

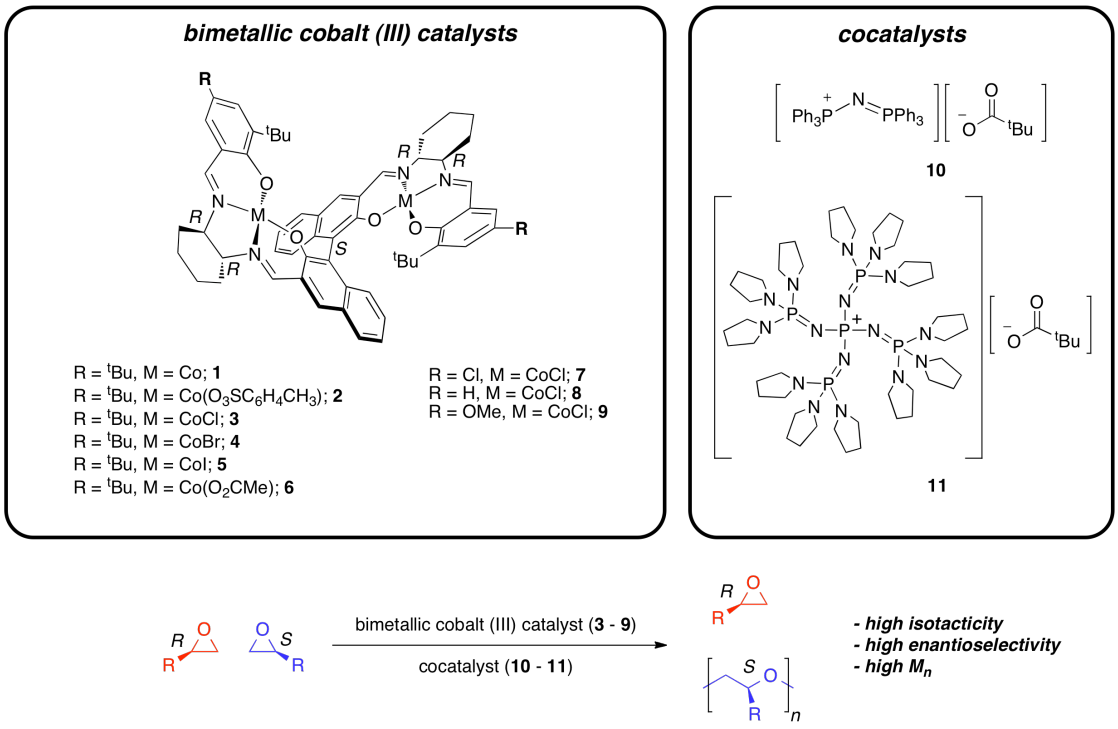

Scheme 3.1. Enantioselective polymerization of racemic epoxides using a bimetallic cobalt (III) catalyst and cocatalyst.

Catalyst **3** contains two optically pure *salen* moieties tethered by a chiral binaphthol linker. The orientation of the *salen* planes creates a chiral cleft that dictates the enantioselectivity of the catalyst and facilitates isoselective polymerization.[7] As shown in Scheme 3.2, we propose that after an epoxide coordinates to a Co inside the cleft, ring opening of the bound epoxide occurs via nucleophilic attack of a halide or alkoxide from the adjacent Co. The ring opening events continue to alternate between the adjacent Co centers yielding isotactic polyether.[8]

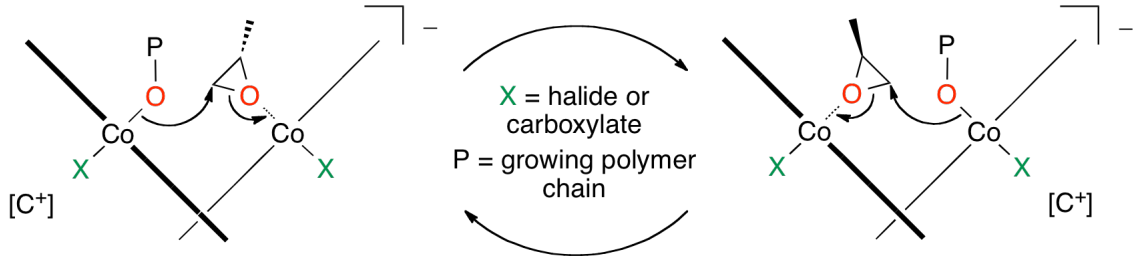

Scheme 3.2. Proposed mechanism of epoxide enchainment.

The activity and selectivity of the catalyst system (**3** with cocatalyst) were greatly improved with the use of new cocatalysts, such as bis(triphenylphosphine)iminium pivalate (**10**) and phosphazenium pivalate (**11**).[9] Monomeric Co(III) *salen* catalysts have been reported to show reactivity differences for epoxide hydroloysis and epoxide/CO_2 copolymerizations due to variations of the Co(III) axial ligands[10] and the substituents in the salicyl moieties.[11] Herein, we describe a systematic study of the effects of varying Co axial ligands and salicyl substituents to attain an improved active catalyst for enantioselective epoxide polymerization.

Bimetallic cobalt (III) catalysts containing a series of axial ligands (X = Br, I, and O_2CMe) were prepared by oxidizing the Co(II) precursor (**1**; Scheme 3.1) in the presence of *para*-toluenesulfonic acid to form the corresponding Co(III) tosylate complex (**2**). Subsequent salt metathesis of **2** yields catalysts **3** – **6**. In addition, a variety of ligand frameworks containing salicylaldehydes with electron-donating/withdrawing *para*-substituents[12] (R = Cl, H and OMe) were synthesized and metallated. Oxidation of the respective Co(II) species yielded catalysts **7** – **9**. Formation of **3** – **9** was confirmed by ^{1}H, ^{13}C, COSY, HSQC and HMBC NMR spectroscopy.

Single crystals of the tetrapyridine adduct of **9** were attained from a mixture of pyridine and toluene. Refinement of the x-ray diffraction data revealed two pyridine molecules bound to each Co center, and two chloride anions were also present in the unit cell (Figure 3.1); further analysis reveals a Co—Co separation of 6.72Å and a naphthol—naphthol dihedral angle of 79.9°. The parameters for the crystal structure of the tetrapyridine adduct of **9** are similar to that of **3**,[5] suggesting that differences in activity and selectivity observed (*vide infra*) may be due to the influence of the electron-donating salicyl substituents in the ligand framework on the Co centers, rather than structural differences.

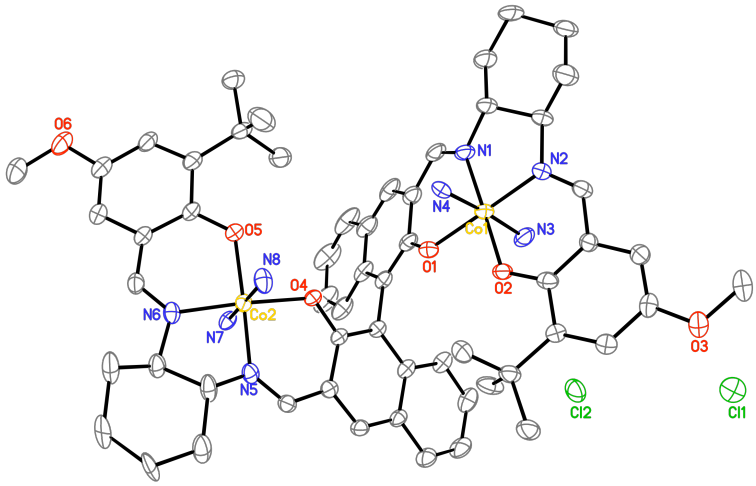

Figure 3.1. Molecular structure of tetrapyridine adduct of **9** (hydrogen atoms were omitted and pyridine ligands truncated for clarity; carbon atoms are also unlabelled). Thermal ellipsoids are at 40% probability level.

All polymerizations using catalysts **3** – **9** were conducted using a Freeslate Core Module 3 robot system in a nitrogen filled glove box. This allowed high precision and consistency for addition of reagents under controlled reaction conditions and permitted systematic screening of the prepared catalysts. Activities and selectivities for the polymerization of propylene oxide (PO) were then studied under identical conditions.

3.2. Results and Discussion

In order to assess the influence of the axial ligand, **3** – **6** were used with cocatalyst **10** for the enantioselective polymerization of PO under identical conditions. At high catalyst loadings (PO:catalyst = 4,000:1), **3** and **4** gave virtually quantitative yields poly(*S*-propylene oxide) (*S*-PPO), while **5** and **6** showed substantially lower conversions (Figure 2.2A). Direct comparison of **3** and **4** at much lower catalyst loadings (PO:catalyst = 16,000:1) shows the latter to be less active (Figure 2.2B). The catalysts **3** – **6** were then used to resolve PO, as shown in Table 2.1. The most active catalyst **3** yielded isotactic PPO with a high *mm* value and *s*-factor (Table 3.1, entry 1), while the least active catalyst **6** had the lowest *mm* value and significantly lower *s*-factor (Table 3.1, entry 4). These results indicate that the highest activity and stereoselectivity can be achieved with chloride as an axial ligand.

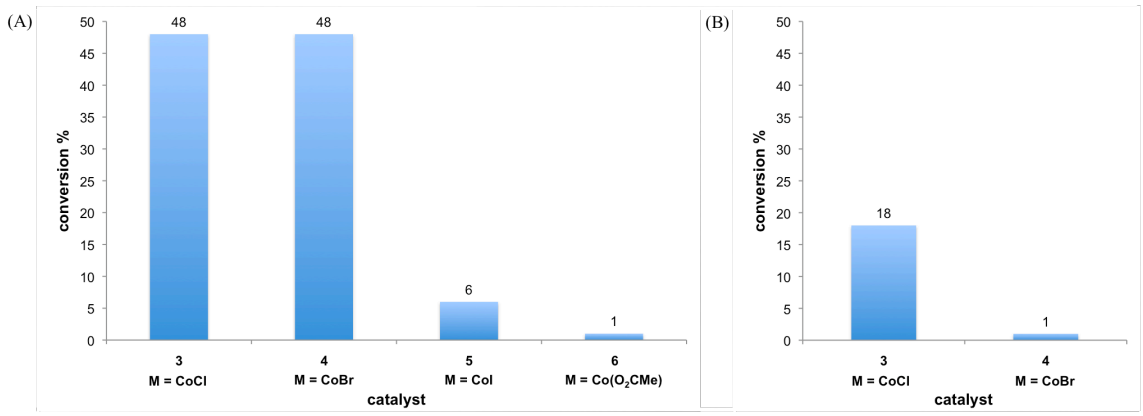

Figure 3.2. (A) Chart comparing conversion of PO using catalysts **3** – **6** at high catalyst loadings; PO:catalyst:**10** = 4,000:1:1, T_{rxn} = 0 °C, t_{rxn} = 15 min. (B) Chart comparing conversion of PO using **3** and **4** at low catalyst loadings; PO:catalyst:**10** = 16,000:1:1, T_{rxn} = 0 °C, t_{rxn} = 15 min.

Table 3.1. Enantioselective polymerization of racemic PO using complexes **3** – **6** with cocatalyst **10**.

entry	cat.	PO/ cat.	t_{rxn} (min)	conv.[b] (%)	Initial TOF[c] (min^{-1})	*mm*[d] (%)	$ee_{(P)}$[e] (%)	M_n[f] (kg/mol)	M_w/M_n[f]	*s*-factor[g]
1	**3**	16,000	5	11	340	99.0	99.3	96	2.3	> 300
2	**4**	10,000	10	9	88	97.7	98.5	58	2.0	140
3	**5**	4,000	30	11	10	95.7	97.0	57	2.4	75
4	**6**	2,000	30	13	17	94.5	96.3	50	2.3	60

[a] Polymerization conditions: [PO] = 2 M in DME; catalyst:**10** = 1:1; T_{rxn} = 0 °C. [b] Determined gravimetrically. [c] TOF = [(moles of prod./moles of cat.)/t_{rxn}]. [d] Determined by ^{13}C NMR spectroscopy. [e] Calculated using: $ee_{(P)} = (2[mm] + [mr] + [rm] - 1)^{1/2}$. [f] Determined by gel-permeation chromatography calibrated with polystyrene standards in tetrahydrofuran at 30 °C. [g] Calculated using: *s*-factor = $\ln[1 - c(1 + ee_{(P)})]/\ln[1 - c(1 - ee_{(P)})]$, where *c* is conversion of PO.

Once the optimal axial substituent had been identified, the effects of introducing electron-withdrawing/donating groups as salicyl substituents in the ligand framework were then studied by screening catalysts **3**, **7**, **8** and **9** with cocatalyst **10** for the synthesis of PPO. As shown in Figure 3.3, **7** (R = Cl) showed the highest conversion of PO, followed by **8**, **3** and **9** respectively. We propose that the electron-withdrawing group in **7** renders the Co centers more Lewis acidic, encouraging the coordination and ring opening events of epoxide for propagation, thus enhancing catalyst activity. The opposite effect is observed with the increasing strength of electron donors (R = H, ^{t}Bu, and OMe; complexes **8**, **3** and **9** respectively). Table 3.2 shows that the catalysts can be used to enantioselectively polymerize PO to form highly isotactic PPO with high *s*-factors at extremely low catalyst loadings.

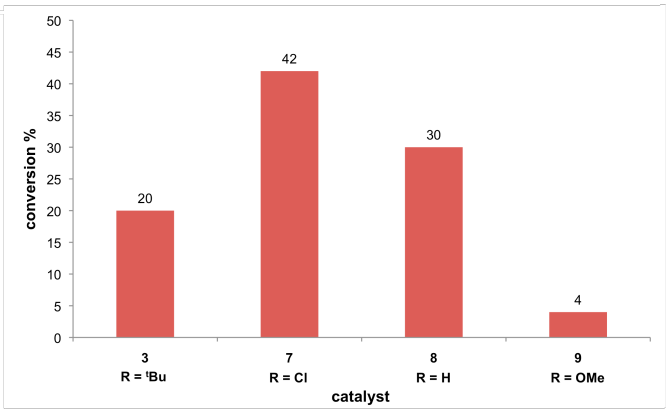

Figure 3.3. Comparison of conversions for catalysts **3**, **7**, **8** and **9** for the polymerization of PO; PO:catalyst:**10** = 20,000:1:1, T_{rxn} = 0 °C, t_{rxn} = 15 min.

Table 3.2. Enantioselective polymerization of racemic PO using complexes **3**, **7**, **8** and **9** with cocatalyst **10**.

entry	cat.	conv.[b] (%)	Initial TOF[c] (min^{-1})	*mm*[d] (%)	$ee_{(P)}$[e]	M_n[f] (kg/mol)	M_w/M_n[f]	*s*-factor[g]
1	**3**	10	180	98.8	99.2	66	3.2	280
2	**7**	30	540	98.2	98.7	166	2.7	250
3	**8**	18	310	99.3	99.5	90	3.3	>300
4[h]	**9**	13	110	99.2	99.5	69	3.1	>300

[a] Polymerization conditions: [PO] = 1 M in DME; PO:catalyst:**10** = 27,000:1:1; T_{rxn} = 0 °C; t_{rxn} = 15 min. [b] Determined gravimetrically. [c] TOF = [(moles of prod./moles of cat.)/t_{rxn}]. [d] Determined by ^{13}C NMR spectroscopy. [e] Calculated using: $ee_{(P)} = (2[mm] + [mr] + [rm] - 1)^{1/2}$. [f] Determined by gel-permeation chromatography calibrated with polystyrene standards in tetrahydrofuran at 30 °C. [g] Calculated using: *s*-factor = $\ln[1 - c(1 + ee_{(P)})]/\ln[1 - c(1 - ee_{(P)})]$, where *c* is conversion of PO. [h] PO:**9**:**10** = 12,000:1:1.

These results establish that the most active catalyst for PO polymerization has (a) a Co center with a chloride axial ligand (Table 3.1, entry 1) and (b) an electron-withdrawing substituent in the ligand framework (Table 3.2, entry 2). Catalyst **7** contains both modifications and displayed exceptional activity for PPO synthesis. The highly active catalyst, **7**, was then tested at extremely low catalyst loadings for polymerization of a range of monosubstituted epoxides.

In previous reports, we discussed the use of excess cocatalyst relative to catalyst for enhancing polymerization at low catalyst loadings.[8] Therefore, **7** was used in combination with a more activating cocatalyst **11**[9] at a catalyst to cocatalyst ratio of 1:4 for the enantioselective polymerization of PO, butene oxide, and hexene oxide at extremely low loadings (epoxide:**7** = 100,000:1) and high epoxide concentrations ([epoxide] = 6M). The monosubstituted terminal epoxides were polymerized successfully to form highly isotactic polyethers with *mm* triads >99% and *s*-factors >300 (Table 3.3, entry 1-3). The polyethers attained display much higher average

molecular weights (M_n) and *mm* values in comparison to previous reports for catalyst **3** at higher catalyst loadings,[4-5] exemplifying the exceptional activity and potential of catalyst **7**.

Table 3.3. Enantioselective polymerization of monosubstituted terminal epoxides using complex **7** with 4 eq. cocatalyst **11**.

entry	Epoxide (R)	conv.[b] (%)	Initial TOF[c] (min^{-1})	*mm*[d] (%)	$ee_{(P)}$[e]	M_n[f] (kg/mol)	M_w/M_n[f]	*s*-factor[g]
1	Me	16	520	99.3	99.5	75	3.0	> 300
2	Et	14	530	99.8	99.8	203	2.8	> 300
3	^{n}Bu	16	480	99.5	99.7	209	2.4	> 300

[a] Polymerization conditions: [epoxide]= 6 M in DME; epoxide:**7**:**11** = 100,000:1:4; T_{rxn}= 0 °C; t_{rxn}= 30 min. [b] Determined gravimetrically. [c] TOF = [(moles of prod./moles of cat.)/t_{rxn}]. [d] Determined by ^{13}C NMR spectroscopy. [e] Calculated using: $ee_{(P)}= (2[mm] + [mr] + [rm] - 1)^{1/2}$. [f] Determined by gel-permeation chromatography calibrated with polystyrene standards in tetrahydrofuran at 30 °C. [g] Calculated using: *s*-factor= $\ln[1 - c(1 + ee_{(P)})]/\ln[1 - c(1 - ee_{(P)})]$, where *c* is conversion of PO.

3.3. Conclusion

In conclusion, a highly active bimetallic cobalt catalyst, **7**, has been developed through systematic variations of the Co axial ligands and salicyl substituents in the ligand framework. When activated by an ionic cocatalyst, catalyst **7** polymerizes a variety of aliphatic epoxides at extremely low catalyst loadings to form highly isotactic polyethers with high M_n values and *s*-factors.

3.4. Experimental

3.4.1. General Considerations

All manipulations of air or water sensitive compounds were carried out under dry nitrogen using a MBraun Labmaster drybox or standard Schlenk line techniques. NMR spectra were recorded on Varian Unity spectrometers INOVA 500 (^{1}H, 500 MHz), or INOVA 600 (^{1}H, 600 MHz). ^{1}H NMR spectra were referenced with residual non- or partially-deuterated solvent shifts ($CHCl_3$ = 7.27 ppm, pyridine-d_4 = 8.74 ppm). ^{13}C NMR spectra were referenced to solvent signals ($CDCl_3$ = 77.23 ppm, pyridine-d_5 = 150.35 ppm). Mass spectrometry analyses were conducted at the School of Chemical Sciences Mass Spectrometry Laboratory at the University of Illinois in Urbana-Champaign.

3.4.2. Polymer Characterization

The polyethers synthesized were characterized using gel permeation chromatography (GPC) using an Agilent PL-GPC 50 integrated system, equipped with UV and refractive index detectors, and 2 PL gel Mini-MIX C columns (5 micron, 4.6 mm ID). The GPC columns were eluted with tetrahydrofuran at 30 °C at 0.3 mL/min and were calibrated with monodisperse polystyrene standards.

3.4.3. NMR Quantification of Polymer Tacticity

The polyethers synthesized display distinct resonances for the stereochemical defects in the polymer chain by ^{13}C NMR spectroscopy. The polyethers synthesized in this paper exhibit triad resolution of the methine carbon, which have been assigned previously. In all cases the methine resonances were used to quantify the triad integral values and to calculate [*mm*]. For polypropylene oxide (PPO), polybutene oxide (PBO) and polyhexene oxide (PHO), the *mr* and *rm* triads are very small relative to the mm triad, and occur in the same area as the ^{13}C-^{13}C satellite signals of the *mm* triad. In the case of PBO and PHO, the *rr* triad resonances also overlapped with the ^{13}C-^{13}C satellite signals of the *mm* triad, whereas in PPO, it was very distinct.

Representative calculation of polymer tacticity in PPO (From ^{13}C NMR integrations of the methine resonances, Figure 3.4)

$[mm]+[mr]+[rm]+[rr] = 1$

$[rr] = 19/1019 = 0.0190$

$[mr + rm] = 2[rr] = 0.0380$

$[mm] = 1 – [mr + rm + rr] = 1 – (0.0190 + 0.0380) = 0.943$

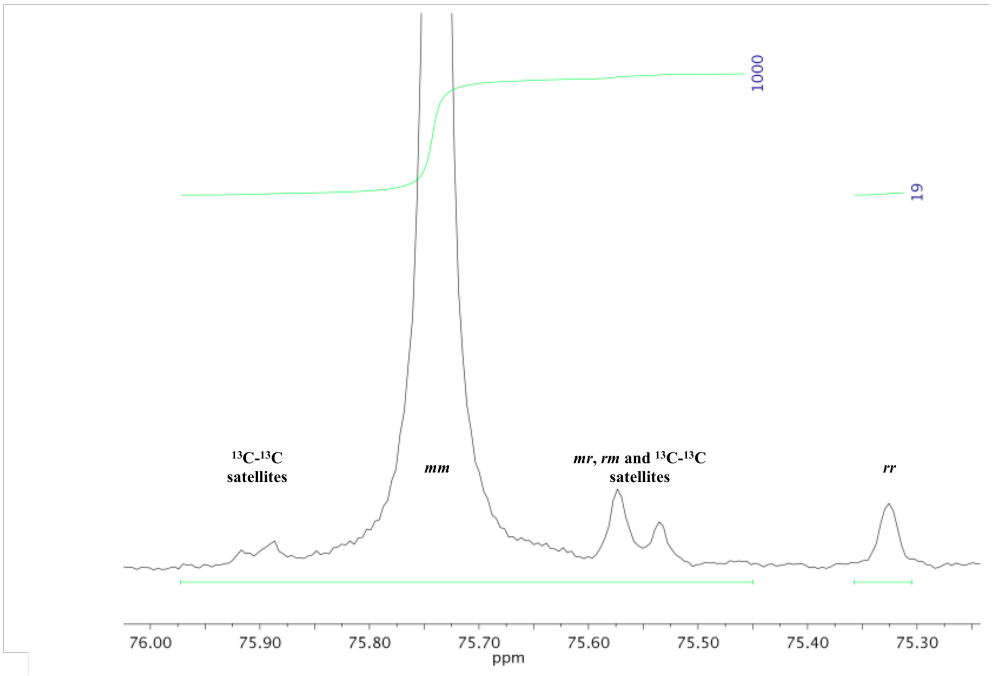

Figure 3.4. Calculation of polymer tacticity of PPO by ^{13}C NMR spectroscopy.

Representative calculation of polymer tacticity in PBO (From ^{13}C NMR integrations of the methine resonances, Figure 3.5; Table 3.3, entry 2)

$[mm]+[mr]+[rm]+[rr] = 1$

$mr + rm + rr = (mr + rm + rr + {}^{13}\text{C}\text{-}{}^{13}\text{C}$ satellite) – (^{13}C-^{13}C satellite) = 12 – 10 = 2

For enantiomorphic site control mechanism, $[mr] = [rm] = [rr]$

Therefore, $mr = rm = rr = 2/3 = 0.667$

$[rr] = 0.667/1021 = 0.000653$

$[mr + rm] = 2[rr] = 0.00131$

$[mm] = 1 – [mr + rm + rr] = 0.998$

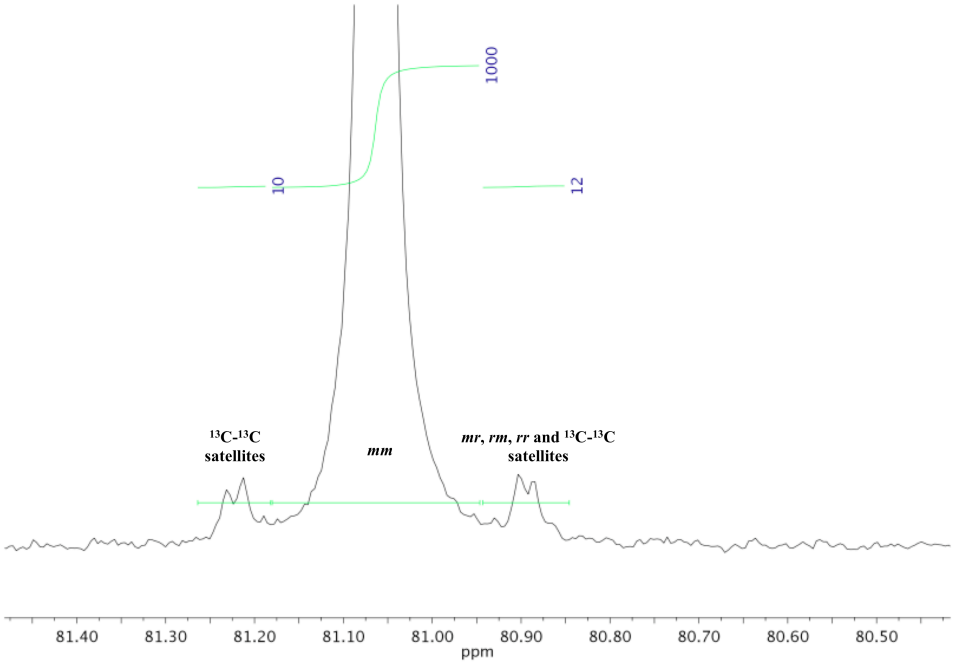

Figure 3.5. Calculation of polymer tacticity of PBO by ^{13}C NMR spectroscopy.

Representative calculation of polymer tacticity in PHO (From ^{13}C NMR integrations of the methine resonances, Figure 3.6; Table 3.3, entry 3)

$[mm]+[mr]+[rm]+[rr] = 1$

$mr + rm + rr = (mr + rm + rr + {}^{13}\text{C-}{}^{13}\text{C satellite}) - ({}^{13}\text{C-}{}^{13}\text{C satellite}) = 21 - 16 = 5$

For enantiomorphic site control mechanism, $[mr] = [rm] = [rr]$

Therefore, $mr = rm = rr = 5/3 = 1.67$

$[rr] = 1.67/1037 = 0.00161$

$[mr + rm] = 2[rr] = 0.00322$

$[mm] = 1 - [mr + rm + rr] = 0.995$

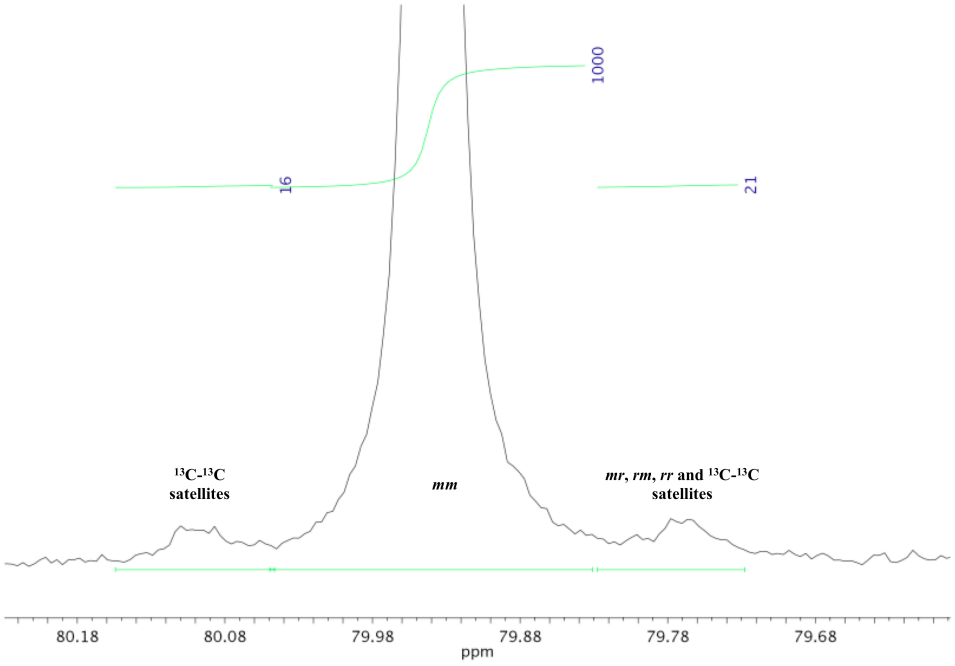

Figure 3.6. Calculation of polymer tacticity of PHO by ^{13}C NMR spectroscopy.

3.4.4. Calculating $ee_{(P)}$ and Selectivity factors (*s*-factor)

The values for [*mm*], [*mr*], [*rm*] and [*rr*], attained from the quantitative ^{13}C NMR spectroscopy of the polyethers were used in equation 1 to calculate polymer *ee*.

$$ee_{(P)} = (2[mm] + [mr] + [rr] - 1)^{1/2} \qquad (1)$$

Corresponding selectivity factors (*s*-factor) were calculated using equation 2, where *c* is conversion of epoxide to polymer. Equation 2 is only valid when $c < 50\%$.

$$s\text{-factor} = ln[1\text{-}c(1+ee_{(P)})]/ln[1\text{-}c(1\text{-}ee_{(P)})] \qquad (2)$$

3.4.5. Materials

HPLC grade methylene chloride and methanol were purchased from Fischer Scientific and purified over solvent columns. 3Å sieves were purchased from Strem, activated by heating at 165 °C under vacuum for 20 hours, and stored in a nitrogen filled glove box. Absolute ethanol

was purchased from Koptec, dried over activated 4Å sieves and degassed by sparging with nitrogen for 2 hours. Dimethoxyethane (DME) was purchased from Sigma-Aldrich, dried over sodium, degassed through multiple freeze-pump-thaw cycles and vacuum transferred to a Straus flask that was stored in a nitrogen filled glove box. All epoxides were purchased from commercial sources, dried over calcium hydride, degassed through multiple freeze-pump-thaw cycles, and also stored in a nitrogen filled glove box. (1*R*, 2*R*)-diaminocyclohexane (99% *ee*), 3-(*tert*-butyl)-2-hydroxybenzaldehyde and cobalt acetate tetrahydrate were purchased from Sigma-Aldrich. (*S*)-1,1'-bi-2-naphthol and 2-(tert-butyl)-4-methoxyphenol were purchased from TCI. Cocatalysts bis(triphenylphosphine)iminium acetate and phosphazenium pivalate were prepared according to reported procedures.[7,9] 3-(*tert*-butyl)-2-hydroxy-5-methoxybenzaldehyde, diformylated (*S*)-1,1'-bi-2-naphthol, and 3-(*tert*-butyl)-5-chloro-2-hydroxybenzaldehyde were also synthesized from previous reports.[12-13] All other reagents were purchased from commercial sources and used as received.

3.4.6. Synthesis of Ligand Framework

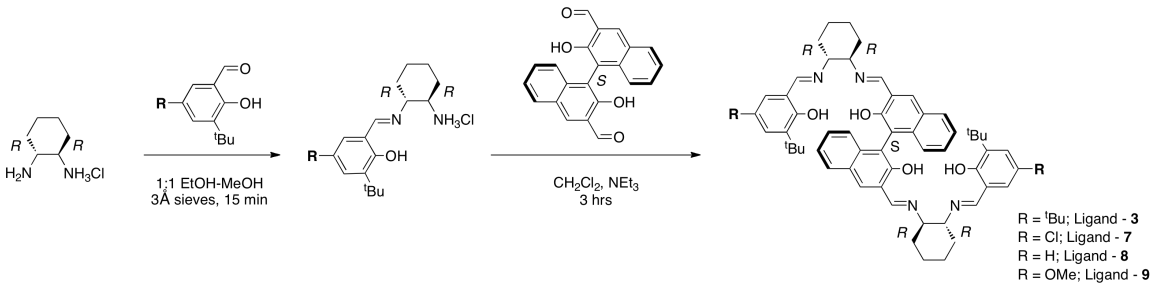

Figure 3.7. Synthesis of Ligands.

The ligands, Co(II) precursors and bimetallic Co(III) complexes (**3** – **9**) were prepared using the modified procedures reported below.

Representative procedure to synthesize ligand framework (Synthesis of Ligand – **3** as shown in Figure 3.7)

The HCl salt of (1*R*, 2*R*)-diaminocyclohexane (0.62 g, 4.1 mmol) and 3,5-di-(*tert*-butyl)-salicylaldehyde (0.96 g, 4.1 mmol) were taken in a 100 mL round bottom flask along with 3Å sieves and a teflon stir bar. A vacuum adaptor was attached to the flask and was placed under nitrogen while stirring. After stirring the solids together for 10 minutes, 20 mL of a 1:1 EtOH-MeOH mixture was canulated into the round bottom flask. On addition of solvent, the contents of the flask turn yellow. After 15 minutes of stirring, a distinct color change is observed from yellow to dark brown. At this point, a solution of diformylated (S)-1,1'-bi-2-napthol (0.70 g, 2.0 mmol) and triethylamine (1.1 mL, 7.9 mmol) in 15 mL anhydrous methylene chloride was added to the reaction mixture and allowed to stir. After 3 hours, a distinct color change from red to dark brown is observed. The reaction mixture was then passed through a plug of Celite, which was washed copiously with methylene chloride. After removal of solvent under reduced pressure, the brown solid was purified by column chromatography (12% ethyl acetate, 2% triethylamine, and 86% hexane) to attain a pure bright yellow solid, Ligand – **3**. Yield = 0.65 g (33%). Full characterization of Ligand – **3** was reported previously.[5]

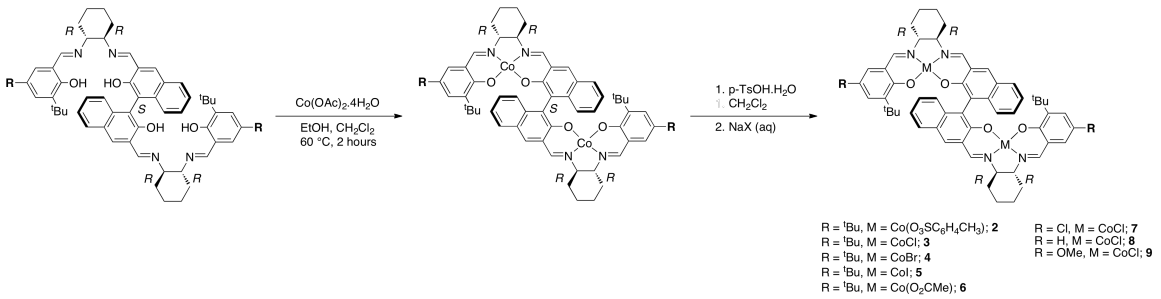

Figure 3.8. Synthesis of complexes from Ligands.

Representative procedure to metallate ligands (Synthesis of Co(II) precursor, **1**)

$Co(OAc)_2 \bullet 4H_2O$ (65 mg, 0.26 mmol) is taken in an oven dried Schlenk flask with a stir bar and placed under nitrogen conditions using Schlenk technique. The contents of the flask are heated carefully using a heat gun under vacuum to remove water from the cobalt salt (turns from pink to dark purple). After the flask cooled to room temperature, 5 mL of EtOH was canulated to the flask, and the contents were stirred to form a purple solution. A yellow solution of Ligand – **3** (0.12 g, 0.12 mmol) in 10 mL of anhydrous methylene chloride was then canulated to the Schlenk flask, causing the cobalt solution to change from purple to dark reddish brown. The flask was closed and placed in an oil bath set at 60 °C. After heating for 2 hrs, solvent was removed by vacuum and a dark brown solid was attained. The solid was collected over a fine glass frit, and washed with methanol (40 mL) and pentane (60 mL x 3). The solid was dried under vacuum over night to yield 0.11 g (84%) of **1**.

Representative procedure to oxidize Co(II) precursor (Synthesis of complex **3**)

1 (0.11 g, 0.10 mmol) was taken in a 20 mL vial with a stir bar and dissolved in 12 mL of methylene chloride. *Para*-toluenesulfonic acid monohydrate (38 mg, 0.20 mmol) was added to the solution. The mixture was stirred and all the solvent was allowed to evaporate. Complex **2**

was attained as a black solid, and redissolved in 20 mL methylene chloride. The solution was washed with brine (40 mL x 4), and dried using Na_2SO_4. Solvent was removed under reduced pressure, and dried under vacuum overnight to yield **3** as a black crystalline solid (88 mg, 76%).[5]

3.4.7. NMR Characterization Specifications

The ligands and complexes were characterized by 1-D and 2-D NMR spectroscopy in $CDCl_3$ or pyridine-d_5 at ambient temperature on a Varian Unity Inova 600 MHz spectrometer using a Varian 5 mm inverse ^1H-{^{13}C,^{15}N} triple-resonance probehead with triple-axis gradients, and/or Varian Unity Inova 500 MHz spectrometers using a Varian 5 mm inverse ^1H-{^{13}C,^{15}N} triple-resonance probehead with Z gradient or a Varian 5 mm dual broadband probehead with Z gradient. NMR data were acquired with the pulse sequences supplied in Vnmrj 2.2D/Chempack 4.1 (Agilent Inc.) and were processed and analyzed using the MestReNova 7.1 software package (2012, Mestrelab Research S. L.). All 2-D spectra were acquired with typical ^1H spectral widths of 0.5 –14.5 ppm and 0.5 – 9.5 ppm for ligands and complexes, respectively. COSY spectra were acquired using the gCOSY sequence with 400 – 600 complex points in the indirectly detected dimension and 1 scan of 0.6 – 0.8 s acquisition time per increment. The resulting matrices were zero filled up to 4k and 8k complex data points in F1 and F2, respectively, and unshifted sine bell (F1), and simultaneous unshifted sine bell and Gaussian (F2) window functions were applied prior to Fourier transformation. TOCSY spectra were acquired with 80ms mixing times using the TOCSY sequence with 200 – 400 complex points in the indirectly detected dimension and 2 or 4 scans of 0.4 s acquisition time per increment. The resulting matrices were zero filled up to 4k x 4k complex data points and Gaussian window functions were applied in both dimensions prior to Fourier transformation. NOESY spectra were acquired with 600 ms mixing times using the

NOESY sequence with 200 – 300 complex points in the indirectly detected dimension and 4 or 8 scans of 0.4 s acquisition time per increment. The resulting matrices were zero filled up to 4k x 4k complex data points and Gaussian window functions were applied in both dimensions prior to Fourier transformation. ROESY spectra were acquired with 200 ms mixing times using the ROESYAD sequence with 200 – 600 complex points in the indirectly detected dimension and 4 or 8 scans of 0.4 s acquisition time per increment. The resulting matrices were zero filled up to 4k x 4k complex data points and Gaussian window functions were applied in both dimensions prior to Fourier transformation. Multiplicity-edited HSQC spectra were acquired using the HSQCAD sequence with a spectral window of -10 – 190 ppm and 400 – 800 complex points in the indirectly detected dimension, and 4 scans of 0.15 s acquisition time per increment. The resulting matrices were zero filled up to 4k x 2k complex data points in F1 and F2, respectively, and Gaussian window functions were applied in the ^{1}H dimension prior to Fourier transformation. HMBC spectra were acquired in phase sensitive mode and optimized for 8 Hz couplings using the gHMBCAD sequence with a spectral window of -10 – 225 ppm and 600 – 1200 complex points in the indirectly detected dimension, and 4 scans of 0.3 s acquisition time per increment. The resulting matrices were zero filled up to 4k x 2k complex data points in F1 and F2, respectively, and simultaneous unshifted sine bell and Gaussian window functions were applied in the ^{1}H dimension prior to Fourier transformation.

3.4.8. Characterization Data for Ligands and Co Complexes

Complex **4**

Yield from Co(II) precursor (**1**) = 54%. Complex **4** was characterized by ^{1}H, ^{13}C, COSY, ROESY, HSQC and HMBC NMR spectroscopy in pyridine-d_5.

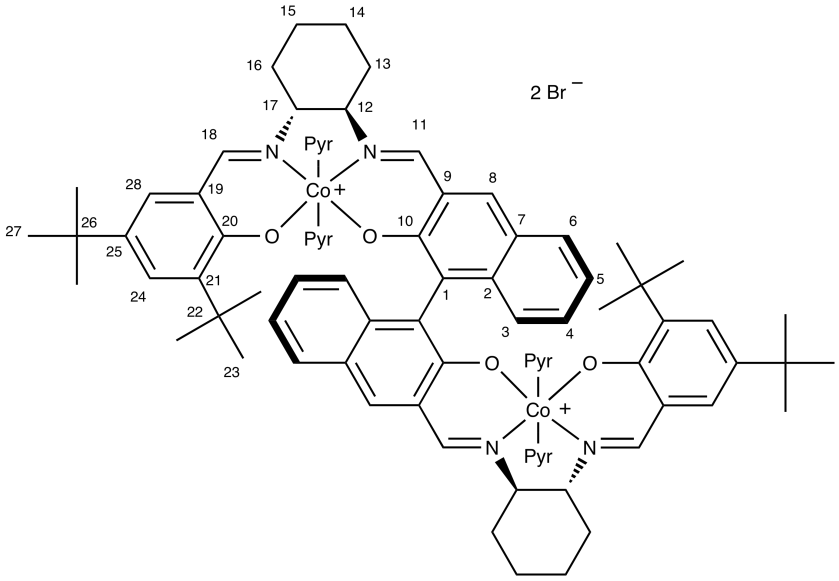

Atom No.	$^{13}C\{^{1}H\}$ NMR δ	^{1}H NMR δ
1	125.30	
2	138.62	
3	125.63	6.36
4	129.16	6.83
5	121.68	7.09
6	130.12	7.88
7	126.85	
8	139.21	8.66
9	123.51	
10	160.65	
11	167.89	9.27
12	74.12	2.47
13	28.90	3.01, 2.97
14	25.18	1.84, 1.02
15	24.75	2.07, 1.72
16	32.72	3.12, 1.24
17	67.25	5.07
18	168.42	8.55

19	116.84	
20	162.14	
21	143.35	
22	35.26	
23	30.34	1.35
24	131.48	7.63
25	136.87	
26	34.06	
27	31.39	1.23
28	130.02	7.43

Complex **5**

Yield from Co(II) precursor (**1**) = 60%. Complex **5** was characterized by ^{1}H, ^{13}C, COSY, ROESY, HSQC and HMBC NMR spectroscopy in pyridine-d_5.

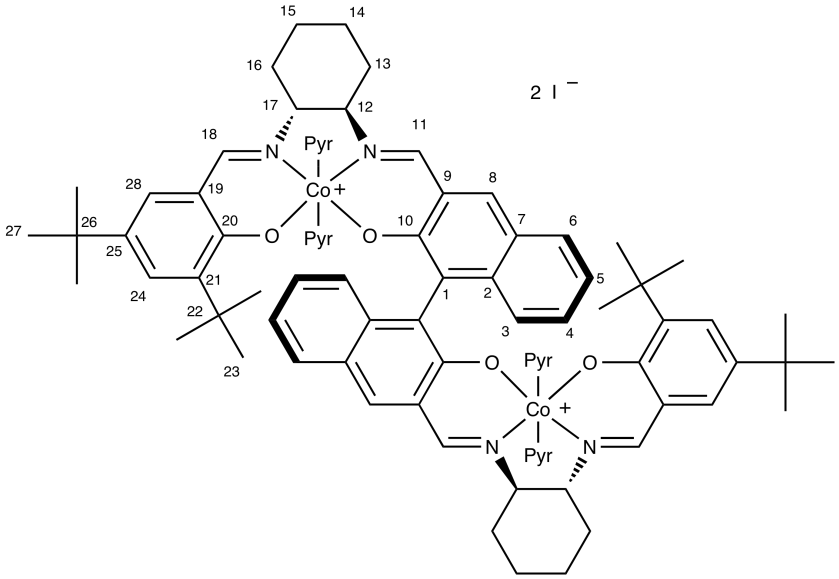

Atom No.	$^{13}C\{^{1}H\}$ NMR δ	^{1}H NMR δ
1	125.46	
2	138.71	
3	125.57	6.33
4	129.37	6.82
5	121.86	7.12
6	130.17	7.92
7	126.90	
8	139.16	8.67
9	123.34	
10	160.57	
11	167.76	9.22

12	73.89	2.54
13	29.00	2.98, 2.75
14	24.98	1.84, 1.08
15	24.81	1.93, 1.75
16	32.49	3.11, 1.30
17	67.48	4.79
18	168.36	8.55
19	116.75	
20	162.17	
21	143.45	
22	35.79	
23	30.34	1.34
24	131.67	7.65
25	137.03	
26	34.10	
27	31.37	1.23
28	130.00	7.42

Complex **6**

Yield from Co(II) precursor (**1**) = 90%. Complex **6** was characterized by ^{1}H, ^{13}C, COSY, ROESY, HSQC and HMBC NMR spectroscopy in pyridine-d_5.

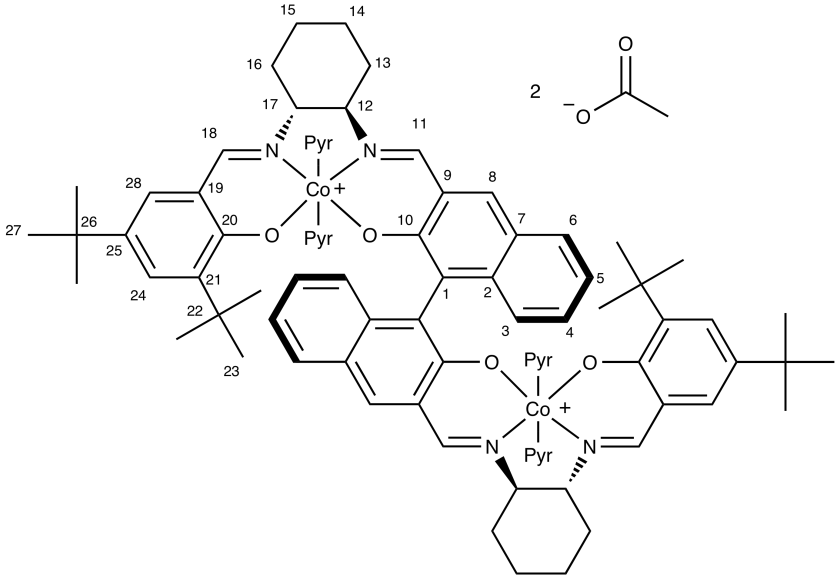

Atom No.	$^{13}C\{^{1}H\}$ NMR δ	^{1}H NMR δ
1	124.88	
2	138.21	
3	125.12	6.28
4	128.74	6.76
5	121.31	7.07
6	129.79	7.91
7	126.49	
8	138.80	8.67
9	123.10	
10	160.14	
11	167.83	9.24
12	73.49	2.45
13	28.52	2.88, 2.55
14	24.60	1.67, 0.98
15	24.50	1.72, 1.65
16	32.05	3.12, 1.21
17	67.23	4.82
18	168.42	8.63
19	116.41	
20	161.67	
21	142.87	
22	35.29	
23	29.93	1.32
24	131.06	7.62
25	136.46	
26	33.64	
27	30.98	1.22
28	129.70	7.45

Ligand – **7** (See Figure 3.7)

Yield = 30%. R_f (12% ethyl Acetate, 88% hexane) = 0.38. HRMS-EI (m/z): calcd for $C_{56}H_{60}Cl_2N_4O_4$, 923.4070; found, 923.4068. Ligand – **7** was characterized by ^{1}H, ^{13}C, COSY, ROESY, HSQC and HMBC NMR spectroscopy in $CDCl_3$.

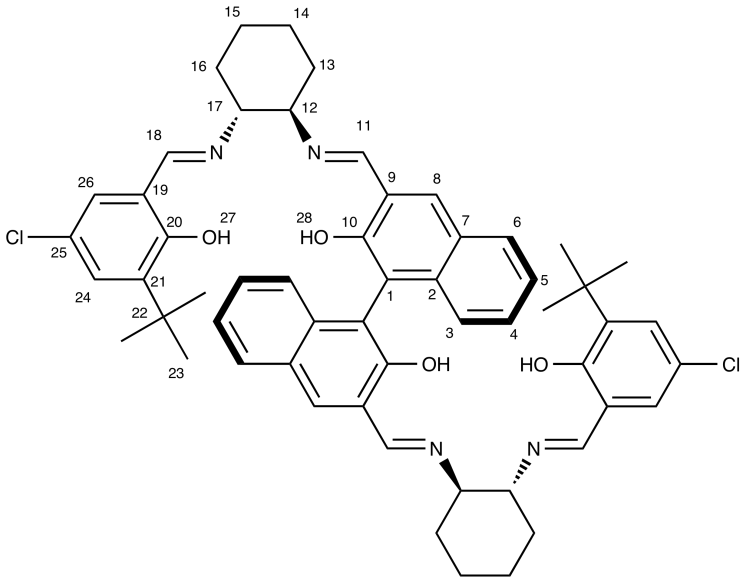

Atom No.	$^{13}C\{^{1}H\}$ NMR δ	^{1}H NMR δ
1	116.23	
2	135.05	
3	124.66	7.11
4	128.15	7.24
5	123.11	7.24
6	128.76	7.77
7	127.37	
8	133.48	7.83
9	120.72	
10	154.50	
11	165.00	8.56
12	73.08	3.41
13	32.83	1.96, 1.66
14	24.10	1.84, 1.45
15	24.03	1.84, 1.40
16	33.13	1.91, 1.70
17	71.66	3.28
18	164.63	8.16
19	119.20	
20	159.00	
21	139.26	
22	34.95	
23	29.11	1.44
24	129.42	7.19
25	122.33	
26	128.63	6.98
27		14.02
28		12.90

Complex **7**

The Co(II) precursor of **7** was prepared in 93% yield and was analyzed by HRMS-EI. HRMS-EI (m/z): calcd for $C_{56}H_{57}Cl_2Co_2N_4O_4$, 1037.2343; found 1037.2343.

Yield of **7** from Co(II) precursor = 71%. Complex **7** was characterized by ^{1}H, ^{13}C, COSY, ROESY, HSQC and HMBC NMR spectroscopy in pyridine-d_5.

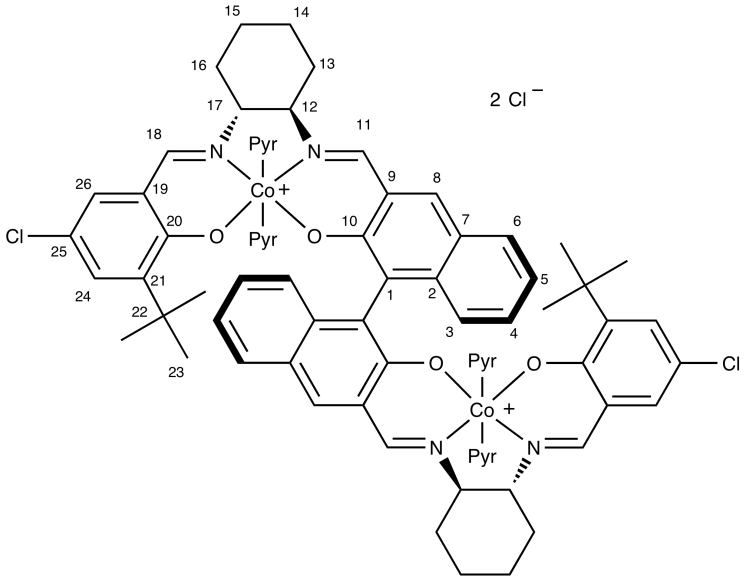

Atom No.	$^{13}C\{^{1}H\}$ NMR δ	^{1}H NMR δ
1	125.15	
2	138.61	
3	125.64	6.36
4	129.26	6.84
5	121.78	7.10
6	130.16	7.81
7	126.92	
8	139.54	8.71
9	123.56	
10	160.38	
11	168.57	9.39
12	74.33	2.51
13	29.00	3.09, 3.04
14	25.28	1.80, 1.02
15	24.81	2.06, 1.70
16	32.73	3.19, 1.29
17	67.57	5.21
18	168.18	8.59
19	118.64	

20	162.65	
21	145.85	
22	35.72	
23	29.76	1.23
24	133.01	7.35
25	118.99	
26	132.62	7.48

Ligand – **8**

Yield = 20%. R_f (20% ethyl acetate, 80% hexane) = 0.37. HRMS-EI (m/z): calcd for $C_{56}H_{63}N_4O_4$, 855.4849; found 855.4846. Ligand – **8** was characterized by ^1H, ^{13}C, COSY, ROESY, HSQC and HMBC NMR spectroscopy in $CDCl_3$.

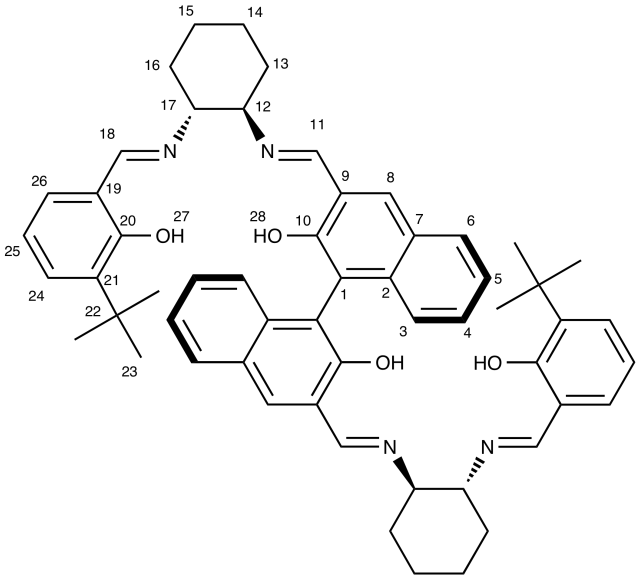

Atom No.	$^{13}C\{^1H\}$ NMR δ	^1H NMR δ
1	116.20	
2	135.05	
3	124.63	7.10
4	128.11	7.23
5	123.11	7.23
6	128.78	7.75
7	127.48	
8	133.50	7.82
9	120.76	
10	154.55	
11	165.21	8.58

12	72.84	3.43
13	32.71	2.00, 1.66
14	24.09	1.83, 1.47
15	24.12	1.86, 1.41
16	33.27	1.92, 1.71
17	71.46	3.21
18	165.79	8.21
19	118.53	
20	160.23	
21	136.94	
22	34.73	
23	29.35	1.47
24	129.30	7.26
25	117.80	6.73
26	129.89	6.97
27		13.97
28		12.95

Complex **8**

The Co(II) precursor of **8** was prepared in 81% yield and was analyzed by HRMS-EI. HRMS-EI (m/z): calcd for $C_{56}H_{59}Co_2N_4O_4$, 969.3122; found 969.3140.

Yield of **8** from Co(II) precursor = 79%. Complex **8** was characterized by ^{1}H, ^{13}C, COSY, ROESY, HSQC and HMBC NMR spectroscopy pyridine-d_5.

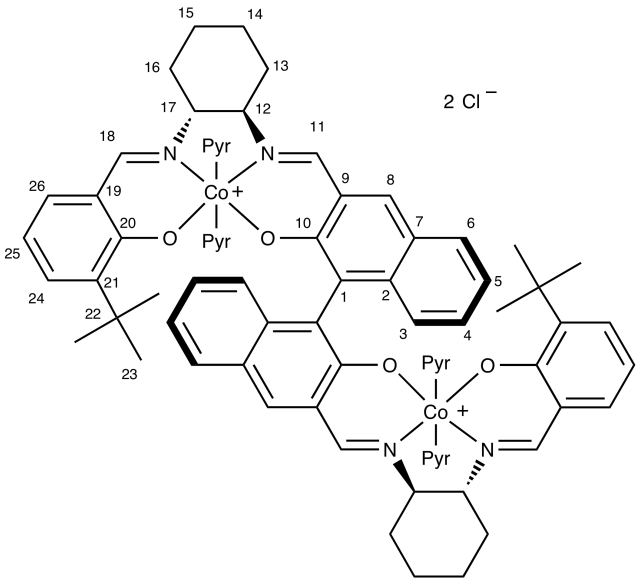

Atom No.	$^{13}C\{^{1}H\}$ NMR δ	^{1}H NMR δ
1	125.21	
2	138.63	
3	125.52	6.33
4	129.05	6.81
5	121.56	7.08
6	130.08	7.84
7	126.81	
8	139.41	8.69
9	123.50	
10	160.50	
11	168.30	9.34
12	74.12	2.45
13	28.97	3.00, 2.92
14	25.17	1.76, 0.97
15	24.75	1.96, 1.65
16	32.59	3.06, 1.18
17	67.32	5.05
18	168.53	8.52
19	117.87	
20	163.96	
21	143.77	
22	35.40	
23	30.16	1.27
24	132.98	7.37
25	115.16	6.55
26	134.69	7.47

Ligand – **9**

Yield = 13%. R_f (20% ethyl acetate, 80% hexane) = 0.37. HRMS-EI (m/z): calcd for $C_{58}H_{67}N_4O_6$, 915.5071; found 915.5061. Ligand – **9** was characterized by ^{1}H, ^{13}C, COSY, ROESY, HSQC and HMBC NMR spectroscopy in $CDCl_3$.

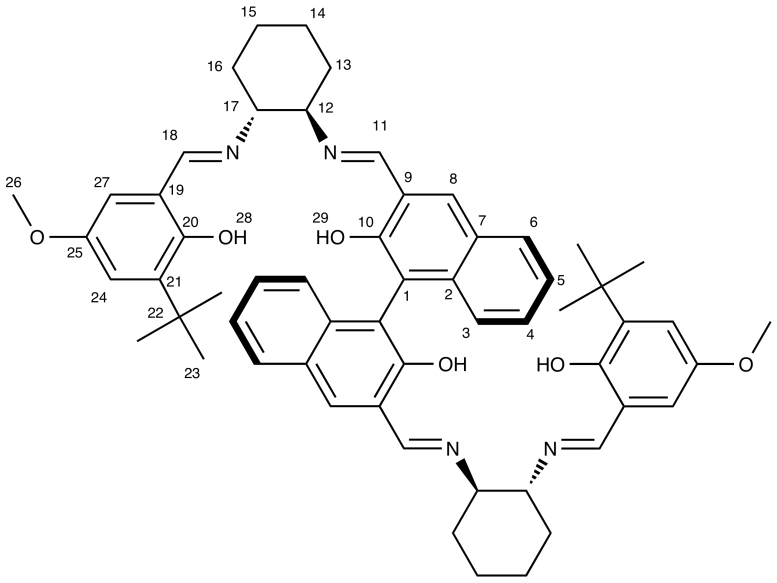

Atom No.	$^{13}C\{^{1}H\}$ NMR δ	^{1}H NMR δ
1	116.17	
2	135.04	
3	124.63	7.09
4	128.10	7.23
5	123.13	7.23
6	128.78	7.75
7	127.50	
8	133.59	7.81
9	120.75	
10	154.49	
11	165.36	8.56
12	72.80	3.42
13	32.57	2.02, 1.66
14	24.05	1.83, 1.46
15	24.16	1.85, 1.40
16	33.23	1.92, 1.72
17	73.36	3.19
18	165.69	8.17
19	117.78	
20	154.74	
21	138.5	
22	34.91	
23	29.28	1.47
24	118.11	6.91
25	151.09	
26	55.76	3.64
27	111.97	6.47
28		13.56
29		12.96

Complex **9**

The Co(II) precursor of **9** was prepared in 89% yield and was analyzed by HRMS-EI. HRMS-EI (m/z): calcd for $C_{58}H_{63}Co_2N_4O_6$, 1029.3373; found 1029.3412.

Yield of **9** from Co(II) precursor = 78%. Complex **9** was characterized by ^{1}H, ^{13}C, COSY, ROESY, HSQC and HMBC NMR spectroscopy in pyridine-d_5.

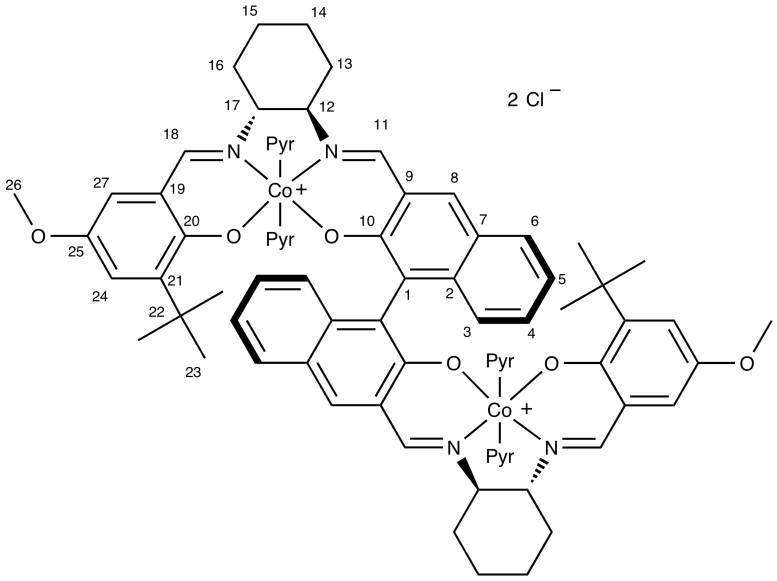

Atom No.	$^{13}C\{^{1}H\}$ NMR δ	^{1}H NMR δ
1	125.38	
2	138.73	
3	125.49	6.35
4	129.12	6.82
5	121.60	7.10
6	130.06	7.87
7	126.88	
8	139.15	8.63
9	123.54	
10	160.73	
11	168.05	9.29
12	74.09	2.52
13	28.94	2.93, 2.93
14	25.13	1.81, 1.01
15	24.81	1.98, 1.69
16	32.69	3.17, 1.27
17	67.47	5.05
18	167.98	8.58

19	116.24	
20	159.04	
21	144.94	
22	35.58	
23	30.03	1.26
24	125.01	7.24
25	149.32	
26	55.64	3.69
27	112.72	7.05

3.4.9. High Throughput Polymerizations

General procedure

The polymerizations were conducted on a Freeslate Core Module 3 robotic platform located inside a MBraun drybox equipped with a balance, liquid and solid dispense options, heated/cooled stirrers, and vortexers. The experiment was designed and executed using Library Studio(TM) and Automation Studio(TM) software. All solutions were dispensed robotically using a positive displacement dispense and disposable PDT tips. 24 8 mL vials each containing a stir bar were loaded into a Al reactor block and tared robotically. The reaction temperature was 0 °C and the stirring rate was 200 rpm. After 15 minutes, each reaction was quenched by addition of a solution of BHT. Volatiles were then removed from the reaction vials using a Speedvac vacuum centrifuge and the vials containing the products were weighed robotically.

Representative polymerization of propylene oxide using **3** *and* **10** (Table 3.2, entry 1)

Stock solutions (1 mg/mL) of **3** and **10** in dimethoxyethane (DME) were prepared in separate 20 mL vials inside a nitrogen filled glove box. Solutions were dispensed using a Freeslate Core Module 3 equipped with a PDT syringe and disposable PDT tips. The experiments were designed using Library Studio. 173 μL of the solution of **3** (0.173 mg, 0.150

μmol) and 95.9μL of the solution of **10** (0.0959 mg, 0.150 μmol) were dispensed into a tared 8 mL vial placed on a 6 X 4 aluminum vial plate. The temperature of the plate was set to 0 °C, and stir rate was set to 200 rpm. 3.15 mL of DME was dispensed into the reaction vial, and then 280 μL of propylene oxide (232 mg, 4.00 mmol) was added. After 15 minutes, the reaction was quenched with 300 μL of 5 mg/mL BHT in hexane solution (1.50 mg BHT, 6.82 mmol). Volatiles were removed from the reaction vial using a vacuum centrifuge and then weighed. Mass of polypropylene oxide attained = 23.5 mg. Conversion = 10.1%. [*mm*]:[*mr* + *rm*]:[*rr*] = 0.988:0.008:0.004. $ee_{(P)}$ = 99.2%. *s*-factor = 280. M_n = 66,000 g/mol, M_w/M_n = 3.2.

Activity comparison of Complexes **3** – **6** (Figure 3.2A)

cat.	mass of cat. (mg)	moles of cat. (μmol)	mass of **10** (mg)	moles of **10** (μmol)	mass of Prod. (mg)	conv. (%)
3	1.15	1.00	0.640	1.00	111.31	48.0
4	1.24	1.00	0.640	1.00	111.92	48.2
5	1.33	1.00	0.640	1.00	13.33	5.74
6	1.20	1.00	0.640	1.00	2.56	1.10

General conditions: Mass of PO added = 232 mg; Number of moles of PO added = 4 mmol; [PO] = 2 M in DME; PO:catalyst:**10** = 4000:1:1; T_{rxn} = 0 °C; t_{rxn} = 15 min; Conversions were determined gravimetrically.

Activity comparison of Complexes **3** and **4** (Figure 3.2B)

cat.	mass of cat. (mg)	moles of cat. (μmol)	mass of **10** (mg)	moles of **10** (μmol)	mass of Prod. (mg)	conv. (%)
3	0.290	0.250	0.160	0.250	18.38	18.4
4	0.310	0.250	0.160	0.250	2.43	1.04

General conditions: Mass of PO added = 232 mg; Number of moles of PO added = 4 mmol; [PO] = 2 M in DME; PO:catalyst:**10** = 16,000:1:1; T_{rxn} = 0 °C; t_{rxn} = 15 min; Conversions were determined gravimetrically.

Activity comparison of Complexes **3**, **7**, **8** and **9** (Figure 3.3)

cat.	mass of cat. (mg)	moles of cat. (μmol)	mass of **10** (mg)	moles of **10** (μmol)	mass of Prod. (mg)	conv. (%)
3	0.230	0.200	0.130	0.200	45.54	19.6
7	0.220	0.200	0.130	0.200	96.65	41.7
8	0.210	0.200	0.130	0.200	69.06	29.8
9	0.210	0.200	0.130	0.200	8.95	3.86

General conditions: Mass of PO added = 232 mg; Number of moles of PO added = 4 mmol; [PO] = 1 M in DME; PO:catalyst:**10** = 20,000:1:1; T_{rxn} = 0 °C; t_{rxn} = 15 min; Conversions were determined gravimetrically.

Polymerizations reported in Table 3.1.

entry	cat.	mass of cat. (mg)	moles of cat. (μmol)	mass of **10** (mg)	moles of **10** (μmol)	mass of prod. (mg)	conv. (%)
1	**3**	0.290	0.250	0.160	0.250	24.95	10.8
2	**4**	0.460	0.400	0.260	0.400	20.33	8.76
3	**5**	2.00	1.50	0.960	1.50	25.54	11.0
4	**6**	1.20	1.00	0.640	1.00	29.06	12.5

General conditions: Mass of PO added = 232 mg; Number of moles of PO added = 4.00 mmol; [PO] = 2 M in DME; T_{rxn} = 0 °C; Conversions were determined gravimetrically; Reactions were quenched by adding 300 μL of 5 mg/mL BHT in hexane solution with a mechanical pipette at different times.

Polymerizations reported in Table 3.2.

entry	cat.	mass of cat. (mg)	moles of cat. (μmol)	mass of **10** (mg)	moles of **10** (μmol)	mass of prod. (mg)	conv. (%)
1	**3**	0.170	0.150	0.100	0.150	23.53	10.1
2	**7**	0.170	0.150	0.100	0.150	70.14	30.2
3	**8**	0.160	0.150	0.100	0.150	40.75	17.6
4	**9**	0.340	0.330	0.210	0.330	30.93	13.3

General conditions: Mass of PO added = 232 mg; Number of moles of PO added = 4 mmol; [PO] = 1 M in DME; PO:catalyst:**10** = 27,000:1:1; T_{rxn} = 0 °C; t_{rxn} = 15 min; Conversions were determined gravimetrically.

Polymerizations reported in Table 3.3.

entry	mass of epoxide (mg)	mass of cat. (mg)	moles of cat. (μmol)	mass of **11** (mg)	moles of **11** (μmol)	mass of prod. (mg)	conv. (%)
1	232.32	0.0400	0.0400	0.180	0.0400	36.17	15.6
2	288.44	0.0400	0.0400	0.180	0.0400	45.57	15.8
3	400.00	0.0400	0.0400	0.180	0.0400	57.56	14.4

General conditions: Number of moles of epoxide added = 4 mmol; [epoxide] = 6 M in DME; epoxide:**7**:**11** = 100,000:1:1; T_{rxn} = 0 °C; t_{rxn} = 30 min; Conversions were determined gravimetrically.

3.4.10. Crystal Data and Refinement for tetrapyridine adduct 9.

Table 3.4. Crystal data and structure refinement for tetrapyridine adduct of **9**.

Identification code	sa3	
Empirical formula	C_{83} H_{87} Cl_2 Co_2 N_9 O_6	
Formula weight	1495.38	
Temperature	173(2) K	
Wavelength	0.71073 Å	
Crystal system	Orthorhombic	
Space group	P2(1)2(1)2(1)	
Unit cell dimensions	a = 11.5431(5) Å	a= 90°
	b = 22.7983(10) Å	b= 90°
	c = 30.4120(14) Å	g = 90°
Volume	8003.3(6) $Å^3$	
Z	4	
Density (calculated)	1.241 Mg/m^3	
Absorption coefficient	0.538 mm^{-1}	
F(000)	3136	
Crystal size	0.60 x 0.40 x 0.20 mm^3	
Theta range for data collection	1.61 to 26.37°	
Index ranges	-14<=h<=14, -26<=k<=28, -35<=l<=38	
Reflections collected	37462	
Independent reflections	16373 [R(int) = 0.0264]	
Completeness to theta = 26.37°	99.9 %	
Absorption correction	Semi-empirical from equivalents	
Max. and min. transmission	0.9001 and 0.7386	
Refinement method	Full-matrix least-squares on F^2	
Data / restraints / parameters	16373 / 172 / 985	
Goodness-of-fit on F^2	1.061	
Final R indices [I>2sigma(I)]	R1 = 0.0513, wR2 = 0.1321	
R indices (all data)	R1 = 0.0721, wR2 = 0.1450	
Absolute structure parameter	0.017(12)	
Largest diff. peak and hole	0.795 and -0.557 e•$Å^{-3}$	

Table 3.5. Atomic coordinates (x 10^4) and equivalent isotropic displacement parameters ($Å^2$x 10^3) for tetrapyridine adduct of **9**. U(eq) is defined as one third of the trace of the orthogonalized U^{ij} tensor.

	x	y	z	U(eq)
Co(1)	1292(1)	8807(1)	6606(1)	43(1)
Co(2)	3640(1)	9277(1)	8579(1)	33(1)
O(1)	2567(2)	8861(1)	6990(1)	40(1)
O(2)	1402(2)	9632(1)	6544(1)	41(1)
O(3)	-624(2)	11099(1)	5334(1)	51(1)
O(4)	3696(2)	9160(1)	7961(1)	34(1)
O(5)	2988(2)	8517(1)	8647(1)	48(1)
O(6)	3491(4)	7027(2)	10058(1)	86(1)
N(1)	1127(3)	7987(1)	6691(1)	52(1)
N(2)	33(3)	8728(2)	6214(1)	54(1)
N(3)	2385(3)	8704(2)	6112(1)	53(1)
N(4)	261(3)	8962(2)	7102(1)	45(1)
N(5)	4152(3)	10069(1)	8545(1)	38(1)
N(6)	3725(2)	9408(1)	9196(1)	37(1)
N(7)	5198(2)	8934(1)	8601(1)	38(1)
N(8)	2059(3)	9586(2)	8535(1)	47(1)
C(1)	3327(3)	8437(2)	7056(1)	41(1)
C(2)	4431(3)	8572(2)	7205(1)	37(1)
C(3)	5265(4)	8113(2)	7277(1)	47(1)
C(4)	6428(4)	8238(2)	7401(1)	58(1)
C(5)	7210(5)	7796(2)	7460(2)	78(2)
C(6)	6925(6)	7210(3)	7411(2)	84(2)
C(7)	5840(6)	7068(2)	7285(2)	81(2)
C(8)	4966(4)	7519(2)	7208(2)	56(1)
C(9)	3859(5)	7391(2)	7069(1)	62(1)
C(10)	3042(4)	7830(2)	6978(1)	47(1)
C(11)	1910(5)	7641(2)	6838(1)	55(1)
C(12)	-35(5)	7784(2)	6579(2)	63(1)
C(13)	-215(5)	7127(2)	6523(2)	75(2)
C(14)	-1483(6)	7006(2)	6403(2)	85(2)

C(15)	-1704(15)	7323(7)	5979(5)	61(4)
C(16)	-1537(17)	7981(8)	6063(11)	73(5)
C(15')	-2140(20)	7443(7)	6082(7)	92(6)
C(16')	-1850(20)	8101(9)	6132(9)	91(5)
C(17)	-404(5)	8115(2)	6165(2)	67(1)
C(18)	-328(4)	9136(2)	5957(1)	53(1)
C(19)	52(3)	9738(2)	5954(1)	41(1)
C(20)	-495(3)	10118(2)	5639(1)	43(1)
C(21)	-184(3)	10686(2)	5624(1)	41(1)
C(22)	622(3)	10907(2)	5926(1)	40(1)
C(23)	1143(3)	10572(2)	6244(1)	37(1)
C(24)	879(3)	9954(2)	6252(1)	42(1)
C(25)	-1484(4)	10910(2)	5042(1)	63(1)
C(26)	1924(3)	10844(2)	6595(1)	45(1)
C(27)	2092(4)	11510(2)	6515(2)	61(1)
C(28)	1355(5)	10766(2)	7046(1)	60(1)
C(29)	3134(3)	10563(2)	6604(2)	62(1)
C(30)	2538(18)	8260(10)	5838(5)	65(5)
C(31)	3270(20)	8230(14)	5488(6)	104(9)
C(32)	4113(18)	8647(12)	5433(6)	92(7)
C(30')	2040(20)	8332(7)	5787(4)	50(4)
C(31')	2650(20)	8335(7)	5405(4)	73(5)
C(32')	3550(20)	8741(8)	5360(5)	82(7)
C(33)	3958(5)	9132(3)	5714(2)	81(2)
C(34)	3207(4)	9124(2)	6064(2)	61(1)
C(35)	-663(3)	9320(2)	7059(1)	55(1)
C(36)	-1379(4)	9463(2)	7397(1)	68(1)
C(37)	-1189(4)	9224(3)	7806(2)	84(2)
C(38)	-240(5)	8869(3)	7854(2)	86(2)
C(39)	460(4)	8740(2)	7505(1)	57(1)
C(40)	4416(3)	9439(1)	7697(1)	31(1)
C(41)	4756(3)	9185(1)	7300(1)	33(1)
C(42)	5480(3)	9495(2)	7004(1)	36(1)
C(43)	5864(3)	9251(2)	6603(1)	45(1)
C(44)	6584(4)	9551(2)	6328(1)	57(1)
C(45)	6979(4)	10111(2)	6432(2)	61(1)

C(46)	6624(3)	10371(2)	6818(1)	52(1)
C(47)	5872(3)	10067(2)	7109(1)	39(1)
C(48)	5577(3)	10307(2)	7507(1)	40(1)
C(49)	4878(3)	10013(2)	7805(1)	35(1)
C(50)	4651(3)	10303(2)	8215(1)	39(1)
C(51)	3800(4)	10403(2)	8940(1)	51(1)
C(52)	4333(6)	11012(2)	9002(1)	75(2)
C(53)	4120(20)	11316(9)	9447(5)	59(4)
C(54)	4324(18)	10803(7)	9797(7)	60(4)
C(53')	3600(20)	11230(5)	9414(3)	92(4)
C(54')	3940(20)	10872(5)	9844(4)	90(5)
C(55)	3543(5)	10241(2)	9746(1)	68(1)
C(56)	4088(4)	10005(2)	9331(1)	48(1)
C(57)	3749(3)	8991(2)	9478(1)	44(1)
C(58)	3508(4)	8392(2)	9402(1)	47(1)
C(59)	3684(4)	8012(2)	9766(1)	55(1)
C(60)	3354(5)	7440(2)	9729(2)	65(1)
C(61)	2824(5)	7248(2)	9341(1)	63(1)
C(62)	2665(4)	7591(2)	8973(1)	53(1)
C(63)	3075(3)	8185(2)	8997(1)	46(1)
C(64)	4105(7)	7212(3)	10438(2)	100(2)
C(65)	2097(5)	7346(2)	8556(2)	63(1)
C(66)	1759(5)	6694(2)	8607(2)	68(1)
C(67)	2886(6)	7378(3)	8162(2)	95(2)
C(68)	990(6)	7681(3)	8476(2)	93(2)
C(69)	6119(3)	9185(2)	8790(1)	51(1)
C(70)	7161(4)	8887(3)	8833(2)	79(2)
C(71)	7240(6)	8326(3)	8678(2)	97(2)
C(72)	6330(6)	8079(2)	8474(2)	81(2)
C(73)	5313(4)	8386(2)	8433(1)	53(1)
C(74)	1762(4)	9931(2)	8195(1)	57(1)
C(75)	738(4)	10244(3)	8190(2)	77(2)
C(76)	-29(4)	10188(3)	8535(2)	97(2)
C(77)	258(4)	9812(3)	8866(2)	91(2)
C(78)	1290(4)	9516(2)	8862(1)	62(1)
Cl(1)	7613(1)	8986(1)	3419(1)	90(1)

Cl(2)	7137(1)	9193(1)	5158(1)	81(1)
N(1S)	4248(9)	10924(4)	4892(3)	174(4)
C(1S)	3944(8)	11403(6)	5124(4)	171(5)
C(2S)	4413(8)	11492(6)	5551(4)	154(4)
C(3S)	5149(8)	11094(7)	5711(3)	149(5)
C(4S)	5366(8)	10621(6)	5482(4)	138(4)
C(5S)	4918(10)	10531(5)	5072(3)	146(4)

Table 3.6. Bond lengths [Å] and angles [°] for tetrapyridine adduct of **9**.

Co(1)-O(1)	1.882(3)	N(7)-C(69)	1.337(5)
Co(1)-N(2)	1.888(3)	N(7)-C(73)	1.356(5)
Co(1)-O(2)	1.893(2)	N(8)-C(74)	1.343(5)
Co(1)-N(1)	1.897(3)	N(8)-C(78)	1.343(5)
Co(1)-N(4)	1.954(3)	C(1)-C(2)	1.388(6)
Co(1)-N(3)	1.977(4)	C(1)-C(10)	1.441(5)
Co(2)-O(4)	1.899(2)	C(2)-C(3)	1.438(5)
Co(2)-O(5)	1.901(3)	C(2)-C(41)	1.474(5)
Co(2)-N(5)	1.902(3)	C(3)-C(8)	1.413(6)
Co(2)-N(6)	1.902(3)	C(3)-C(4)	1.424(7)
Co(2)-N(8)	1.962(3)	C(4)-C(5)	1.365(6)
Co(2)-N(7)	1.962(3)	C(5)-C(6)	1.384(8)
O(1)-C(1)	1.321(4)	C(6)-C(7)	1.349(9)
O(2)-C(24)	1.301(5)	C(7)-C(8)	1.460(7)
O(3)-C(21)	1.387(4)	C(8)-C(9)	1.377(7)
O(3)-C(25)	1.401(5)	C(9)-C(10)	1.402(6)
O(4)-C(40)	1.319(4)	C(10)-C(11)	1.440(7)
O(5)-C(63)	1.312(4)	C(12)-C(13)	1.523(6)
O(6)-C(60)	1.384(6)	C(12)-C(17)	1.527(7)
O(6)-C(64)	1.420(7)	C(13)-C(14)	1.534(8)
N(1)-C(11)	1.281(6)	C(14)-C(15)	1.502(12)
N(1)-C(12)	1.459(6)	C(14)-C(15')	1.587(14)
N(2)-C(18)	1.284(6)	C(15)-C(16)	1.534(14)
N(2)-C(17)	1.494(5)	C(16)-C(17)	1.378(19)
N(3)-C(30)	1.324(18)	C(15')-C(16')	1.544(12)
N(3)-C(34)	1.355(6)	C(16')-C(17)	1.68(2)
N(3)-C(30')	1.361(17)	C(18)-C(19)	1.441(6)
N(4)-C(39)	1.345(5)	C(19)-C(24)	1.406(5)
N(4)-C(35)	1.350(6)	C(19)-C(20)	1.439(6)
N(5)-C(50)	1.272(5)	C(20)-C(21)	1.344(6)
N(5)-C(51)	1.480(5)	C(21)-C(22)	1.399(5)
N(6)-C(57)	1.282(5)	C(22)-C(23)	1.371(5)
N(6)-C(56)	1.482(5)	C(23)-C(24)	1.442(5)

C(23)-C(26)	1.529(5)	C(57)-C(58)	1.412(6)
C(26)-C(28)	1.529(6)	C(58)-C(63)	1.409(5)
C(26)-C(29)	1.537(6)	C(58)-C(59)	1.422(5)
C(26)-C(27)	1.550(5)	C(59)-C(60)	1.363(6)
C(30)-C(31)	1.357(12)	C(60)-C(61)	1.399(7)
C(31)-C(32)	1.374(13)	C(61)-C(62)	1.377(6)
C(32)-C(33)	1.41(2)	C(62)-C(63)	1.436(6)
C(30')-C(31')	1.360(13)	C(62)-C(65)	1.533(6)
C(31')-C(32')	1.397(15)	C(65)-C(68)	1.509(8)
C(32')-C(33)	1.47(3)	C(65)-C(67)	1.508(7)
C(33)-C(34)	1.372(7)	C(65)-C(66)	1.543(6)
C(35)-C(36)	1.358(6)	C(69)-C(70)	1.388(6)
C(36)-C(37)	1.376(7)	C(70)-C(71)	1.366(9)
C(37)-C(38)	1.370(8)	C(71)-C(72)	1.344(9)
C(38)-C(39)	1.365(7)	C(72)-C(73)	1.374(7)
C(40)-C(41)	1.398(5)	C(74)-C(75)	1.381(6)
C(40)-C(49)	1.449(5)	C(75)-C(76)	1.378(7)
C(41)-C(42)	1.418(5)	C(76)-C(77)	1.362(9)
C(42)-C(43)	1.413(5)	C(77)-C(78)	1.368(7)
C(42)-C(47)	1.415(5)	N(1S)-C(5S)	1.303(12)
C(43)-C(44)	1.363(6)	N(1S)-C(1S)	1.347(13)
C(44)-C(45)	1.393(7)	C(1S)-C(2S)	1.424(14)
C(45)-C(46)	1.376(6)	C(2S)-C(3S)	1.334(16)
C(46)-C(47)	1.421(5)	C(3S)-C(4S)	1.307(15)
C(47)-C(48)	1.372(5)	C(4S)-C(5S)	1.367(13)
C(48)-C(49)	1.387(5)	O(1)-Co(1)-N(2)	178.05(15)
C(49)-C(50)	1.435(5)	O(1)-Co(1)-O(2)	86.83(11)
C(51)-C(56)	1.530(5)	N(2)-Co(1)-O(2)	94.78(14)
C(51)-C(52)	1.531(7)	O(1)-Co(1)-N(1)	93.34(14)
C(52)-C(53)	1.541(14)	N(2)-Co(1)-N(1)	85.11(16)
C(52)-C(53')	1.588(11)	O(2)-Co(1)-N(1)	177.12(14)
C(53)-C(54)	1.600(15)	O(1)-Co(1)-N(4)	89.18(12)
C(54)-C(55)	1.574(15)	N(2)-Co(1)-N(4)	92.01(15)
C(53')-C(54')	1.592(10)	O(2)-Co(1)-N(4)	86.50(13)
C(54')-C(55)	1.540(10)	N(1)-Co(1)-N(4)	90.63(14)
C(55)-C(56)	1.511(6)	O(1)-Co(1)-N(3)	88.87(14)

N(2)-Co(1)-N(3)	90.04(16)	C(30')-N(3)-Co(1)	116.1(10)
O(2)-Co(1)-N(3)	89.94(13)	C(39)-N(4)-C(35)	116.7(4)
N(1)-Co(1)-N(3)	92.94(14)	C(39)-N(4)-Co(1)	122.1(3)
N(4)-Co(1)-N(3)	176.03(14)	C(35)-N(4)-Co(1)	121.1(3)
O(4)-Co(2)-O(5)	89.51(10)	C(50)-N(5)-C(51)	123.3(3)
O(4)-Co(2)-N(5)	93.93(11)	C(50)-N(5)-Co(2)	125.5(3)
O(5)-Co(2)-N(5)	173.85(13)	C(51)-N(5)-Co(2)	110.9(3)
O(4)-Co(2)-N(6)	175.03(12)	C(57)-N(6)-C(56)	119.4(3)
O(5)-Co(2)-N(6)	93.24(12)	C(57)-N(6)-Co(2)	123.0(3)
N(5)-Co(2)-N(6)	83.70(13)	C(56)-N(6)-Co(2)	115.5(2)
O(4)-Co(2)-N(8)	90.84(12)	C(69)-N(7)-C(73)	118.6(3)
O(5)-Co(2)-N(8)	88.04(14)	C(69)-N(7)-Co(2)	124.9(3)
N(5)-Co(2)-N(8)	86.81(14)	C(73)-N(7)-Co(2)	116.4(3)
N(6)-Co(2)-N(8)	93.38(12)	C(74)-N(8)-C(78)	118.1(3)
O(4)-Co(2)-N(7)	86.92(12)	C(74)-N(8)-Co(2)	120.0(3)
O(5)-Co(2)-N(7)	89.74(12)	C(78)-N(8)-Co(2)	121.4(3)
N(5)-Co(2)-N(7)	95.53(12)	O(1)-C(1)-C(2)	119.8(3)
N(6)-Co(2)-N(7)	88.96(12)	O(1)-C(1)-C(10)	121.8(4)
N(8)-Co(2)-N(7)	176.86(14)	C(2)-C(1)-C(10)	118.5(3)
C(1)-O(1)-Co(1)	124.5(2)	C(1)-C(2)-C(3)	120.1(3)
C(24)-O(2)-Co(1)	126.8(2)	C(1)-C(2)-C(41)	120.6(3)
C(21)-O(3)-C(25)	117.0(3)	C(3)-C(2)-C(41)	119.3(3)
C(40)-O(4)-Co(2)	123.7(2)	C(8)-C(3)-C(4)	117.4(4)
C(63)-O(5)-Co(2)	125.8(2)	C(8)-C(3)-C(2)	120.8(4)
C(60)-O(6)-C(64)	116.3(4)	C(4)-C(3)-C(2)	121.7(4)
C(11)-N(1)-C(12)	122.4(4)	C(5)-C(4)-C(3)	120.8(5)
C(11)-N(1)-Co(1)	125.7(3)	C(4)-C(5)-C(6)	122.8(6)
C(12)-N(1)-Co(1)	111.9(3)	C(7)-C(6)-C(5)	118.9(5)
C(18)-N(2)-C(17)	120.5(3)	C(6)-C(7)-C(8)	121.2(5)
C(18)-N(2)-Co(1)	124.4(3)	C(9)-C(8)-C(3)	118.3(4)
C(17)-N(2)-Co(1)	114.3(3)	C(9)-C(8)-C(7)	122.8(5)
C(30)-N(3)-C(34)	112.3(6)	C(3)-C(8)-C(7)	118.9(5)
C(30)-N(3)-C(30')	26.5(6)	C(8)-C(9)-C(10)	122.2(4)
C(34)-N(3)-C(30')	124.5(9)	C(9)-C(10)-C(11)	117.1(4)
C(30)-N(3)-Co(1)	130.9(6)	C(9)-C(10)-C(1)	119.9(4)
C(34)-N(3)-Co(1)	116.4(3)	C(11)-C(10)-C(1)	122.8(4)

N(1)-C(11)-C(10)	124.1(4)	C(28)-C(26)-C(27)	107.9(4)
N(1)-C(12)-C(13)	117.6(5)	C(23)-C(26)-C(27)	111.2(3)
N(1)-C(12)-C(17)	107.0(3)	C(29)-C(26)-C(27)	107.2(3)
C(13)-C(12)-C(17)	110.9(4)	N(3)-C(30)-C(31)	127.9(14)
C(12)-C(13)-C(14)	109.5(5)	C(32)-C(31)-C(30)	120.1(14)
C(15)-C(14)-C(13)	106.3(7)	C(31)-C(32)-C(33)	112.3(13)
C(15)-C(14)-C(15')	24.2(10)	C(31')-C(30')-N(3)	117.8(12)
C(13)-C(14)-C(15')	119.3(8)	C(30')-C(31')-C(32')	118.1(13)
C(14)-C(15)-C(16)	107.8(14)	C(33)-C(32')-C(31')	124.4(12)
C(17)-C(16)-C(15)	111.9(12)	C(34)-C(33)-C(32')	110.9(10)
C(16')-C(15')-C(14)	116.6(12)	C(34)-C(33)-C(32)	122.7(7)
C(15')-C(16')-C(17)	103.7(13)	C(32')-C(33)-C(32)	28.7(7)
C(16)-C(17)-N(2)	123.4(9)	N(3)-C(34)-C(33)	122.4(5)
C(16)-C(17)-C(12)	110.0(12)	N(4)-C(35)-C(36)	123.5(4)
N(2)-C(17)-C(12)	106.6(3)	C(35)-C(36)-C(37)	119.5(4)
C(16)-C(17)-C(16')	15.3(16)	C(38)-C(37)-C(36)	117.2(5)
N(2)-C(17)-C(16')	111.1(8)	C(39)-C(38)-C(37)	121.2(5)
C(12)-C(17)-C(16')	108.6(9)	N(4)-C(39)-C(38)	121.8(4)
N(2)-C(18)-C(19)	126.5(4)	O(4)-C(40)-C(41)	120.1(3)
C(24)-C(19)-C(18)	122.5(4)	O(4)-C(40)-C(49)	122.0(3)
C(24)-C(19)-C(20)	121.1(4)	C(41)-C(40)-C(49)	117.8(3)
C(18)-C(19)-C(20)	116.4(3)	C(40)-C(41)-C(42)	120.5(3)
C(21)-C(20)-C(19)	118.9(3)	C(40)-C(41)-C(2)	119.4(3)
C(20)-C(21)-O(3)	125.2(3)	C(42)-C(41)-C(2)	120.0(3)
C(20)-C(21)-C(22)	120.2(3)	C(43)-C(42)-C(47)	117.2(3)
O(3)-C(21)-C(22)	114.5(4)	C(43)-C(42)-C(41)	122.4(3)
C(23)-C(22)-C(21)	123.6(4)	C(47)-C(42)-C(41)	120.4(3)
C(22)-C(23)-C(24)	117.5(3)	C(44)-C(43)-C(42)	121.5(4)
C(22)-C(23)-C(26)	121.8(3)	C(43)-C(44)-C(45)	121.4(4)
C(24)-C(23)-C(26)	120.6(3)	C(46)-C(45)-C(44)	119.4(4)
O(2)-C(24)-C(19)	123.8(3)	C(45)-C(46)-C(47)	120.2(4)
O(2)-C(24)-C(23)	117.8(3)	C(48)-C(47)-C(42)	119.2(3)
C(19)-C(24)-C(23)	118.4(4)	C(48)-C(47)-C(46)	120.4(4)
C(28)-C(26)-C(23)	109.0(3)	C(42)-C(47)-C(46)	120.3(4)
C(28)-C(26)-C(29)	109.1(4)	C(47)-C(48)-C(49)	121.9(3)
C(23)-C(26)-C(29)	112.3(3)	C(48)-C(49)-C(50)	116.8(3)

C(48)-C(49)-C(40)	120.2(3)	C(67)-C(65)-C(62)	112.4(4)
C(50)-C(49)-C(40)	123.0(3)	C(68)-C(65)-C(66)	106.9(4)
N(5)-C(50)-C(49)	125.0(3)	C(67)-C(65)-C(66)	106.2(4)
N(5)-C(51)-C(56)	105.5(3)	C(62)-C(65)-C(66)	112.1(4)
N(5)-C(51)-C(52)	117.1(4)	N(7)-C(69)-C(70)	121.4(5)
C(56)-C(51)-C(52)	110.8(3)	C(71)-C(70)-C(69)	118.9(5)
C(53)-C(52)-C(51)	116.8(11)	C(72)-C(71)-C(70)	120.1(5)
C(53)-C(52)-C(53')	23.1(8)	C(71)-C(72)-C(73)	119.7(5)
C(51)-C(52)-C(53')	99.7(9)	N(7)-C(73)-C(72)	121.3(5)
C(52)-C(53)-C(54)	103.4(14)	N(8)-C(74)-C(75)	122.0(4)
C(53)-C(54)-C(55)	116.3(16)	C(76)-C(75)-C(74)	119.5(5)
C(54')-C(53')-C(52)	110.9(8)	C(77)-C(76)-C(75)	117.6(4)
C(55)-C(54')-C(53')	104.2(9)	C(76)-C(77)-C(78)	121.1(5)
C(54')-C(55)-C(56)	111.6(8)	N(8)-C(78)-C(77)	121.4(4)
C(54')-C(55)-C(54)	18.0(10)	C(5S)-N(1S)-C(1S)	119.6(8)
C(56)-C(55)-C(54)	97.7(9)	N(1S)-C(1S)-C(2S)	119.6(9)
N(6)-C(56)-C(55)	116.1(4)	C(3S)-C(2S)-C(1S)	118.5(11)
N(6)-C(56)-C(51)	105.6(3)	C(4S)-C(3S)-C(2S)	119.4(11)
C(55)-C(56)-C(51)	110.4(3)	C(3S)-C(4S)-C(5S)	122.5(12)
N(6)-C(57)-C(58)	127.0(3)		
C(63)-C(58)-C(57)	122.6(3)		
C(63)-C(58)-C(59)	121.7(4)		
C(57)-C(58)-C(59)	115.6(3)		
C(60)-C(59)-C(58)	118.6(4)		
C(59)-C(60)-O(6)	124.0(4)		
C(59)-C(60)-C(61)	119.4(4)		
O(6)-C(60)-C(61)	116.5(4)		
C(62)-C(61)-C(60)	124.5(4)		
C(61)-C(62)-C(63)	116.7(4)		
C(61)-C(62)-C(65)	121.5(4)		
C(63)-C(62)-C(65)	121.8(4)		
O(5)-C(63)-C(58)	122.8(4)		
O(5)-C(63)-C(62)	118.6(3)		
C(58)-C(63)-C(62)	118.6(3)		
C(68)-C(65)-C(67)	110.9(5)		
C(68)-C(65)-C(62)	108.2(4)		

N(1S)-C(5S)-C(4S)	120.2(11)

Symmetry transformations used to generate equivalent atoms:

Table 3.7. Anisotropic displacement parameters ($Å^2 x\ 10^3$) for tetrapyridine adduct of **9**. The anisotropic displacement factor exponent takes the form: $-2p^2[\ h^2\ a^{*2}U^{11} + ...\ + 2\ h\ k\ a^*\ b^*\ U^{12}\ ]$

	U^{11}	U^{22}	U^{33}	U^{23}	U^{13}	U^{12}
Co(1)	53(1)	33(1)	42(1)	0(1)	-2(1)	-16(1)
Co(2)	29(1)	39(1)	32(1)	3(1)	0(1)	1(1)
O(1)	41(1)	32(1)	45(1)	-2(1)	1(1)	-5(1)
O(2)	38(1)	33(1)	52(1)	8(1)	-9(1)	-8(1)
O(3)	58(2)	54(2)	40(1)	-1(1)	-6(1)	11(1)
O(4)	31(1)	39(1)	32(1)	3(1)	8(1)	-7(1)
O(5)	53(2)	54(2)	37(1)	6(1)	1(1)	-19(1)
O(6)	133(3)	69(2)	55(2)	24(2)	4(2)	-31(2)
N(1)	76(2)	38(2)	41(2)	-4(1)	7(2)	-28(2)
N(2)	64(2)	56(2)	43(2)	5(2)	-10(2)	-28(2)
N(3)	76(2)	37(2)	48(2)	9(2)	7(2)	-8(2)
N(4)	37(2)	53(2)	46(2)	0(2)	-13(1)	-17(2)
N(5)	43(2)	37(2)	36(2)	1(1)	-10(1)	9(1)
N(6)	32(1)	48(2)	33(1)	2(1)	-5(1)	10(1)
N(7)	35(1)	39(2)	39(2)	12(1)	4(1)	6(1)
N(8)	31(2)	75(2)	36(2)	-3(2)	-2(1)	9(2)
C(1)	61(2)	26(2)	37(2)	4(2)	13(2)	2(2)
C(2)	46(2)	31(2)	33(2)	4(1)	11(2)	4(2)
C(3)	64(3)	36(2)	42(2)	10(2)	20(2)	13(2)
C(4)	54(2)	54(2)	66(3)	26(2)	14(2)	23(2)
C(5)	72(3)	71(3)	92(4)	37(3)	20(3)	36(3)
C(6)	75(4)	71(4)	107(5)	37(3)	31(3)	39(3)
C(7)	132(5)	35(2)	75(3)	20(2)	46(4)	36(3)
C(8)	74(3)	38(2)	57(3)	11(2)	18(2)	12(2)
C(9)	114(4)	26(2)	47(2)	8(2)	24(3)	10(2)

C(10)	71(3)	32(2)	39(2)	-1(2)	8(2)	-5(2)
C(11)	95(3)	26(2)	44(2)	6(2)	8(2)	-15(2)
C(12)	88(3)	54(2)	47(2)	-1(2)	-4(2)	-41(2)
C(13)	115(4)	50(3)	60(3)	1(2)	-4(3)	-40(3)
C(14)	116(4)	65(3)	74(3)	3(2)	-5(3)	-64(3)
C(15)	45(7)	53(6)	84(8)	5(6)	-13(5)	-19(5)
C(16)	66(8)	56(6)	97(11)	13(6)	-27(8)	-11(7)
C(15')	117(11)	77(8)	83(9)	-8(7)	-17(9)	-70(7)
C(16')	99(9)	75(7)	98(10)	20(8)	-40(9)	-74(7)
C(17)	90(3)	52(3)	57(3)	1(2)	-18(2)	-42(2)
C(18)	56(2)	61(3)	42(2)	-4(2)	-4(2)	-27(2)
C(19)	43(2)	49(2)	30(2)	-3(2)	4(2)	-10(2)
C(20)	38(2)	57(2)	34(2)	-3(2)	8(2)	-7(2)
C(21)	34(2)	57(2)	33(2)	4(2)	8(1)	12(2)
C(22)	40(2)	35(2)	45(2)	-6(2)	4(2)	5(2)
C(23)	34(2)	34(2)	43(2)	1(1)	4(2)	2(1)
C(24)	37(2)	42(2)	47(2)	-5(2)	6(2)	-9(2)
C(25)	65(3)	82(3)	41(2)	-3(2)	-11(2)	20(3)
C(26)	45(2)	31(2)	61(2)	3(2)	-14(2)	-5(2)
C(27)	73(3)	35(2)	74(3)	2(2)	-27(2)	-6(2)
C(28)	81(3)	51(2)	48(2)	-4(2)	-14(2)	-12(3)
C(29)	42(2)	40(2)	105(4)	4(2)	-28(2)	-6(2)
C(30)	42(8)	88(11)	65(8)	-8(7)	18(6)	-29(8)
C(31)	90(13)	180(20)	48(8)	-39(10)	19(8)	-67(14)
C(32)	54(9)	145(19)	76(9)	11(10)	15(7)	-45(10)
C(30')	54(9)	53(6)	43(5)	-10(4)	-3(6)	5(7)
C(31')	92(13)	75(8)	52(7)	15(6)	-11(7)	13(8)
C(32')	104(17)	101(11)	42(6)	20(7)	24(8)	51(12)
C(33)	98(4)	68(3)	78(4)	26(3)	25(3)	-10(3)
C(34)	63(3)	38(2)	82(3)	8(2)	7(2)	-5(2)
C(35)	36(2)	77(3)	52(2)	8(2)	-12(2)	-17(2)
C(36)	31(2)	113(4)	61(3)	7(3)	-9(2)	7(3)
C(37)	44(2)	156(6)	52(3)	-3(3)	-1(2)	8(3)
C(38)	69(3)	148(6)	42(2)	10(3)	-9(2)	20(4)
C(39)	51(2)	75(3)	45(2)	5(2)	-7(2)	-2(2)
C(40)	22(1)	32(2)	38(2)	10(1)	0(1)	5(1)

C(41)	31(2)	30(2)	37(2)	4(1)	3(1)	6(1)
C(42)	26(2)	40(2)	43(2)	12(2)	5(1)	10(1)
C(43)	44(2)	43(2)	48(2)	9(2)	12(2)	14(2)
C(44)	50(2)	71(3)	48(2)	12(2)	21(2)	17(2)
C(45)	45(2)	75(3)	61(3)	19(2)	16(2)	-11(2)
C(46)	40(2)	62(3)	54(2)	11(2)	7(2)	-10(2)
C(47)	27(2)	47(2)	42(2)	15(2)	-1(1)	-4(2)
C(48)	36(2)	38(2)	47(2)	7(2)	-6(2)	-8(2)
C(49)	30(2)	37(2)	39(2)	4(2)	-3(1)	2(1)
C(50)	42(2)	32(2)	43(2)	3(2)	-11(2)	-2(2)
C(51)	74(3)	47(2)	32(2)	-5(2)	-11(2)	27(2)
C(52)	144(5)	39(2)	42(2)	-1(2)	-22(3)	20(3)
C(53)	85(12)	51(7)	41(7)	-17(5)	-41(7)	21(7)
C(54)	99(11)	57(7)	25(6)	-25(5)	0(7)	51(6)
C(53')	193(13)	41(4)	41(4)	-19(3)	-36(6)	25(7)
C(54')	190(13)	48(4)	32(4)	-6(3)	1(6)	52(6)
C(55)	105(4)	66(3)	31(2)	-3(2)	-12(2)	31(3)
C(56)	63(3)	45(2)	34(2)	3(2)	-11(2)	13(2)
C(57)	43(2)	57(2)	32(2)	4(2)	-3(2)	0(2)
C(58)	52(2)	52(2)	37(2)	7(2)	8(2)	-10(2)
C(59)	67(3)	61(3)	38(2)	9(2)	0(2)	-12(2)
C(60)	82(4)	63(3)	51(2)	16(2)	8(2)	-17(2)
C(61)	93(3)	53(3)	43(2)	9(2)	13(2)	-24(2)
C(62)	59(3)	58(3)	42(2)	3(2)	12(2)	-16(2)
C(63)	48(2)	53(2)	36(2)	9(2)	8(2)	-10(2)
C(64)	156(6)	88(4)	57(3)	28(3)	-14(4)	-32(4)
C(65)	83(3)	57(3)	47(2)	3(2)	12(2)	-35(2)
C(66)	92(4)	53(3)	60(3)	0(2)	7(3)	-27(2)
C(67)	139(5)	103(4)	44(3)	-22(3)	25(3)	-70(4)
C(68)	105(5)	71(3)	102(4)	6(3)	-44(4)	-21(3)
C(69)	32(2)	78(3)	41(2)	2(2)	0(2)	7(2)
C(70)	46(2)	135(5)	54(3)	-3(3)	-7(2)	29(3)
C(71)	86(4)	143(6)	61(3)	13(3)	0(3)	78(4)
C(72)	99(4)	74(3)	70(3)	23(3)	19(3)	44(3)
C(73)	60(3)	42(2)	56(2)	13(2)	16(2)	12(2)
C(74)	42(2)	95(4)	35(2)	5(2)	-4(2)	14(2)

C(75)	51(3)	131(5)	48(2)	7(3)	-7(2)	39(3)
C(76)	46(3)	179(7)	66(3)	-14(4)	-1(3)	48(3)
C(77)	40(2)	198(7)	35(2)	-6(3)	2(2)	26(3)
C(78)	34(2)	112(4)	39(2)	0(2)	-3(2)	5(2)
Cl(1)	84(1)	81(1)	104(1)	-12(1)	5(1)	16(1)
Cl(2)	85(1)	110(1)	47(1)	-13(1)	2(1)	-26(1)
N(1S)	251(11)	155(7)	115(6)	-6(5)	-108(7)	28(7)
C(1S)	96(6)	186(10)	232(12)	-38(10)	-88(7)	30(6)
C(2S)	75(5)	233(12)	152(9)	-63(8)	28(6)	-24(7)
C(3S)	73(5)	279(16)	94(6)	46(8)	-16(5)	-67(8)
C(4S)	86(5)	199(12)	130(8)	71(7)	-1(6)	-35(7)
C(5S)	184(9)	173(9)	82(5)	41(5)	-17(6)	-6(8)

Table 3.8. Hydrogen coordinates (x 10^4) and isotropic displacement parameters ($Å^2$ x 10^3) for tetrapyridine adduct of **9**.

	x	y	z	U(eq)
H(4A)	6662	8633	7444	69
H(5A)	7983	7895	7538	94
H(6A)	7484	6913	7466	101
H(7A)	5642	6667	7246	97
H(9A)	3642	6992	7033	75
H(11A)	1733	7235	6857	66
H(12A)	-560	7914	6821	76
H(13A)	-17	6922	6800	90
H(13B)	299	6976	6288	90
H(14A)	-1616	6580	6367	102
H(14B)	-2005	7154	6637	102
H(15A)	-2503	7246	5876	73
H(15B)	-1156	7186	5750	73
H(16A)	-1769	8203	5797	88
H(16B)	-2046	8105	6308	88
H(15C)	-1962	7325	5776	110
H(15D)	-2983	7391	6126	110
H(16C)	-2212	8264	6401	109
H(16D)	-2130	8326	5874	109
H(17A)	67	7941	5922	80
H(18A)	-902	9030	5748	64
H(20A)	-1067	9970	5443	51
H(22A)	820	11311	5908	48
H(25A)	-1725	11238	4856	94
H(25B)	-2151	10764	5208	94
H(25C)	-1176	10594	4857	94
H(27A)	1336	11705	6514	91
H(27B)	2475	11570	6231	91
H(27C)	2573	11675	6750	91
H(28A)	586	10948	7043	90
H(28B)	1835	10953	7271	90

H(28C)	1279	10347	7111	90
H(29A)	3062	10141	6658	93
H(29B)	3597	10743	6838	93
H(29C)	3516	10627	6320	93
H(30A)	2084	7920	5893	78
H(31A)	3191	7920	5281	125
H(32A)	4731	8613	5228	110
H(30B)	1396	8079	5826	60
H(31B)	2474	8068	5175	88
H(32B)	3926	8768	5082	99
H(33A)	4392	9479	5659	98
H(34A)	3266	9423	6280	74
H(35A)	-821	9482	6777	66
H(36A)	-2006	9725	7351	82
H(37A)	-1694	9303	8046	101
H(38A)	-66	8709	8134	103
H(39A)	1105	8488	7548	69
H(43A)	5613	8869	6523	54
H(44A)	6821	9374	6060	68
H(45A)	7490	10312	6239	73
H(46A)	6881	10755	6889	62
H(48A)	5859	10686	7580	48
H(50A)	4891	10699	8243	47
H(51A)	2940	10450	8930	61
H(52A)	5180	10979	8959	90
H(52B)	4032	11271	8767	90
H(53A)	3313	11468	9466	71
H(53B)	4665	11643	9494	71
H(54A)	4199	10966	10095	72
H(54B)	5145	10680	9778	72
H(53C)	3751	11653	9463	110
H(53D)	2768	11179	9353	110
H(54C)	4791	10886	9896	108
H(54D)	3542	11031	10106	108
H(55A)	3630	9968	9997	81
H(55B)	2715	10341	9705	81

H(56A)	4948	10004	9371	57
H(57A)	3952	9095	9771	53
H(59A)	4024	8154	10030	66
H(61A)	2557	6854	9331	76
H(64A)	4150	6887	10648	150
H(64B)	3699	7543	10574	150
H(64C)	4889	7333	10354	150
H(66A)	2458	6460	8659	103
H(66B)	1377	6559	8338	103
H(66C)	1229	6650	8857	103
H(67A)	3592	7152	8220	143
H(67B)	3090	7788	8105	143
H(67C)	2489	7215	7905	143
H(68A)	1168	8099	8440	139
H(68B)	467	7628	8726	139
H(68C)	617	7534	8208	139
H(69A)	6059	9576	8896	61
H(70A)	7810	9071	8968	94
H(71A)	7938	8111	8715	116
H(72A)	6391	7692	8359	97
H(73A)	4678	8212	8283	63
H(74A)	2272	9961	7951	69
H(75A)	563	10497	7951	92
H(76A)	-733	10403	8542	117
H(77A)	-266	9754	9102	109
H(78A)	1465	9255	9097	74
H(1SB)	3421	11681	5002	206
H(2SA)	4206	11827	5720	184
H(3SA)	5512	11154	5988	178
H(4SA)	5855	10329	5606	166
H(5SA)	5095	10180	4917	175

3.5. References and Notes

(1) (a) *Comprehensive Asymmetric Catalysis;* Jacobsen, E. N.; Pfaltz, A.; Yamamoto, H., Eds.; Springer: Berlin 1999. (b) *Stereoselective Polymerization with Single Site Catalysts*; Baugh, L. S.; Canich, J. M., Eds.; CRC Press: Boca Raton, FL, 2007. (c) Halpern, J.; Trost, B. M. *Proc. Nat. Acad. Sci. U. S. A.* **2004**, *101*, 5347.

(2) *Aziridines and Epoxides in Organic Synthesis*; Yudin, A., Ed.; Wiley: New York, 2006.

(3) Kuran, W. *Prog. Polym. Sci.* **1998**, *23*, 919.

(4) Hirahata, W.; Thomas, R. M.; Lobkovsky, E. B.; Coates, G. W. *J. Am. Chem. Soc.* **2008**, *130*, 17658.

(5) Thomas, R. M.; Widger, P. C. B.; Ahmed, S. M.; Jeske, R. C.; Hirahata, W.; Lobkovsky, E. B.; Coates, G. W. *J. Am. Chem. Soc.* **2010**, *132*, 16520.

(6) (a) Wilms, D.; Stiriba, S. E.; Frey, H. *Acc. Chem. Res.* **2010**, *43*, 129. (b) Stevens, M. P. *Polymer Chemistry*; Oxford University Press: New York, 1999; Chapter 11.

(7) Widger, P. C. B.; Ahmed, S. M.; Hirahata, W.; Thomas, R. M.; Lobkovsky, E. B.; Coates, G. W. *Chem. Commun.* **2010**, *46*, 2935.

(8) Ahmed, S. M.; Poater, A.; Childers, M. I.; LaPointe, A. M.; Widger, P. C. B.; Lobkovsky, E. B.; Cavallo, L.; Coates, G. W.; Manuscript in preparation.

(9) Widger, P. C. B.; Ahmed, S. M.; Coates, G. W. *Macromolecules* **2011**, *44*, 5666.

(10) (a) Nielsen, L. P. C.; Stevenson, C. P.; Blackmond, D. G.; Jacobsen, E. N. *J. Am. Chem. Soc.* **2004**, *126*, 1360. (b) Nielsen, L. P. C.; Zuend, S. J.; Ford, D. D.; Jacobsen, E. N. *J. Org. Chem.* **2012**, *77*, 2486. (c) Cohen, C. T.; Chu, T.; Coates, G. W. *J. Am. Chem. Soc.* **2005**, *127*, 10869. (d) Cohen, C. T.; Thomas, C. M.; Peretti, K. L.; Lobkovsky, E.

B.; Coates, G. W. *Dalton Trans.* **2006**, 237. (e) Cohen, C. T.; Coates, G. W. *J. Polym. Sci., Part A: Polym. Chem.* **2006**, *44*, 5182.

(11) (a) Palucki, M.; Finney, N. S.; Pospisil, P. J.; Guler, M. L.; Ishida, T.; Jacobsen, E. N. *J. Am. Chem. Soc.* **1998**, *120*, 948. (b) Norrby, P.-O.; Linde, C.; Aakermark, B. *J. Am. Chem. Soc.* **1995**, *117*, 11035. (c) Jacobsen, E. N.; Zhang, W.; Guler, M. L. *J. Am. Chem. Soc.* **1991**, *113*, 6703. (d) Hormnirun, P.; Marshall, E. L.; Gibson, V. C.; Pugh, R. I.; White, A. J. P. *Proc. Nat. Acad. Sci. U. S. A.* **2006**, *103*, 15343. (e) Darensbourg, D. J.; Phelps, A. L. *Inorg. Chem.* **2005**, *44*, 4622.

(12) (a) Nomura, N.; Ishii, R.; Yamamoto, Y.; Kondo, T. *Chem. Eur. J.* **2007**, *13*, 4433. (b) Casiraghi, G.; Casnati, G.; Puglia, G.; Sartori, G.; Terenghi, G. *J. Chem. Soc., Perkin Trans. 1* **1980**, 1862.

(13) (a) Zhang, H. C.; Huang, W. S.; Pu, L. *J. Org. Chem.* **2001**, *66*, 481; (b) Kozitsyna, N. Y.; Bukharkina, A. A.; Martens, M. V.; Vargaftik, M. N.; Moiseev, II *J. Organomet. Chem.* **2001**, *636*, 69.